2015-06-01

# Identifying and Characterizing Yeast PAS Kinase 1 Substrates Reveals Regulation of Mitochondrial and Cell Growth Pathways

Desiree DeMille
*Brigham Young University - Provo*

# Identifying and Characterizing Yeast PAS Kinase 1 Substrates Reveals Regulation of Mitochondrial and Cell Growth Pathways

Desiree DeMille

A dissertation submitted to the faculty of
Brigham Young University
in partial fulfillment of the requirements for the degree of

Doctor of Philosophy

Julianne H. Grose, Chair
William R. McCleary
Laura C. Bridgewater
David M. Thomson
Steven M. Johnson

Department of Microbiology & Molecular Biology

Brigham Young University

June 2015

ABSTRACT

Identifying and Characterizing Yeast PAS Kinase 1 Substrates Reveals Regulation of Mitochondrial and Cell Growth Pathways

Desiree DeMille
Department of Microbiology & Molecular Biology, BYU
Doctor of Philosophy

Glucose allocation is an important cellular process that is misregulated in the interrelated diseases obesity, diabetes and cancer. Cells have evolved critical mechanisms for regulating glucose allocation, one of which is sensory protein kinases. PAS kinase is a key sensory protein kinase that regulates glucose allocation in yeast, mice and man; and is a novel therapeutic target for the treatment of metabolic diseases such as obesity, diabetes and cancer. Despite its importance, the molecular mechanisms of PAS kinase function are largely unknown. Through large-scale protein-interaction studies, we have identified 93 novel binding partners for PAS kinase which help to expand its role in glucose allocation as well as suggest novel roles for PAS kinase including mitochondrial metabolism, cell growth/division, protein modification, stress tolerance, and gene/protein expression. From a subset of these binding partners, we identified 5 in vitro substrates of PAS kinase namely Mot3, Utr1, Zds1, Cbf1 and Pbp1. Additionally, we have further characterized Pbp1 and Cbf1 as PAS kinase substrates through both in vitro and in vivo evidence as well as phenotypic analysis. Evidence is provided for the PAS kinase-dependent phosphorylation and activation of Pbp1, which in turn inhibits cell proliferation through the sequestration of TORC1. In contract, PAS kinase-dependent phosphorylation of Cbf1 inhibits its activity, decreasing cellular respiration. This work elucidates novel molecular mechanisms behind PAS kinase function in both mitochondrial and cell growth pathways in eukaryotic cells, increasing our understanding of the regulation of central metabolism.

Keywords: PAS kinase, Psk1, Cbf1, Pbp1, respiration, glucose allocation, diabetes, metabolism

ACKNOWLEDGMENTS

I would like to express appreciation for my mentor Dr. Julianne Grose especially for her enthusiasm and dedication to our research. I am grateful for her time and effort spent in helping me to succeed.

I would like to give a big thank you to all of my graduate committee members, as well as other faculty whom I have had the opportunity to collaborate with, for their ideas and advice with troubleshooting.

Finally, I would like to dedicate this dissertation to my loving, supportive and patient family, Lee, Kai and Mya.

TABLE OF CONTENTS

LIST OF TABLES

LIST OF FIGURES

# CHAPTER 1: PAS kinase: A nutrient sensing regulator of glucose homeostasis

Desiree DeMille and Julianne H. Grose*

Department of Microbiology and Molecular Biology
Brigham Young University, Provo, UT 84602

*Address correspondence to:

Julianne H. Grose
Department of Microbiology and Molecular Biology
Brigham Young University, Provo, UT 84602
E-mail: julianne_grose@byu.edu

ABSTRACT

Per-Arnt-Sim (PAS) kinase (PASK, PASKIN, and PSK) is a member of the group of nutrient sensing protein kinases. These protein kinases sense the energy or nutrient status of the cell and regulate cellular metabolism appropriately. PAS kinase responds to glucose availability and regulates glucose homeostasis in yeast, mice and man. Despite this pivotal role, the molecular mechanisms of PAS kinase regulation and function are largely unknown. This review focuses on what is known about PAS kinase, including its conservation from yeast to man, identified substrates, associated phenotypes and role in metabolic disease.

INTRODUCTION

A cell's ability to accurately coordinate its metabolism with nutrient availability is essential for proper health. Metabolic diseases are becoming a pandemic with more than one in 10 adults in the world being obese (World Health Organization), often leading to further disease such as diabetes, heart disease and cancer [National Cancer Institute, (1–3)]. Glucose metabolism is central to these metabolic diseases (4) making it crucial to understand the cellular mechanisms behind glucose allocation. Protein kinases are a key cellular mechanism for proper glucose allocation by enabling the simultaneous control of multiple proteins to direct glucose away from some pathways while stimulating others.

An individual cell may express hundreds of different protein kinases. It is estimated that there are 122 protein kinase homologs in yeast (5), 540 in mice (6), and 518 in humans (7), which phosphorylate over 30% of the proteome (8). Thus, it is not surprising that aberrant kinase function is associated with several human diseases and that protein kinases are one of the top drug targets for treating disease (9).

Per-Arnt-Sim (PAS) kinase (PASK, PASKIN, and PSK) has recently been shown to play pivotal roles in glucose homeostasis in yeast, mice, and man. This review will discuss what is known about PAS kinase activation and function, including its conservation from yeast to man, identified substrates, associated phenotypes and role in metabolic disease.

## Conservation and functional domains of PAS kinase

Nutrient sensing protein kinases regulate multiple targets in response to nutrient status, enabling a single enzyme to facilitate the appropriate cellular response. PAS kinase is a member of the group of nutrient sensing protein kinases and contains both a sensory PAS domain and a serine/threonine catalytic kinase domain (10,11). Both the PAS and kinase domains of PAS kinase are highly conserved from yeast to man (10,11), displaying significant amino acid conservation among organisms (Figure 1.1). *Saccharomyces cerevisiae* is the only organism in which two orthologs of PAS kinase have been identified, namely Psk1 and Psk2 (10). Duplications of genes are common in yeast due to a whole-genome duplication that occurred in an early ancestor (12–16). Most duplicate genes were eventually lost, while a few acquired accessory functions that allowed for their selection and maintenance, suggesting differential functions for the Psk1 and Psk2 proteins. Blast alignment of the yeast Psk1 protein with human PASK (hPASK) indicates 27% identity and 56% similarity for the PAS domain and 38% identity and 56% similarity for the kinase domain, arguing the evolutionary importance of these two domains. As the only reported mammalian protein to contain both a sensory PAS and protein kinase domain, it is no surprise that PAS kinase plays a key role in metabolic regulation in response to nutrient status.

The mechanism by which PAS kinase activity is regulated is unknown, but it is likely

through its N-terminal PAS domain. PAS domains often play important roles in mediating protein-protein interactions, signal transfer, and subcellular localization by regulating an attached functional domain (17). They are known to react to a variety of intracellular stimuli including light, oxygen, redox state, or metabolites and can bind small ligands to trigger appropriate downstream responses (18). As expected for a regulatory domain, removal of the hPASK PAS domain increases catalytic activity (10) while addition of purified PAS domain inhibits the activity in trans (10,19). The NMR structure of the hPASK PAS domain is similar to the oxygen sensor FixL (11), which is able to sense oxygen through a heme ligand. Amezcua et al. screened over 750 organic compounds and found that the hPASK PAS domain selectively bound nine related but non-biologically relevant small molecules with high affinity within its hydrophobic core (19). They provide evidence that hPASK PAS domain binds directly to the kinase domain and that ligand binding disrupts this interaction. Together, these results suggest small organic molecules bind to the inhibitory PAS domain, releasing it from the kinase domain. However, the exact biologically relevant ligand is yet to be determined.

The C-terminal end of PAS kinase contains a catalytic serine/threonine kinase domain that belongs to the CAMK family based on both amino acid sequence and protein structure (20). Most protein kinases require phosphorylation of at least one amino acid within the activation loop of their kinase domain to be activated (21). hPASK contains an activation loop threonine (T1116) that is not conserved in yeast (see Figure 1.1). In addition, biochemical assays and crystallographic evidence indicate that activation loop phosphorylation is not necessary for hPASK activation (20). Together this data led to an investigation of the structural features of PAS kinase that enable activation in the absence of activation loop phosphorylation (20). The kinase domain of hPASK adopts the classical two-lobe structure typical of eukaryotic protein

kinases but contains a unique additional β-hairpin replacing part of the αC helix. Other kinases that do not require activation loop phosphorylation typically have a negatively charged or nonpolar residue in their activation loop, whereas hPASK has a phosphorylatable threonine residue. Although not necessary for activation, hPASK autophosphorylation within the activation loop has been shown to increase catalytic activity (10). Hence, activation loop phosphorylation may regulate activity in certain cellular contexts or in response to particular substrates.

These biochemical and structural investigations into the role of the PAS and kinase domains have led to the current model for PAS kinase regulation summarized in Figure 1.2. The PAS domain binds to the kinase domain and inhibits catalytic activity. Under activating conditions, a small metabolite binds to the PAS domain causing a conformational change, releasing PAS domain binding and activating the kinase domain. In addition, autophosphorylation or transphosphorylation of PAS kinase could lead to stable activation by disrupting the PAS and kinase domain interaction.

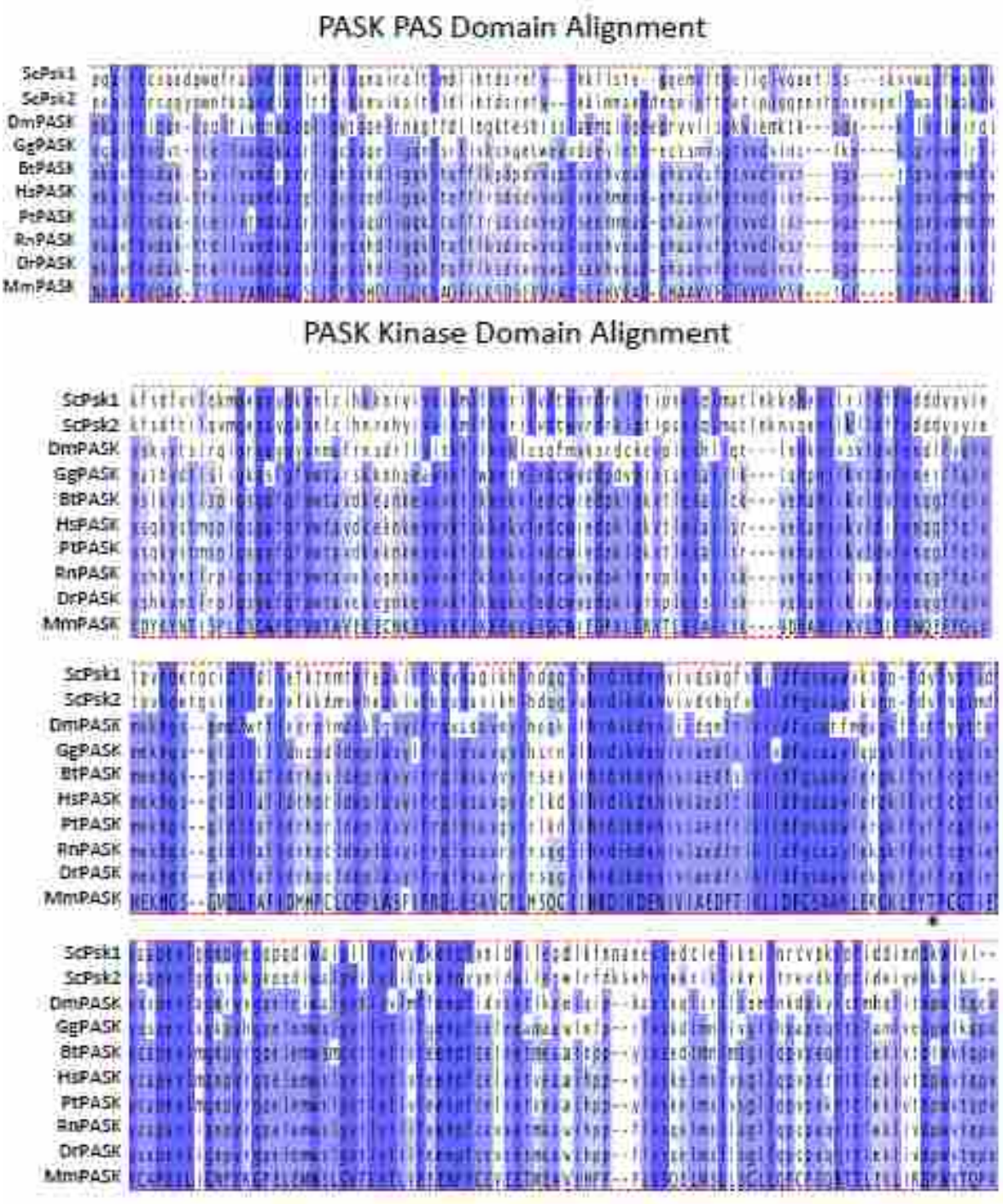


FIGURE 1.1. Alignment of the PAS kinase PAS domain and kinase domain amino acid sequences from various model organisms. The amino acid sequence from *S. cerevisiae* Psk1 (ScPsk1), *S. cerevisiae* Psk2 (ScPsk2), *D. melanogaster* (DmPASK), *G. gallus* (GgPASK), *B. taurus* (BtPASK), *H. sapiens* (HsPASK), *P. troglodytes* (PtPASK), *R. norvegicus* (RtPASK), *D. rerio* (DrPASK), and *M. musculus* (MmPASK) were obtained from GenBank and aligned using the Clustal Omega and Jalview software (49,50). The semiconserved phosphorylation loop threonine is indicated by an asterisk. No discernable PASK homologs were found for the model organisms *A. thaliana*, *O. sativa*, *C. elegans*, or *A. mellifera*. [Color figure can be viewed in the online issue, which is available at wileyonlinelibrary.com.]

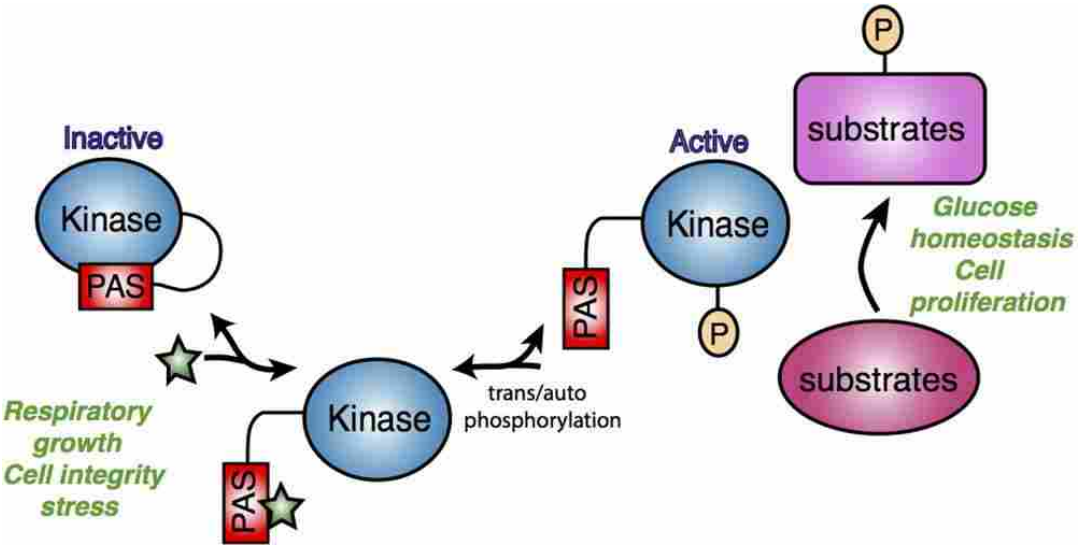


FIGURE 1.2. A current model for PAS kinase regulation and function. The PAS domain binds to and inhibits the kinase domain. Under activating growth conditions, such as growth that stimulates respiration or cell integrity stress, a small metabolite (indicated by the star) may bind the PAS domain, releasing it from the kinase domain. Auto or transphosphorylation may also activate PAS kinase or stabilize transient metabolite activation. PAS kinase then phosphorylates downstream targets to regulate glucose metabolism as well as cell proliferation. [Color figure can be viewed in the online issue, which is available at wileyonlinelibrary.com.]

Activation and regulation of PAS kinase

While the underlying molecular mechanisms behind PAS kinase regulation are yet to be determined, growth conditions that activate both yeast and mammalian PAS kinase have been reported (Table 1.1). In yeast, PAS kinase is activated by two different pathways, the cell integrity stress pathway or the glucose repression pathway (22). Although the precise mechanisms of activation by the cell integrity pathway are unknown, both Psk1 and Psk2 are activated by cell wall or membrane stress as well as overexpression of the cell integrity sensor-transducer *WSC1*. In contrast, only one of the two PAS kinase homologs, Psk1, is activated by the glucose repression pathway. The yeast homolog of (AMP)-activated protein kinase (AMPK), otherwise known as *SNF1*, is the master commander of the glucose repression pathway and controls the shift from fermentation to respiration when glucose levels are low. *SNF1* is

necessary and sufficient for Psk1 activation by non-glucose carbon sources that either require or favor respiration. This activation is both transcriptional as well as post-transcriptional. The second yeast homolog, Psk2, is transcriptionally downregulated and thus inactivated by carbon sources that stimulate respiration, suggesting differential roles for Psk1 and Psk2.

Similar to yeast PAS kinase, hPASK is activated by conditions that stimulate high respiration in Min-6 pancreatic β-cells suggesting a conserved pathway of activation. In contrast to yeast, high glucose levels trigger high respiration rates in these cells, with an increase in both hPASK mRNA and protein (23). Further support is provided in a recent study by Hurtado-Carneiro et al., in which PASK is activated by glucose and glucagon-like peptide-1 (GLP-1), a peptide whose levels increase after a meal to signal nutrient availability to the central nervous system (24). Conversely, hPASK decreased in pancreatic islets of type 2 diabetics where high glucose may be expected (25). These differences could be due to differing genetic backgrounds including the low level of hPASK mRNA in normal tissue verses cell lines (26) or altered hPASK levels in a disease state.

In addition to activation by growth conditions that stimulate respiration, mammalian PASK has been shown to be activated through the binding of different phospholipids (27). Monophosphorylated phosphatidylinositols proved to be the strongest binding phospholipids and caused the highest auto-phosphorylation of PASK. In contrast, diphosphorylated and triphosphorylated phosphatidylinositols inhibited PASK auto-phosphorylation. Also important to note is that rather than binding to the sensory PAS domain, monophosphorylated phosphatidylinositols bind to the kinase domain. These results suggest a multi-ligand regulation of PASK activity through the interaction of phospholipids with the kinase domain and an unidentified metabolite with the PAS domain.

TABLE 1.1. Cellular conditions known to activate PAS kinase in yeast and mammalian cells

| Organism (cells) | Activation pathway | Cellular growth conditions | Genetic modifiers | Study |
|---|---|---|---|---|
| *S. cerevisiae* | Cell integrity stress | CW, CPZ, SDS, high temp (37˚C) | *WSC1*$^{OE}$ | (22) |
| | Glucose repression | Non-glucose carbon sources | *reg1* *snf1* | (22) |
| *M. musculus* (Min-6) | High glucose | High glucose | | (23) |
| hPASK in vitro | Phospholipids | In vitro assay | | (27) |

Calcofluor white (CW) elicits cell wall stress, chlorpromazine (CPZ) elicits cell membrane stress while sodium dodecyl sulfate (SDS) elicits a more general cell stress. Non-glucose carbon sources tested include ethanol, glycerol, galactose, and raffinose. Growth on these non-glucose carbon sources as sole carbon source either requires or favors respiration in yeast, whereas high glucose favors high respiration rates in Min-6 cells. OE stands for overexpression.

## PAS kinase phenotypes and substrates

Since the discovery of PAS kinase in 2001 (10,11) studies in humans, mice, and yeast have been performed to better understand its regulation and function. Both phenotypic analysis (summarized in Table 1.2) and substrate discovery (summarized in Table 1.3) have been used to elucidate its role and cellular importance, however, the underlying molecular mechanisms behind its function are largely unknown.

In humans, a rare mutation in hPASK (hPASK G1117E) may be a genetic modifier of Maturity-Onset Diabetes of the Young (MODY) since it was found in one of eighteen patients with MODY (28). This mutation was found to cause increased basal insulin secretion from pancreatic cells when transfected into mouse islets. In addition, activated hPASK is involved in the regulation of glucose induced preproinsulin and pancreatic duodenum homeobox-1 (PDX1) gene expression, a key transcription factor involved in both pancreatic development and insulin gene expression (23,29). In human islets, overexpression of hPASK also causes an inhibition of glucagon secretion at various glucose concentrations (25). Glucagon is a hormone that is

secreted by the pancreas to stimulate glucose secretion when blood glucose is low. Together these findings suggest that hPASK may play a key role in the pathophysiology of type 2 diabetes.

In addition to the rare hPASK G1117E mutation being associated with diabetes, several PASK-deficiency phenotypes have been associated with symptoms of metabolic syndrome and diabetes in mice (25,30). Initial studies indicate no abnormalities in development, growth, or reproductive functions in PASK knockout mice (26). However, when placed on a high fat diet, PASK knockout mice gain less weight, are hypermetabolic, and display reduced insulin and triglyceride levels when compared to their wild type littermates (30). Furthermore, they are more insulin sensitive and glucose tolerant. Additional studies found increased glucose and glucagon levels following 16 H of fasting, as well as decreased insulin levels in knockout mice (25). Besides these phenotypes associated with diabetes, a recent study showed that female PASK-deficient mice have an increased ventilatory response to acute hypoxia treatment; however, they are unable to reach ventilatory acclimatization after chronic hypoxia exposure (31). A major regulator of glucose consumption is the availability of oxygen, with glucose consumption being higher in hypoxic tissues (32–34). This suggests a potential link between oxygen sensing and PASK, resulting in altered regulation of glucose metabolism.

In addition to knockout phenotypes, the identification of bona fide PAS kinase substrates is critical to understanding its cellular role as well as contribution to metabolic disease. Four mammalian PASK substrates have been reported, namely pancreatic duodenal homeobox-1 (Pdx-1), glycogen synthase (Gsy), eukaryotic translation elongation factor 1A1 (eEF1A1), and ribosomal protein S6 (S6).

The mammalian substrate, Pdx-1, was identified by da Silva et al. as a direct in vitro

substrate for hPASK and there is evidence that hPASK also controls Pdx-1 expression (23,29). Pdx-1 is an essential transcription factor found in β-cells that plays a key role in regulating genes crucial for glucose sensing and insulin gene expression (35). Accordingly, mutations in Pdx-1 have been associated with the development of MODY (36).

Glycogen metabolism is an important process that is tightly regulated to maintain proper glucose and energy homeostasis. PAS kinase has been shown to negatively regulate Gsy, the enzyme responsible for glycogen synthesis, in both yeast (37) and mammals (38). Rutter et al. provided the first evidence by showing direct in vitro phosphorylation of yeast Gsy2, and decreased Gsy activity in vivo (37). Wilson et al. then demonstrated the in vitro phosphorylation of Gsy by mammalian PASK and provided in vivo evidence for its negative regulation (38). Finally, Gsy was identified in a large scale peptide microarray assay for hPASK substrates, along with other proteins central to glycogen metabolism and glycolysis (27). Together, these results provide compelling evidence for conserved PASK-dependent phosphorylation and regulation of Gsy.

The role of PAS kinase in glucose homeostasis is expanded in yeast through its well-characterized substrate Ugp1 (UDP-glucose pyrophosphorylase). Ugp1 is responsible for the production of UDP-glucose, which is the primary glucose donor for most glucose-dependent cellular reactions. In yeast, the two major storage forms of glucose are glycogen and trehalose. Phenotypes associated with PAS kinase deficiency are centered on hyperaccumulation of each of these storage molecules. Surprisingly, PAS kinase-dependent phosphorylation does not affect the enzymatic activity of Ugp1 (39) but rather partitions UDP-glucose to be used towards structural components at the expense of glycogen storage (22). PAS kinase-deficient yeast accumulates excess glycogen in a phospho-Ugp1 dependent manner (37). In addition, they are

unable to grow on non-glucose carbon sources at high temperatures (i.e., Galactose, 39˚C) due to a defect in cell wall structural components (37,39). To determine potential pathways that might be involved with the PAS kinase-deficient growth phenotype, a high-copy suppressor screen was performed (37). A number of different genetic suppressors were found including genes involved in glucose metabolism such as phosphoglucomutase (*PGM1*, *PGM2*) and the glucose derepression gene *SIP1*, as well as genes involved in translational control.

A role for PAS kinase in translational control is also suggested by both mammalian and yeast substrates. Yeast and mammalian two-hybrid screening as well as copurification studies identified translation elongation factor 1 alpha 1 (eEF1A1) as a binding partner of hPASK (40). hPASK phosphorylates eEF1A1, colocalizes in HeLa and sperm cells, and increases translation efficiency. Additionally, Schlafali et al. show ribosomal protein S6 as an in vitro and in vivo target of PAS kinase (27). Finally, several ribosomal proteins appeared to be phosphorylated by PAS kinase in a high throughput screen [website publication only (41)], further substantiating a role of PAS kinase in translational regulation.

*S. cerevisiae* has proved to be a valuable model organism in searching for PAS kinase substrates, providing additional support for the role of PAS kinase in translation. The Caf20, Tif11, and Sro9 proteins, all of which are involved in translational regulation, were shown to be phosphorylated by Psk2 in vitro (37). In addition, when overexpressed, Psk2 is able to rescue growth of a *stm1* mutant, which encodes for translation initiation factor eIF4B (37). The abundance of evidence from both yeast and mammalian studies strongly supports a role for PAS kinase in the regulation of translation.

Besides glucose and translational regulation, recent studies have suggested the involvement of yeast PAS kinase in the Target of Rapamycin TOR2 pathway (42). Tor2 is a

well-studied, essential nutrient responsive protein kinase that regulates growth and cell-cycle dependent polarization of the actin cytoskeleton. A *tor2*$^{ts}$ mutant can be rescued by overexpression of its downstream substrate Rho1, or Rho1 activating GDP/GTP exchange factors such as Rom2 (43). In addition, overexpression of yeast PAS kinase, either Psk1 or Psk2, is also able to suppress the *tor2*$^{ts}$ mutant (42). This suppression is dependent on the phosphorylation of Ugp1, which forms a complex with Rom2. Although the downstream pathways activated through this association are unknown, this suppression of the *tor2*$^{ts}$ mutant supports novel roles for PAS kinase in the regulation of cell proliferation. Previous studies indicate that activation of AMPK or mTOR signaling pathways was not dependent on PASK function in mammalian cells (30). In contrast, recent studies show that knockdown of PASK mRNA impairs AMPK and mTOR/S6K1 response to glucose in neuroblastoma cells (24), supporting an overlap of PASK and TOR function.

Although numerous PAS kinase substrates have been identified, the in vivo effects of phosphorylation of these proteins are largely unknown. In addition, these proteins are not likely to explain the pleiotropic effects seen in PASK-deficient mice, including reduced triglyceride accumulation and weight gain as well as increased metabolism and insulin sensitivity. In looking for a consensus sequence for PAS kinase phosphorylation targets, studies show that hPASK prefers basic residues at the -3 and -5 positions upstream of the serine or threonine phosphoacceptor in substrate peptides (20), and shows a strong preference for arginine at -3 position (20,27). The Ugp1 serine11 phosphorylation site, which is the one bona fide in vivo phosphorylation target of yeast PAS kinase, matches this consensus sequence found for hPASK, providing a basis for predicting in vivo phosphorylation site preferences (20).

TABLE 1.2. Phenotypes associated with PAS kinase in yeast, mice and man

| Organism | Genotype | Growth Conditions | Phenotypes | Study |
|---|---|---|---|---|
| *S. cerevisiae* | *psk1⁻ psk2⁻* | Galactose, 39˚C | Growth inhibition | [37] |
| | | Glucose (log & SP) | Glycogen hyperaccumulation | |
| | | | Trehalose hyperaccumulation | |
| | *psk2⁻* | Galactose, 39˚C | Limited growth | [37] |
| | | Glucose (log & SP) | Intermediate glycogen hyperaccumulation | |
| | | | Intermediate trehalose hyperaccumulation | |
| | *psk1⁻* | Glucose (log & SP) | Intermediate glycogen hyperaccumulation | [37] |
| | | | Intermediate trehalose hyperaccumulation | |
| | $PSK2^{OE}stm1^{-}$ | Glucose, 37˚C | Rescues growth of *stm1⁻* mutant | [37] |
| | $psk2^{-}rom2^{-}$ | Glucose, 37˚C | Exacerbates growth of $rom2^{ts}$ mutant | [22] |
| | $PSK2^{OE}tor2^{ts}$ | Glucose, 37˚C | Overexpression rescues $tor2^{ts}$ | [42] |
| | $PSK2^{OE}UGP1^{OE}$ | Galactose, 37˚C | Overexpression rescues $UGP1^{OE}$ toxicity | [39, 48] |
| *M. musculus* | $pask^{-/-}$ | 16 hour fasting | Increased fasting plasma glucose & glucagon | [25] |
| | | Glucose (10mM) | Impaired inhibition of glucagon secretion | |
| | | Insulin (20mM) | Decreased islet and whole pancreas insulin | |
| | | | Increased glucagon secretion | |
| | $hPASK^{OE}$ | Glucose (1mM) | Inhibited glucagon release in TC1-9 islets | [25] |
| | $pask^{-/-}$ | Glucose (1mM) | Constitutive glucagon release in TC1-9 islets | [25] |
| | $pask^{-/-}$ | Glucose (1mM) | Decreased insulin levels | [30] |
| | | High fat diet (45%) | Glucose tolerant | |
| | | | Insulin sensitive | |
| | | | Less weight gain | |
| | | | Hypermetabolic (higher $O_2$ consumption, $CO_2$ production and heat generation) | |
| | | | Reduced liver triglyceride accumulation | |
| | | | Increased ATP production | |
| | $pask^{-/-}$ | Acute hypoxia | Higher hypoxic ventilatory response | [31] |

| | | | |
|---|---|---|---|
| | hPASK(KD)$^{OE}$ | Decreased intracellular insulin in TC1-9 cells | [25] |
| | hPASK G1117E | Hyperinsulin secretion in CD1 islets | [28] |
| *H. sapiens* | hPASK G1117E | MODY associated | [28] |

Log is log/exponential phase, SP is stationary phase, OE is overexpression and MODY is Maturity-Onset Diabetes of the Young.

TABLE 1.3. Summary of PAS kinase substrates reported from studies of yeast and hPASK

| Organism | Substrate | Evidence | Study |
|---|---|---|---|
| *S. cerevisiae* | Ugp1<br>UDP-glucose Pyrophosphorylase | *In vitro* kinase assay with Psk2<br>PSK-dependent *in vivo* phosphorylation<br>UGP1-S11A mutant mimics *psk1*$^{-}$*psk2*$^{-}$ mutant | [22,37,39] |
| | Caf20<br>Cap Associated Factor | *In vitro* kinase assay with Psk2 | [39] |
| | Tif11 (eIF1A)<br>Translation Initiation Factor | *In vitro* kinase assay with Psk2 | [39] |
| | Sro9<br>Suppressor of Rho3 | *In vitro* kinase assay with Psk2 | [39] |
| | Gsy2<br>Glycogen Synthase | *In vitro* kinase assay with Psk2 | [39] |
| *H. sapiens* | Gsy<br>Glycogen Synthase | *In vitro* kinase assay with hPASK<br>Copurification | [38] |
| | eEF1A1<br>Eukaryotic Translation Elongation Factor | Yeast and mammalian two-hybrid<br>Copurification<br>*In vitro* kinase assay with hPASK<br>Colocalization | [40] |

| | | |
|---|---|---|
| S6<br>Ribosomal Protein S6 | *In vitro* kinase assay with hPASK<br>*In vivo* phosphorylation assay | [27] |
| Pdx-1<br>Pancreatic Duodenal Homeobox-1 | *In vitro* kinase assay with hPASK | [29] |

The protein abbreviation and description are given for each substrate.

## CONCLUSIONS

Nutrient sensing kinases play a critical role in controlling glucose metabolism by simultaneously regulating interrelated metabolic pathways in response to glucose. Three nutrient sensing kinases, AMPK, TOR, and PASK play key roles in proper glucose regulation. AMPK responds to cellular energy levels and upregulates energy producing pathways while inhibiting energy consumption pathways [for a recent review see (44)]. TOR responds to amino acids and other nutrients to regulate growth and proliferation [for a recent review see (45)]. PAS kinase, the focus of this review, is regulated by glucose levels and is necessary for glucose homeostasis. Integration of the AMPK, PASK, and TOR pathways would link cellular energy status with glucose allocation and cell proliferation. Recently, PAS kinase has been shown to integrate with the AMPK and TOR pathways in both yeast and mammalian cells. In yeast, AMPK (*SNF1*) is necessary and sufficient for Psk1 activation (22), and overexpression of either *PSK1* or *PSK2* rescues the $tor2^{ts}$ growth defect (42). In mammalian cells, PAS kinase may integrate with the mTOR pathway through phosphorylation of S6, a target of mTOR (27). The well-studied AMPK and mTOR pathways are primary drug targets for the treatment of diabetes and cancer. Metformin, an AMPK activator, has been the most commonly prescribed drug for the treatment of type 2 diabetes for almost 20 years and is currently in 60 clinical trials for treatment of a wide

variety of cancers [for a recent review see (46)]. mTOR inhibitors have also been shown to be an effective treatment against a wide variety of cancers [for a recent review see (47)]. Since PAS kinase is regulated by AMPK and affects targets downstream of TOR in both yeast and mammalian cells, it may prove to be a valuable nonessential target for the treatment of diabetes and cancer. In support of PAS kinase as a therapeutic target, PAS kinase is implicated in the development of MODY (28), and phenotypes seen in the PASK-deficient mice are directly related to development of obesity, diabetes, and cardiovascular disease (30).

Despite its obvious importance, the molecular mechanisms behind PAS kinase function are largely unknown, with few verified substrates reported. A better understanding of PAS kinase regulation and function will not only increase our understanding of conserved, basic pathways of metabolism, but may lead to novel therapeutic drug targets for the treatment of metabolic disease.

REFERENCES


1. Sciacca L, Vigneri R, Tumminia A, Frasca F, Squatrito S, Frittitta L, Vigneri P: Clinical and molecular mechanisms favoring cancer initiation and progression in diabetic patients. *Nutr Metab Cardiovasc Dis* 2013.

2. Palomer X, Salvado L, Barroso E, Vazquez-Carrera M: An overview of the crosstalk between inflammatory processes and metabolic dysregulation during diabetic cardiomyopathy. *Int J Cardiol* 2013.

3. Van de Voorde J, Pauwels B, Boydens C, Decaluwe K: Adipocytokines in relation to cardiovascular disease. *Metabolism* 2013.

4. Gillies RJ, Robey I, Gatenby RA: Causes and consequences of increased glucose metabolism of cancers. *J Nucl Med* 2008, 49 Suppl 2:24S-42S.

5. Zhu H, Klemic JF, Chang S, Bertone P, Casamayor A, Klemic KG, Smith D, Gerstein M, Reed MA, Snyder M: Analysis of yeast protein kinases using protein chips. *Nat Genet* 2000, 26(3):283-289.

6. Caenepeel S, Charydczak G, Sudarsanam S, Hunter T, Manning G: The mouse kinome: discovery and comparative genomics of all mouse protein kinases. *Proc Natl Acad Sci U S A* 2004, 101(32):11707-11712.

7. Manning G, Whyte DB, Martinez R, Hunter T, Sudarsanam S: The protein kinase complement of the human genome. *Science* 2002, 298(5600):1912-1934.

8. Cohen P: The regulation of protein function by multisite phosphorylation--a 25 year update. *Trends Biochem Sci* 2000, 25(12):596-601.

9. Melnikova I, Golden J: Targeting protein kinases. *Nat Rev Drug Discov* 2004, 3(12):993-994.

10. Rutter J, Michnoff CH, Harper SM, Gardner KH, McKnight SL: PAS kinase: an evolutionarily conserved PAS domain-regulated serine/threonine kinase. *Proc Natl Acad Sci U S A* 2001, 98(16):8991-8996.

11. Hofer T, Spielmann P, Stengel P, Stier B, Katschinski DM, Desbaillets I, Gassmann M, Wenger RH: Mammalian PASKIN, a PAS-serine/threonine kinase related to bacterial oxygen sensors. *Biochem Biophys Res Commun* 2001, 288(4):757-764.

12. Taylor BL, Zhulin IB: PAS domains: internal sensors of oxygen, redox potential, and light. *Microbiol Mol Biol Rev* 1999, 63(2):479-506.

13. Byrne KP, Wolfe KH: Consistent patterns of rate asymmetry and gene loss indicate widespread neofunctionalization of yeast genes after whole-genome duplication. *Genetics* 2007, 175(3):1341-1350.

14. Conant GC, Wolfe KH: Increased glycolytic flux as an outcome of whole-genome duplication in yeast. *Mol Syst Biol* 2007, 3:129.

15. Grassi L, Fusco D, Sellerio A, Cora D, Bassetti B, Caselle M, Lagomarsino MC: Identity and divergence of protein domain architectures after the yeast whole-genome duplication event. *Mol Biosyst* 2010, 6(11):2305-2315.

16. Maclean CJ, Greig D: Reciprocal gene loss following experimental whole-genome duplication causes reproductive isolation in yeast. *Evolution* 2011, 65(4):932-945.

17. Sugino RP, Innan H: Estimating the time to the whole-genome duplication and the duration of concerted evolution via gene conversion in yeast. *Genetics* 2005, 171(1):63-69.

18. Henry JT, Crosson S: Ligand-binding PAS domains in a genomic, cellular, and structural context. *Annu Rev Microbiol* 2011, 65:261-286.

19. Amezcua CA, Harper SM, Rutter J, Gardner KH: Structure and interactions of PAS kinase N-terminal PAS domain: model for intramolecular kinase regulation. *Structure* 2002, 10(10):1349-1361.

20. Kikani CK, Antonysamy SA, Bonanno JB, Romero R, Zhang FF, Russell M, Gheyi T, Iizuka M, Emtage S, Sauder JM *et al*: Structural bases of PAS domain-regulated kinase (PASK) activation in the absence of activation loop phosphorylation. *J Biol Chem* 2010, 285(52):41034-41043.

21. Johnson LN, Noble ME, Owen DJ: Active and inactive protein kinases: structural basis for regulation. *Cell* 1996, 85(2):149-158.

22. Grose JH, Smith TL, Sabic H, Rutter J: Yeast PAS kinase coordinates glucose partitioning in response to metabolic and cell integrity signaling. *EMBO J* 2007, 26(23):4824-4830.

23. da Silva Xavier G, Rutter J, Rutter GA: Involvement of Per-Arnt-Sim (PAS) kinase in the stimulation of preproinsulin and pancreatic duodenum homeobox 1 gene expression by glucose. *Proc Natl Acad Sci U S A* 2004, 101(22):8319-8324.

24. Hurtado-Carneiro V, Roncero I, Blazquez E, Alvarez E, Sanz C: PAS Kinase as a Nutrient Sensor in Neuroblastoma and Hypothalamic Cells Required for the Normal Expression and Activity of Other Cellular Nutrient and Energy Sensors. *Molecular neurobiology* 2013.

25. da Silva Xavier G, Farhan H, Kim H, Caxaria S, Johnson P, Hughes S, Bugliani M, Marselli L, Marchetti P, Birzele F *et al*: Per-arnt-sim (PAS) domain-containing protein kinase is downregulated in human islets in type 2 diabetes and regulates glucagon secretion. *Diabetologia* 2011, 54(4):819-827.

26. Katschinski DM, Marti HH, Wagner KF, Shibata J, Eckhardt K, Martin F, Depping R, Paasch U, Gassmann M, Ledermann B *et al*: Targeted disruption of the mouse PAS domain serine/threonine kinase PASKIN. *Mol Cell Biol* 2003, 23(19):6780-6789.

27. Schlafli P, Troger J, Eckhardt K, Borter E, Spielmann P, Wenger RH: Substrate preference and phosphatidylinositol monophosphate inhibition of the catalytic domain of the Per-Arnt-Sim domain kinase PASKIN. *The FEBS journal* 2011, 278(10):1757-1768.

28. Semplici F, Vaxillaire M, Fogarty S, Semache M, Bonnefond A, Fontes G, Philippe J, Meur G, Diraison F, Sessions RB *et al*: Human mutation within Per-Arnt-Sim (PAS) domain-containing protein kinase (PASK) causes basal insulin hypersecretion. *J Biol Chem* 2011, 286(51):44005-44014.

29. An R, da Silva Xavier G, Hao HX, Semplici F, Rutter J, Rutter GA: Regulation by Per-Arnt-Sim (PAS) kinase of pancreatic duodenal homeobox-1 nuclear import in pancreatic beta-cells. *Biochem Soc Trans* 2006, 34(Pt 5):791-793.

30. Hao HX, Cardon CM, Swiatek W, Cooksey RC, Smith TL, Wilde J, Boudina S, Abel ED, McClain DA, Rutter J: PAS kinase is required for normal cellular energy balance. *Proc Natl Acad Sci U S A* 2007, 104(39):15466-15471.

31. Soliz J, Soulage C, Borter E, van Patot MT, Gassmann M: Ventilatory responses to acute and chronic hypoxia are altered in female but not male Paskin-deficient mice. *Am J Physiol Regul Integr Comp Physiol* 2008, 295(2):R649-658.

32. Krebs HA: The Pasteur effect and the relations between respiration and fermentation. *Essays Biochem* 1972, 8:1-34.

33. Racker E WR: Limiting factors in glycolysis of ascites tumour cells and the pasteur effect. *Regulation of Cell Metabolism* 1958:205-229.

34. Wu R: Regulatory mechanisms in carbohydrate metabolism. V. Limiting factors of glycolysis in HeLa cells. *J Biol Chem* 1959, 234:2806-2810.

35. Boucher MJ, Selander L, Carlsson L, Edlund H: Phosphorylation marks IPF1/PDX1 protein for degradation by glycogen synthase kinase 3-dependent mechanisms. *J Biol Chem* 2006, 281(10):6395-6403.

36. Jonsson J, Carlsson L, Edlund T, Edlund H: Insulin-promoter-factor 1 is required for pancreas development in mice. *Nature* 1994, 371(6498):606-609.

37. Rutter J, Probst BL, McKnight SL: Coordinate regulation of sugar flux and translation by PAS kinase. *Cell* 2002, 111(1):17-28.

38. Wilson WA, Skurat AV, Probst B, de Paoli-Roach A, Roach PJ, Rutter J: Control of mammalian glycogen synthase by PAS kinase. *Proc Natl Acad Sci U S A* 2005, 102(46):16596-16601.

39. Smith TL, Rutter J: Regulation of glucose partitioning by PAS kinase and Ugp1 phosphorylation. *Mol Cell* 2007, 26(4):491-499.

40. Eckhardt K, Troger J, Reissmann J, Katschinski DM, Wagner KF, Stengel P, Paasch U, Hunziker P, Borter E, Barth S *et al*: Male germ cell expression of the PAS domain kinase

PASKIN and its novel target eukaryotic translation elongation factor eEF1A1. *Cell Physiol Biochem* 2007, 20(1-4):227-240.

41. Brandon L. Probst SX, Leeju Wu, Carolyn H. Michnoff, Olga Jetter, Luping Qin, Jared Rutter and Steven L. McKnight: Two Distinct High Throughput Screens of PAS Kinase Yield Convergent Insight to Enzyme Function. http://wwwmcknightlabcom/Documents/publications/PASK_HTSpdf:http://www.mcknightlab.com/Documents/publications/PASK_HTS.pdf.

42. Cardon CM, Beck T, Hall MN, Rutter J: PAS kinase promotes cell survival and growth through activation of Rho1. *Sci Signal* 2012, 5(209):ra9.

43. Schmidt A, Bickle M, Beck T, Hall MN: The yeast phosphatidylinositol kinase homolog TOR2 activates RHO1 and RHO2 via the exchange factor ROM2. *Cell* 1997, 88(4):531-542.

44. Mihaylova MM, Shaw RJ: The AMPK signalling pathway coordinates cell growth, autophagy and metabolism. *Nat Cell Biol* 2011, 13(9):1016-1023.

45. Laplante M, Sabatini DM: mTOR signaling in growth control and disease. *Cell* 2012, 149(2):274-293.

46. Quinn BJ, Kitagawa H, Memmott RM, Gills JJ, Dennis PA: Repositioning metformin for cancer prevention and treatment. *Trends in endocrinology and metabolism: TEM* 2013.

47. Khan KH, Yap TA, Yan L, Cunningham D: Targeting the PI3K-AKT-mTOR signaling network in cancer. *Chin J Cancer* 2013, 32(5):253-265.

# CHAPTER 2: A comprehensive protein-protein interactome for yeast PAS kinase 1 reveals direct inhibition of respiration through the phosphorylation of Cbf1

Desiree DeMille[a], Benjamin T. Bikman[b], Andrew D. Mathis[c], John T. Prince[c], Jordan T. Mackay[a], Steven W. Sowa[a], Tacie D. Hall[a], and Julianne H. Grose[a]

[a]Department of Microbiology and Molecular Biology, [b]Department of Physiology and Developmental Biology, and [c]Department of Chemistry, Brigham Young University, Provo, UT 84602

*Address correspondence to:

Julianne H. Grose
Department of Microbiology and Molecular Biology
Brigham Young University, Provo, UT 84602
E-mail: julianne_grose@byu.edu

ABSTRACT

Per-Arnt-Sim (PAS) kinase is a sensory protein kinase required for glucose homeostasis in yeast, mice, and humans, yet little is known about the molecular mechanisms of its function. Using both yeast two-hybrid and copurification approaches, we identified the protein–protein interactome for yeast PAS kinase 1 (Psk1), revealing 93 novel putative protein binding partners. Several of the Psk1 binding partners expand the role of PAS kinase in glucose homeostasis, including new pathways involved in mitochondrial metabolism. In addition, the interactome suggests novel roles for PAS kinase in cell growth (gene/protein expression, replication/cell division, and protein modification and degradation), vacuole function, and stress tolerance. In vitro kinase studies using a subset of 25 of these binding partners identified Mot3, Zds1, Utr1, and Cbf1 as substrates. Further evidence is provided for the in vivo phosphorylation of Cbf1 at T211/T212 and for the subsequent inhibition of respiration. This respiratory role of PAS kinase is consistent with the reported hypermetabolism of PAS kinase–deficient mice, identifying a possible molecular mechanism and solidifying the evolutionary importance of PAS kinase in the regulation of glucose homeostasis.

## INTRODUCTION

Sensory protein kinases sense the nutrient or stress status of the cell and adjust metabolic processes accordingly. Per-Arnt-Sim (PAS) kinase is a sensory protein kinase with a conserved N-terminal sensory PAS domain and a C-terminal S/T kinase domain required for congruous glucose homeostasis in yeast, mice, and humans (for recent reviews see Hao and Rutter, 2008; Grose and Rutter, 2010; Cardon and Rutter, 2012; DeMille and Grose, 2013). A single point mutation (G1117E) in human PAS kinase has been associated with maturity-onset diabetes of the

young, is seemingly hyperactive, and produces basal insulin hypersecretion when expressed in mouse islets (Semplici et al., 2011). This role of PAS kinase in insulin secretion had been reported in mice, where PAS kinase is essential for glucose-responsive preproinsulin and pancreatic duodenum homeobox 1 gene expression in Min6 cells (da Silva Xavier et al., 2004; Fontes et al., 2009). PAS kinase–deficient mice also display increased insulin sensitivity, as well as resistance to fat and triglyceride accumulation, when placed on a high fat diet (Hao et al., 2007). These mice are hypermetabolic, consuming more oxygen while gaining less weight than their wild type littermates despite the same food intake and physical activity. Yeast PAS kinase also has a conserved role in glucose homeostasis through the phosphorylation of Ugp1, a well-characterized substrate and a key enzyme in glucose allocation (Rutter et al., 2002; Smith and Rutter, 2007; Cardon and Rutter, 2012; Grose et al., 2007). Despite this crucial role of PAS kinase in eukaryotic glucose homeostasis, little is known about the molecular mechanisms of its function, including protein substrates. This lack of understanding is predominately due to the difficulty in elucidating protein kinase function.

Protein kinases play critical roles in disease development due to their ability to simultaneously regulate multiple interrelated pathways (recent reviews include Eglen and Reisine, 2011; Zhang and Daly, 2012; Fang et al., 2013; Gallinetti et al., 2013; Lal et al., 2013), yet they are difficult to study. This difficulty is primarily due to the abundance of eukaryotic protein kinases and their multiple and overlapping targets, with hundreds of protein kinases that phosphorylate >50% of the proteome, often at multiple sites within a single protein (Johnson and Hunter, 2005; Sopko and Andrews, 2008; Mok et al., 2011; Knight et al., 2012; Graves et al., 2013). This overlapping function makes it difficult to perturb a single kinase due to cellular feedback mechanisms. A fruitful method for identifying protein kinase substrates is to identify

direct protein–protein interactions (Johnson and Hunter, 2005). The two widespread approaches for identifying protein binding partners are the yeast two-hybrid (Y2H; Fields and Song, 1989) and copurification followed by quantitative mass spectrometry (Jessulat et al., 2011; Dunham et al., 2012; Kean et al., 2012; Marcilla and Albar, 2013).

The first protein–protein interactome for PAS kinase is reported here, obtained through both comprehensive Y2H and copurification approaches. The 93 identified putative binding partners support and expand the role of PAS kinase in glucose homeostasis, including new pathways involved in mitochondrial metabolism. The relevance of our interactome is demonstrated through in vitro kinase assays using 25 identified putative binding partners. In addition, in vivo evidence is provided for the PAS kinase 1 (Psk1)–dependent phosphorylation and inhibition of Cbf1, a novel substrate involved in the regulation of mitochondrial respiration. These results are consistent with yeast PAS kinase partitioning glucose away from respiration and may explain the mechanism by which PAS kinase–deficient mice display a hypermetabolic phenotype.

## RESULTS

### Identification of ΔN692Psk1, a construct with increased protein-binding proficiency

Initial Y2H screens employing full-length yeast Psk1 as bait yielded only false positive hits despite it being a functional construct (functionality of the bait was verified by its ability to rescue Ugp1 toxicity, as previously described; Grose et al., 2009). This difficulty in detecting binding partners is consistent with the classic notion that kinase/substrate interactions are transient, making them difficult to detect by conventional protein–protein interaction screens. To identify Psk1 constructs with increased protein–protein interaction capabilities, Y2H screens

were conducted using various Psk1 truncations as bait (Figure 2.1A) and a genomic library as prey (pJG428; James et al., 1996). These Psk1 truncations were previously isolated from a screen for hyperactive mutants that suppress Ugp1 toxicity (Grose et al., 2009), and all corresponding bait constructs were verified as functional by this same assay. One truncation, beginning at amino acid 693 (ΔN692Psk1), yielded multiple true positive hits from the Y2H screen, suggesting enhanced binding proficiency (Figure 2.1B). These hits were tested against the full-length protein and showed very weak but reproducible growth above background, suggesting the ΔN692Psk1 construct increased the strength of the Y2H interactions. The bona fide Psk1 substrate Ugp1 was not used as prey because epitope tags are known to destroy the ability of Psk1 to phosphorylate Ugp1 (Smith and Rutter, 2007).

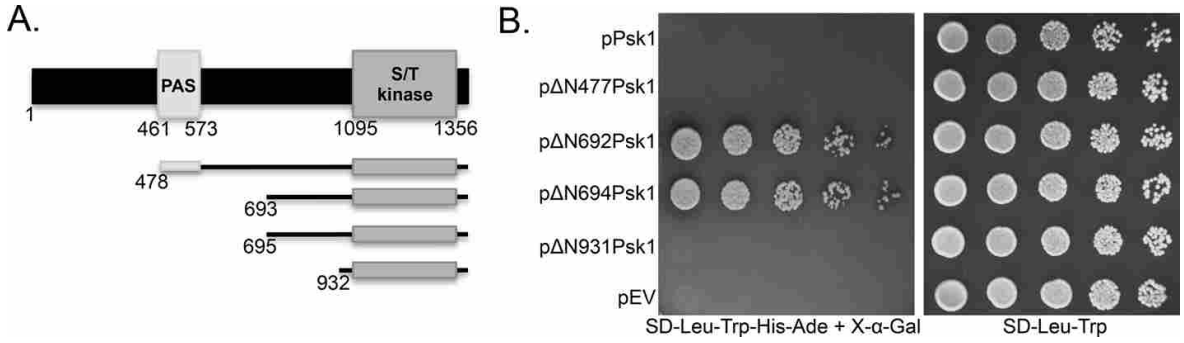


FIGURE 2.1. A Psk1 Y2H construct with increased protein–protein interaction proficiency. (A) A diagram of previously isolated hyperactive truncations of Psk1 (Grose et al., 2009) that were screened for their ability to bind protein partners in a Y2H screen. (B) The relative Y2H interaction strength of each Psk1 truncation is shown using Pbp1, a Psk1 binding partner identified in this study by both Y2H and copurification approaches. Y2HGold cells (Clontech) containing the Pbp1 prey (pJG1001) were cotransformed with bait plasmids harboring full-length Psk1 (pJG441), truncated Psk1 (pΔN477Psk1 [pJG1005], pΔN692Psk1 [pJG598], pΔN694Psk1 [pJG1006], pΔN931Psk1 [pJG568]) or empty vector (pJG425). Overnights were grown in SD-Leu-Trp for plasmid maintenance, diluted fivefold serially, and plated on Y2H selective media (SD-Leu-Trp-His-Ade + X-α-Gal), as well as a control plate (SD-Leu-Trp). Plates were incubated at 30°C for 3–4 d until colonies were apparent. The Y2H Gold strain contains four reporters under the control of three different Gal4-responsive promoters (Clontech), allowing selection for histidine (His) or adenine (Ade) biosynthesis, as well as blue colony formation on media containing X-α-Gal.

PAS kinase binding partners identified through Y2H and copurification

The Psk1 truncation ΔN692Psk1 was then used to perform large-scale Y2H screens for Psk1 binding partners. Advantages of the Y2H approach include the identification of direct protein–protein interactions and sensitivity due to transcriptional amplification of an interaction. This sensitivity may be particularly useful when studying protein kinases due to transient interactions with substrates; however, the yeast two-hybrid can also yield false positives that allow growth independent of the bait. To minimize false positives, the Y2HGold strain was used, which harbors four different reporters controlled by three different GAL4-responsive promoters (Clontech Matchmaker Gold Yeast Two-hybrid System). Y2H screens were conducted with three yeast genomic libraries (James et al., 1996) and two cDNA libraries (this study). From ~40 million transformants or matings screened (Table 2.1), 28 Psk1 binding partners were identified (Table 2.2). Each of these binding partners was verified by purifying the prey plasmid from yeast and retransforming into naive Y2HGold along with the ΔN692Psk1 bait or an empty bait plasmid. Remarkably, 100% of the binding partners were dependent on the Psk1 plasmid and were thus true positives in the Y2H assay.

An alternative sensitive and reliable approach for identifying protein binding partners is copurification followed by quantitative mass spectrometry (MS). Full-length Psk1 fused with histidine (HIS), Myc, or FLAG epitopes was affinity purified in triplicate, and samples were subjected to quantitative liquid chromatography (LC)–tandem MS. Sixty-seven putative binding partners were identified for Psk1 (Table 2.3). Most of the reported proteins were only present in the Psk1 samples, not the empty vector control, and were identified in at least two of three independent replicates. For abundant proteins found in both samples, the cutoff was set at ≥ 3.4x the protein score in the Psk1 sample. For the HIS-epitope purifications, the ΔN692Psk1

construct was also used. Remarkably, 85% of the full-length or ΔN692Psk1 binding partners retrieved in the HIS-tag purifications were also identified with significance in at least one of the samples of the alternate construct, suggesting that the truncated form of Psk1 behaves similar to wild type and was only necessary in the Y2H screen. This could be due to differences in sensitivity or alternate folding of the Y2H fusion construct. A majority of the proteins in Table 2.3 were obtained from the HIS purifications. This is likely due to the increased expression of the HIS construct in yeast when compared with the FLAG or Myc constructs (unpublished data), as well as the six replicates (three for full-length and three for truncated Psk1) compared with three for FLAG or Myc. PAS kinase 2 (Psk2), a Psk1 homolog arising from whole-genome duplication, was the only protein that was retrieved from more than one of the copurification approaches. It is common, however, to retrieve different proteins when using different epitopes due to differences in purification methods and/or epitope effects on the fusion protein (Breitkreutz et al., 2010). This interaction suggests that Psk1/Psk2 heterodimers exist within the cell and is consistent with the tendency for kinases to dimerize (Endicott et al., 2012).

The Y2H screen retrieved all novel binding partners, whereas the copurification screens retrieved both expected and novel binding partners. The copurification screen retrieved several proteins known to regulate PAS kinase or interact with Ugp1, the only well-characterized Psk1 substrate. The Snf1 protein kinase, master commander of the shift from respiration to fermentation in yeast (for recent reviews see Hardie, 2007; Hedbacker and Carlson, 2008), and its β subunits Gal83 and Sip2 were all identified with significance in both the HIS-tagged full-length and ΔN692Psk1 samples. The Snf1 protein kinase is necessary and sufficient for Psk1 activation by carbon sources that stimulate respiration (Grose et al., 2007). We recently validated this direct interaction between Psk1 and Gal83 via the yeast two-hybrid (unpublished

data). The Ssd1 protein was also identified in both the HIS-tagged full-length and ΔN692Psk1 samples and was recently shown to interact with phosphorylated Ugp1 (Cardon and Rutter, 2012).

Only two of the putative Psk1 binding partners were identified in both screens (Pbp1 and Prb1). This incongruous result is not surprising, given the diverse strengths of each approach, as previously reported (Rajagopala et al., 2012). Copurification is likely to yield larger protein complexes, whereas the Y2H primarily identifies direct protein–protein interactions. Neither the Y2H or copurification screens identified Ugp1, the well-characterized PAS kinase substrate. For the Y2H, this may be explained by the inability of PAS kinase to phosphorylate epitope-tagged Ugp1 (Smith and Rutter, 2007). For the copurification screen, Ugp1 was abundant in all of the samples (both the Psk1 samples and the control) due to its high abundance in the cell and did not pass our stringent cutoff. In addition to the proteins reported in Table 2.3, all Psk1 copurification constructs retrieved various ribosomal proteins (see the footnote to Table 2.3). This may also be due to the high expression of ribosomal proteins in yeast cells. Further work is needed to verify these putative binding partners.

TABLE 2.1. Libraries screened in the yeast two-hybrid

| Library name | Library type | Number of matings/transformants |
|---|---|---|
| pJG427 | Genomic library cloned into pGAD-C1 reading frame | 4,825,880 |
| pJG428 | Genomic library cloned into pGAD-C2 reading frame | 2,071,560 |
| pJG429 | Genomic library cloned into pGAD-C3 reading frame | 7,461,150 |
| pJG1074 | cDNA isolated from stationary-phase yeast and cloned into pGADT7 | 24,000,000 |
| pJG1098 | cDNA isolated from exponential-phase yeast and cloned into pGADT7 | 2,000,000 |
| Total | | 40,358,590 |

The genomic libraries were a generous gift from David Stillman, University of Utah, and James et al. (1996), and cDNA libraries were prepared for this study using Clontech's Make Your Own "Mate & Plate" Library System. The mRNA from yeast grown to either stationary phase or exponential phase was isolated (RNeasy Mini Kit; Qiagen). Y2H Gold cells (Clontech) containing pJG598 were mated with yeast containing cDNA libraries (JGY1074 or JGY1098) or transformed with genomic libraries (pJG427, pJG428, and pJG429). Cells were plated on SD-Leu-Trp-His-Ade or SGal-Leu-Trp-His-Ade to select for yeast two-hybrid protein-protein interactions.

TABLE 2.2. Psk1 binding partners identified by the yeast two-hybrid.

| Gene | Human Homolog | Name Description | Loc | # hits | Gen/ cDNA | G/D | Construct (total # of aa) | G |
|---|---|---|---|---|---|---|---|---|
| GLUCOSE METABOLISM | | | | | | | | |
| KRE6 | | Killer toxin REsistant | C/V/ER | 1 | Gen | G | aa300-550 (720) | M |
| MTH1 | | MSN Three Homolog | C | 1 | Gen | G | aa1-433 (433) | S |
| STD1 | PSMD8[1] | Suppressor of Tbp Deletion | C | 1 | Gen | G | aa124-444 (444) | M |
| YAP6 | | Yeast homolog of AP-1 | C | 14 | Gen | G/D | aa41-383 (383) | S |
| GENE/PROTEIN EXPRESSION | | | | | | | | |
| CBF1 | USF1[1] | Centromere Binding Factor | C/N/M | 3 | Gen | G | aa202-351 (351) | M |
| GCD14 | TRMT61A[2] | General Control Nonderepressible | C/N | 2 | cDNA | D | aa152-383 (383) | S |
| HAP2 | NFYA[1] | Heme Activator Protein | C/N | 2 | cDNA | D | aa56-249 (265) | M |
| IES6 | | Ino Eighty Subunit | N | 108 | cDNA | D | aa1-166 (166) | S |
| MOT3 | PLAGL1[3] | Modifier of Transcription | C/N | 1 | Gen | G | aa311-490 (490) | S |
| NOB1 | NOB1[2] | Nin1(One) Binding protein | C/N | 1 | cDNA | D | aa230-459 (459) | S |
| PBP1 | ATXN2[1] | Pab1p-Binding Protein | C/N/M | 44 | Gen | D | aa356-,197-722 (722) | S |
| PMD1 | | Paralog of MDS3 | C | 2 | Both | D | aa1482-1753 (1753) | S |
| SAP30 | NCOR2[3] | SIT4 protein phosphatase Associated Protein | N | 1 | cDNA | D | aa110-201 (201) | S |
| SIR4 | NOLC1[1] | Silent Information Regulator | C/N | 4 | Gen | G | aa1094-1358 (1358) | M |
| SSN2 | | Suppressor of SNf1 | C/N | 8 | Both | G/D | aa504-703 (1420) | S |
| TOM1 | WWP1[1] | Temp. Organization in Mitotic nucleus | N | 4 | Gen | G/D | aa2055-2459 (3268) | M |

| | | | | | | | | |
|---|---|---|---|---|---|---|---|---|
| REPLICATION/CELL DIVISION | | | | | | | | |
| FOB1 | | FOrk Blocking less | C/N | 11 | Gen | D | aa3-421 (566) | M |
| IBD2 | | Inhibition of Bud Division 2 | C | 50 | Gen | G/D | aa106-,183-351 (351) | M |
| ZDS1 | | Zillion Different Screens | C | 2 | Gen | G | aa795-915 (915) | S |
| ZDS2 | | Zillion Different Screens | C/N | 6 | Gen | G | aa692-,516-942 (942) | S |
| AMINO ACID BIOSYNTHESIS/CATABOLISM | | | | | | | | |
| CYS3 | CTH[2] | CYStathionine gamma-lyase | C | 6 | cDNA | D | aa169-394 (394) | S |
| LYS14 | MBD6[1] | LYSine requiring | C/N | 1 | Gen | D | aa179-790 (790) | M |
| PROTEIN/RNA DEGRADATION | | | | | | | | |
| PRB1 | PCSK9[1] | PRoteinase B | C | 3 | Gen | G/D | aa80-249 (635) | S |
| RPM2 | | RNase P Mitochondrial | M | 2 | cDNA | D | aa740-1202 (1202) | W |
| MITOCHONDRIAL FUNCTION | | | | | | | | |
| NFS1 | NFS1[2] | NiFS-like cysteine desulfurase | M | 7 | Gen | D | aa20-,70-497 (497) | S |
| UNKNOWN | | | | | | | | |
| YFR006W | PEPD[2] | | C | 1 | cDNA | D | aa47-186 (535) | S |
| YIL108W | | | C | 9 | Gen | D | aa3-498 (696) | M |
| YNL144C | | | M | 2 | Gen | G/D | aa1-600 (740) | M |

Y2H Gold cells (Clontech) containing pJG598 (ΔN692Psk1 fused to the GAL4 BD) were mated with cDNA libraries produced with Clontech's Make Your Own "Mate & Plate" Library System (JGY1074 or JGY1098) or transformed with genomic libraries (pJG427, pJG428, and pJG429; James et al., 1996). Cells were plated on SD-Leu-Trp-His-Ade or SGal-Leu-Trp-His-Ade to select for yeast two-hybrid protein–protein interactions. Plasmids were purified from colonies that arose, sequenced, and verified as true positives by transforming back into naive Y2H Gold cells containing the bait (pJG598) or empty bait plasmid (pJG425) and then restreaking on yeast two-hybrid selective media. Columns indicate the gene symbol, human homolog (where applicable, and database retrieved from [1]MIT Isobase, [2]NCBI HomoloGene, [3]NCBI Blast), gene name description, cellular localization (from the Saccharomyces Genome Database and FunSpec), number of times the protein was retrieved from the screen, the prey library used in the screen (Genomic [Gen] or cDNA library), the carbon source used (either galactose [G] or dextrose [D]), the amino acids present in the prey construct, with the total known amino acids for the protein given in parentheses, and the strength of growth, which is an indication of the interaction strength (S, strong; M, medium; W, weak). For localization, C corresponds to cytoplasm, M to mitochondrion, N to nucleus, ER to endoplasmic reticulum, and V to vacuole.

TABLE 2.3. Psk1 binding partners identified by copurification, followed by quantitative mass spectrometry

| Gene | Human Homolog | Name Description | Loc | In Psk1 only | Psk1/ EV Ratio | In ΔN692 only | ΔN692/ EV Ratio |
|---|---|---|---|---|---|---|---|
| GLUCOSE METABOLISM | | | | | | | |
| GAL2 | SLC2A10[1] | GALactose metabolism | C | 1 | | 2 | |
| GAL83 | PRKAB2[3] | GALactose metabolism | C | 2 | | 2 | |
| GLK1 | IGFBP4[1] | GLucoKinase | C | 1 | | 2 | |
| GND1 | PGD[1] | 6-phosphogluconate dehydrogenase | C/N/M | 2 | | 1 | |
| HXK2 | HK1[2] | HeXoKinase | C | 1 | | 2 | |
| PSK2 | PASK[1] | PAS kinase 2 | C/M | 3,2[#] | | 2 | |
| SIP2 | PRKAB2[2] | Snf1-Interacting Protein | C/PM | 1 | 5.2 | | 4.6 |
| SNF1 | PRKAA2[2] | Sucrose NonFermenting | C/M | | 5.1, 5.2 | | 3.8 |
| TDH2 | GAPDH[2] | Triose-phosphate DeHydrogenase | C/N/W | 2[†] | | | |
| TDH3 | GAPDH[2] | Triose-phosphate DeHydrogenase | C/N/W | 2[†] | | | |
| GENE/PROTEIN EXPRESSION | | | | | | | |
| ABF1 | | ARS-Binding Factor 1 | C/N | 1 | 5.9, 4.7 | | |
| BMH1 | YWHAZ[1] | Brain Modulosignalin Homolog | C | 3 | | 1 | |
| BMH2 | YWHAE[1] | Brain Modulosignalin Homolog | C/N | 3 | | 1 | |
| EAF6 | MED15[1] | Esa1p-Associated Factor | C/N | 1 | | 2 | |
| EFT1 | EEF2[2] | Elongation Factor Two | C | 1 | | 2 | |
| EFT2 | EEF2[2] | Elongation Factor Two | C | 1 | | 2 | |
| HUB1 | UBL5[1] | Homologous to UBiquitin | C | 2 | | | |
| INO2 | | INOsitol requiring | N | 1 | | 2 | |
| LSM12 | LSM12[1] | Like SM | C/N | 2 | | 1 | |

| | | | | | | | |
|---|---|---|---|---|---|---|---|
| PAB1 | PABPC1[2] | Poly(A) Binding protein | C | 2 | | | |
| PBP1 | ATXN2[1] | Pab1p-Binding Protein | C/N/M | 1 | 4.3 | | 3.4, 3.7 |
| SSD1 | DIS3[1] | Suppressor of SIT4 Deletion | C/N | 2 | 5.97 | 1 | 5.3 |
| SSZ1 | HSPA8[3] | Hsp70 protein | C | 1 | | 2 | |
| TEF1 | EEF1A1[1] | Translation Elongation Factor | C | 2[†] | | | |
| VTS1 | SAMD4A[1] | VTi1-2 Suppressor | C | 2 | | | |
| | | REPLICATION/CELL DIVISION | | | | | |
| CDC33 | EIF4E[1] | Cell Division Cycle | C | | 4.2, 26.6 | | 22.72 |
| MYO1 | MYH11[1], MYH9[2] | MYOsin | C/B | 1 | | 2 | |
| NUM1 | | NUclear Migration | B/M | 3 | | 2 | |
| TUB2 | TUBB[2] | TUBulin | C | 1 | | 2 | |
| | | AMINO ACID BIOSYNTHESIS/CATABOLISM | | | | | |
| ASN2 | ASNS[1] | ASparagiNe requiring | C | 1 | | 2 | |
| CAR2 | OAT[2] | Catabolism of Arginine | C/N | 2 | | 2 | |
| GAD1 | SGPL1[1] | GlutAmate Decarboxylase | C | 2 | | 1 | |
| ILV1 | SRR[1] | IsoLeucine-plus-Valine requiring | M | 1 | | 2 | |
| | | PROTEIN/RNA DEGRADATION | | | | | |
| DPM1 | DPM1[1] | Dolichol Phosphate Mannose synthase | ER/M | 1 | | 2 | |
| HSP82 | HSP90AA1[2] | Heat Shock Protein 90 | C/N | 1 | | 2 | |
| HTZ1 | H2AFV[2] | Histone Two A Z1 | N | 2 | | 1 | |
| LCL2 | | Long Chronological Lifespan 2 | C | | | 2 | |
| PRB1 | PCSK9[1] | PROteinase B | C | 1 | 6.0, 8.7 | 1 | 6.4 |
| YDJ1 | DNAJA1[1], DNAJA2[2] | Yeast dnaJ | C/N | 1 | | 2 | |
| | | MITOCHONDRIAL FUNCTION | | | | | |
| AIM32 | | Altered Inheritance rate of Mitochondria | C/M | 2 | | 1 | |
| ATP1 | ATP5A1[2] | ATP synthase | C/M | 1 | | 2 | |
| ATP2 | ATP5B[2] | ATP synthase | M | 2 | | 1 | |
| COQ4 | COQ4[2] | COenzyme Q | C/M | 1 | | 2 | |
| MIR1 | SLC25A3[1] | Mitochondrial phosphate carrier | M | 2 | | 1 | |
| MMT2 | SLC30A9[1] | Mitochondrial Metal Transporter | C/M | | | 2 | |
| MRM1 | MRM1[2] | Mitochondrial rRNA Methyltransferase | M | 1 | | 2 | |
| QCR6 | | ubiQuinol-cytochrome C oxidoReductase | C/M | | | 2 | |
| | | STRESS TOLERANCE | | | | | |
| AHP1 | PRDX5[1] | Alkyl HydroPeroxide reductase | C/N | 2 | | 3 | |
| DLD3 | D2HGDH[1] | D-Lactate Dehydrogenase | C/N | 1 | | 2 | |
| IPP1 | PPA1[1], PPA2[2] | Inorganic PyroPhosphatase | C/N | 2 | | 2 | |
| NST1 | STIM1[1] | Negatively affects Salt Tolerance | C | 1 | | 2 | |
| TPS3 | | Trehalose-6-Phosphate Synthase | C | 1 | | 2 | |
| UTH1 | | yoUTH | V | 1 | | 2 | |
| YHB1 | NGB[1] | Yeast HemogloBin-like Protein | C/M | 1 | | 2 | |
| | | STEROL METABOLISM | | | | | |
| ERG9 | FDFT1[2] | ERGosterol biosynthesis | C/ER | 1 | | 2 | |
| OSH7 | OSBPL8[2], OSBPL9[1] | OxySterol binding protein Homolog | C/N/M | 1 | | 2 | |
| | | NUCLEOTIDE BIOSYNTHESIS | | | | | |
| IRA1 | NF1[1] | Inhibitory Regulator of RAS-cAMP pathway | C/M | 2 | | 1 | |
| IRA2 | NF1[1] | Inhibitory Regulator of RAS-cAMP pathway | C/M | 1 | 4.8 | | 4.0, 4.9 |
| URA2 | CAD[1] | URAcil requiring | C/M | 2 | | 2 | |
| UTR1 | NADK[3] | Unidentified TRanscript(NAD kinase) | C/N | 2 | | 1 | |
| | | PROTEIN TRANSPORT/MODIFICATION | | | | | |
| BUL1 | | Binds Ubiquitin Ligase | C | 1 | | 2 | |
| CPR5 | PPIB[2] | Cyclosporin-sensitive Proline Rotamase | C/V | | | 2 | |
| GVP36 | | Golgi Vesicle Protein | C | 1 | | 2 | |
| PPH21 | PPP2CA[2] | Protein PHosphatase 21 | C/N | 1 | | 2 | |
| | | VACUOLAR FUNCTION | | | | | |
| VMA1 | ATP6V1A[2] | Vacuolar Membrane Atpase | C/V | 1 | | 2 | |
| VNX1 | | Vacuolar Na+/H+ eXchanger | C/ER | 1 | | 2 | |
| | | UNKNOWN | | | | | |
| JIP4 | | Jumonji domain Interacting Protein | M | 1 | | 2 | |

HIS-tagged full-length (pJG858) or ΔN692Psk1 (pJG960), as well as full-length FLAG (pJG1217) and Myc-tagged Psk1 (pJG1181), were purified in triplicate and associated proteins analyzed by quantitative mass spectrometry. Most of the reported proteins were only present in the Psk1 samples, not the empty vector control, and were identified in at least two of three independent replicates. For abundant proteins found in both samples, the cutoff was set at ≥ 3.4 times the protein score in the Psk1 sample. Columns indicate the gene symbol, human homolog (database retrieved from [1]MIT Isobase, [2]NCBI HomoloGene, or [3]NCBI Blast), gene name description, cellular localization (from the Saccharomyces Genome Database

and FunSpec), number of times the protein was retrieved from the full-length Psk1 sample but not the control, ratio of protein in the full-length HIS-, Myc-, or FLAG-tagged Psk1 compared with control, number of times retrieved from the HIS-tagged ΔN692Psk1 sample but not the control, and the ratio of protein in the ΔN692Psk1 sample compared with control. Proteins retrieved from each purification are either unmarked (HIS), or marked with # (Myc) or † (FLAG). EV, empty vector. For localization: C, cytoplasm; M, mitochondrion; N, nucleus; ER, endoplasmic reticulum; PM, plasma membrane; W, cell wall; V, vacuole; B, Bud. Several ribosomal proteins were also identified in both full-length and ΔN692Psk1 and not in the EV; however, they are excluded from the list due to their high abundance in the cell, which makes them likely false positives (RPL10, RPL15A, RPL15B, RPL1A, RPL1B, RPL29, RPL7A, RPL7B, RPP0, RPS17A, RPS17B, RPS18A, RPS18B, RPS19A, RPS19B, RPS24A, RPS3, and RPS7A).

Validation of the Psk1 interactome through in vitro kinase assays

The Psk1 interactome may include Psk1 substrates, proteins that regulate Psk1 activity, or proteins present in a larger complex. To identify novel Psk1 substrates, 25 random putative binding partners were expressed in bacteria, purified, and evaluated by in vitro kinase assays with radiolabeled ATP (Figure 2.2). Thirty-eight putative Psk1 binding partners were randomly chosen for this analysis; however, 13 did not express well for purification.

Psk1 directly phosphorylated Cbf1, Mot3, Osh7, Zds1, and Utr1 (Figure 2.2A). The phosphorylation of Mot3 was faint, so we purified the truncated, hyperactive Psk1 and verified phosphorylation (Figure 2.2B). Other binding partners were also assayed using this truncation but were not phosphorylated (unpublished data), suggesting that the truncated kinase is specific for its substrates.

To show Psk1 dependence and rule out contaminating kinases, a kinase-dead mutant of Psk1 (D1230A) was designed and constructed. This mutation is predicted to abolish the terminal hydrogen–accepting aspartic acid in the canonical kinase domain from sequence alignment with PKA (Taylor et al., 2004). The D1230A mutant expressed well and displayed no detectable kinase activity, as assessed by both in vitro kinase assays using Ugp1 (Figure 2.2C) and in vivo activity assays (Grose et al., 2009) for suppression of Ugp1 toxicity (unpublished data). Four of

the five in vitro substrates (Cbf1, Mot3, Zds1, and Utr1) were Psk1 dependent (Figure 2.2C). Osh7 was phosphorylated by both wild type and kinase-dead constructs, suggesting a contaminating kinase activity that masks Psk1 activity.

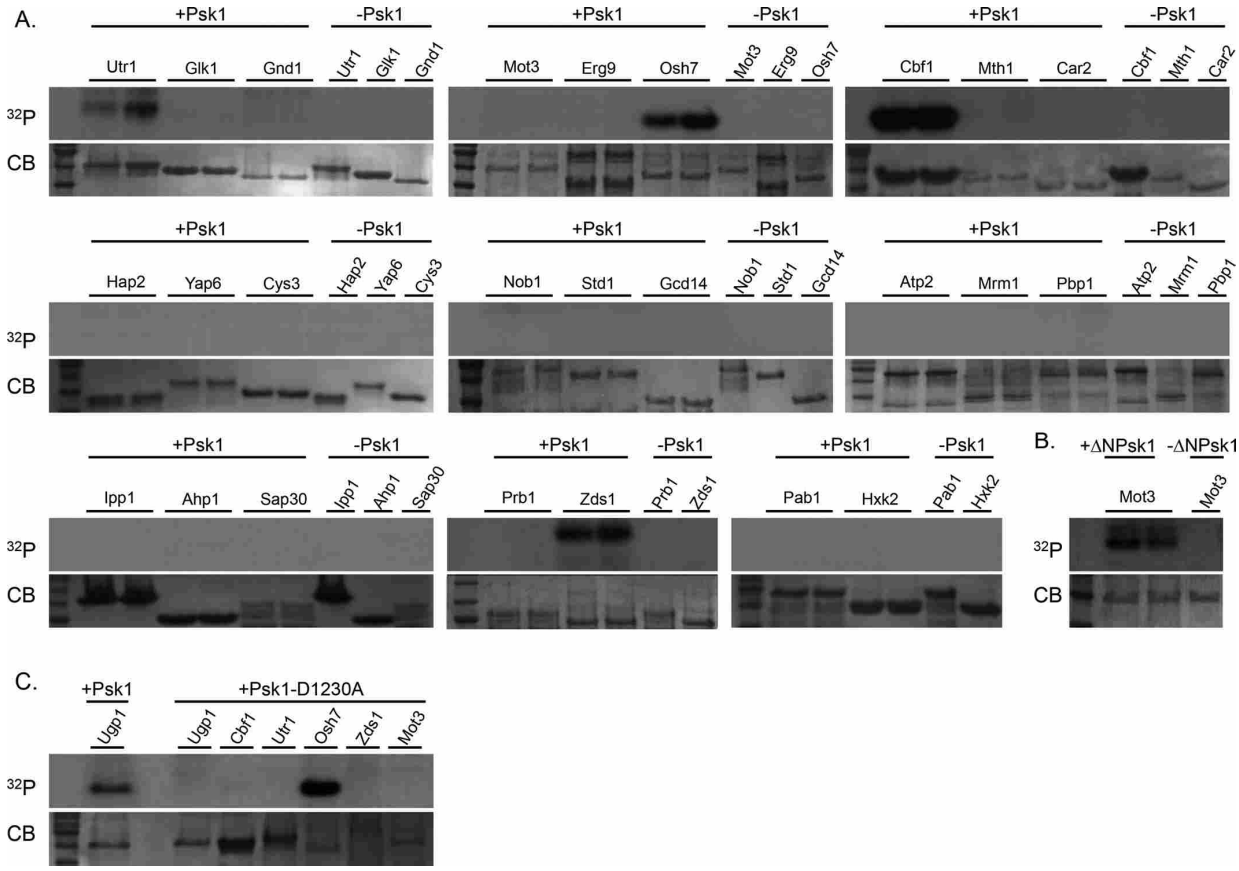


FIGURE 2.2. Evidence for in vitro phosphorylation of Psk1 binding partners. A subset of 25 Psk1 binding partners was expressed and purified from *E. coli* BL21 cells and then assayed for in vitro phosphorylation by Psk1. (A) Utr1, Osh7, Cbf1, and Zds1 were shown to be phosphorylated by Psk1 in vitro. (B) Mot3 displayed faint bands with full-length Psk1 and was confirmed as an in vitro Psk1 substrate using a hyperactive Psk1 truncation (ΔN931Psk1). (C) Cbf1, Utr1, Zds1, and Mot3 were verified as Psk1 substrates using a kinase-dead mutant (Psk1-D1230A). For kinase assays, purified proteins were incubated with radiolabeled ATP ($^{32}$P) in the presence or absence of purified Psk1. Kinase reactions were visualized on 8 or 12% SDS–PAGE gels, stained with Coomassie brilliant blue (CB), and exposed on x-ray film.

## Bioinformatic analysis of the Psk1 interactome revealed both known and novel functions

FunSpec (Robinson et al., 2002) was used to reveal the basic processes of Psk1 function.

FunSpec determines the number of proteins within a set that belong to each Gene Ontology (GO) process and calculates the probability of these proteins being co-identified, given a random pool of the yeast gene products. Thirty-one different GO processes were significantly enriched ($p < 0.05$) in our interactome (Figure 2.3A). These processes identified pathways that regulate Psk1, as well as pathways in which Psk1 is likely to function. The most significant process enriched includes the Snf1 kinase, which was been mentioned earlier in this article as necessary and sufficient for Psk1 activation (Grose et al., 2007). In fact, the Snf1 kinase (or subunits Gal83 and Sip2) are found in five of the enriched GO processes: signal transduction ($p = 7.256e^{-06}$), replicative cell aging ($p = 2.081e^{-03}$), cell adhesion ($p = 3.936e^{-03}$), the regulation of complex formation ($p = 3.936e^{-03}$), and the negative regulation of translation ($p = 8.206e^{-03}$). The related processes of glucose metabolism ($p = 1.37e^{-05}$, including the GLK1, HXK2, TDH2, TDH3, and STD1 proteins), glycolysis ($p = 5.829e^{-04}$, including the GLK1, HXK2, TDH2, and TDH3 proteins), and glucose import ($p = 5.834e^{-04}$, including the GLK1 and HXK2 proteins) were all enriched due to these related proteins. TDH2 and TDH3 are also involved in the reactive oxygen species metabolic process ($p = 1.156e^{-03}$), and GLK1 and HXK2 also function in the mannose metabolic process ($p = 1.156e^{-03}$). Mannose biosynthesis is related to the known role of Psk1 in the regulation of β-1,6 glucan biosynthesis (Rutter et al., 2002; Smith and Rutter, 2007; Grose et al., 2009). Specifically, PAS kinase–deficient yeast display decreased β-1,6 glucan levels, increased sensitivity to cell wall–disturbing agents (Smith and Rutter, 2007), and increased glycogen accumulation (Rutter et al., 2002). In addition, there were six processes in which IRA1/IRA2 function was also enriched, including the positive regulation of RAS GTPase ($p = 5.834e^{-04}$). These proteins are also involved in the regulation of glycogen and trehalose biosynthesis (Chvojka et al., 1981).

The processes of ATP metabolism and ATP hydrolysis–coupled protein transport were also enriched ($p = 1.071e^{-05}$ and $1.594e^{-03}$, respectively) and include the ATP1, ATP2, and VMA1 proteins that are critical for ATP synthesis. In addition, the interactome supports a mitochondrial role for Psk1, in that the proteins are enriched for mitochondrial targets (Figure 2.3B). A mitochondrial role for Psk1 would be novel but consistent with the hypermetabolic phenotype of PAS kinase–deficient mice. Specifically, they consume more $O_2$ and release more $CO_2$ than their wild type littermates, suggesting increased respiration rates (Hao et al., 2007).

We were surprised that none of the pathways identified by FunSpec were lipid pathways, because of the dramatically altered liver triglyceride accumulation seen in PAS kinase–deficient mice (Hao et al., 2007) and because the yeast Psk1 interactome is enriched with proteins that have a human homolog (Tables 2.2 and 2.3). Approximately 73% of the putative Psk1 binding partners appear to have a human homolog, whereas only 20–30% of the yeast proteome is reportedly conserved from yeast to humans (Makino and McLysaght, 2012). This fact was used to identify lipid-related proteins using the Human Protein Reference Database (www.hsls.pitt.edu/obrc/index.php?page=URL1055173331). Diseases associated with human homologs of the interactome proteins revealed several involved in cholesterol/triglyceride homeostasis and cardiac disease (Table 2.4).

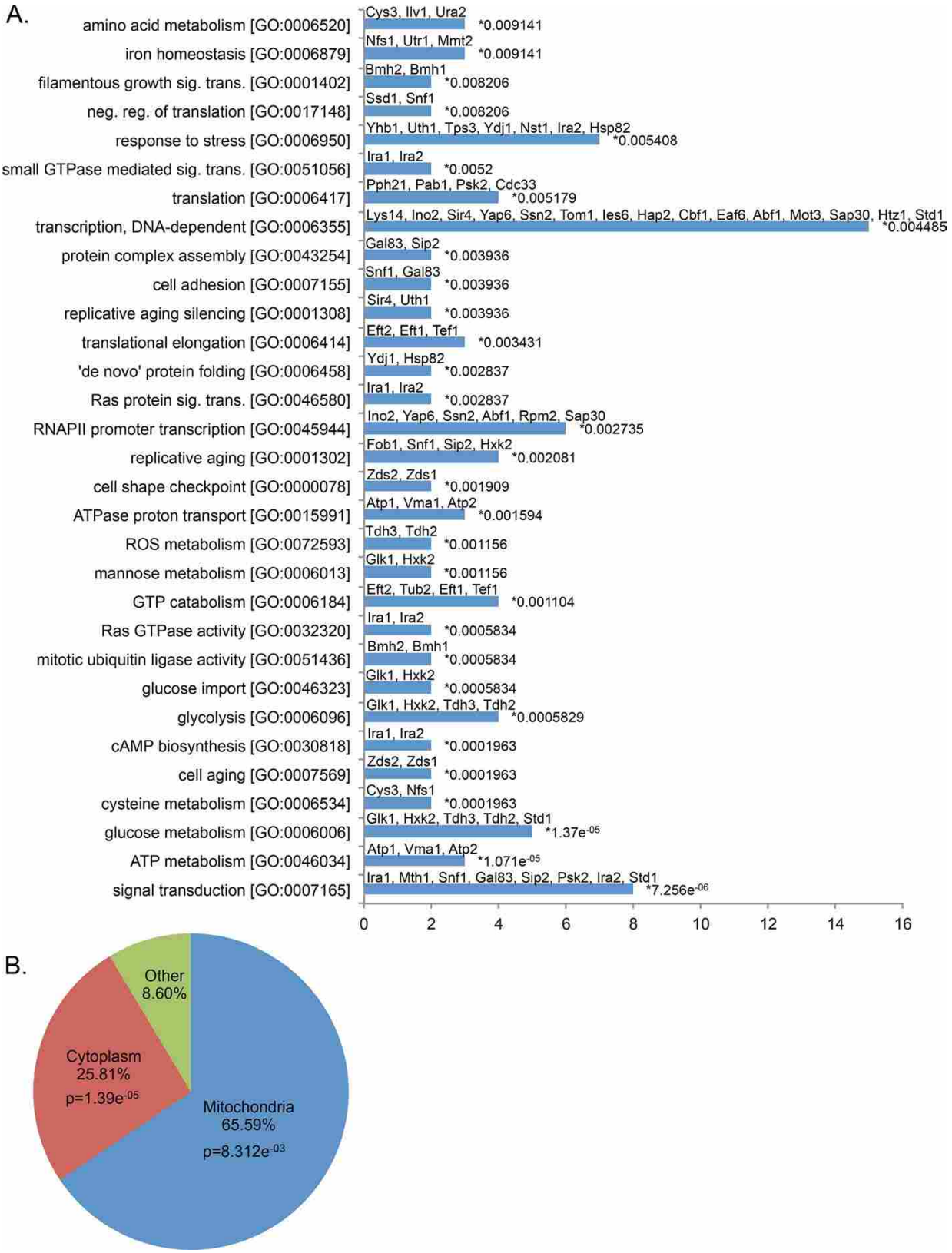


FIGURE 2.3. Enrichment of GO processes and cellular localization for the putative Psk1 binding partners. (A) GO processes enriched in the Psk1 interactome with corresponding p-values from FunSpec

(Robinson et al., 2002) analysis. Putative Psk1 binding partners belonging to each process are provided above the bar. GO process names are simplified due to space constraints, and abbreviations include signal transduction (sig. trans.) and negative regulation (neg. reg.). (B) FunSpec analysis reveals enrichment of proteins localized to the cytoplasm and mitochondria. Percentage of proteins from the Psk1 interactome and corresponding p-values are reported. Of the 93 putative binding partners, eight were not enriched in either the cytoplasm or mitochondria and were placed in an "other" category.

TABLE 2.4. Diseases associated with PAS kinase binding partners reveal a trend toward cardiac/lipid-related disease

| Yeast Gene | Human Homolog | Associated Disease |
|---|---|---|
| | CARDIAC/LIPID-RELATED | |
| *CBF1* | USF1 | Familial combined hyperlipidemia |
| *GAL2* | SLC2A10 | Arterial tortuosity syndrome |
| *IRA1* | NF1 | Neurofibromatosis-Noonan syndrome |
| *IRA2* | NF1 | Neurofibromatosis-Noonan syndrome |
| *MIR1* | SLC25A3 | Mitochondrial phosphate carrier deficiency |
| *MYO1* | MYH11 | Familial thoracic aortic aneurysm |
| *PRB1* | PCSK9 | Familial hypercholesterolemia |
| | BLOOD/ANEMIA | |
| *HXK2* | HK1 | Hexokinase deficiency hemolytic anemia |
| *MYO1* | MYH9 | May-Hegglin anomaly |
| | CANCERS | |
| *IRA1* | NF1 | Juvenile myelomonocytic leukemia |
| *IRA2* | NF1 | Juvenile myelomonocytic leukemia |
| | OTHER | |
| *CAR2* | OAT | Gyrate atrophy |
| *CYS3* | CTH | Cystathioninuria |
| *DPM1* | DPM1 | Congenital disorder of glycosylation type Ie |
| *PBP1* | ATXN2 | Spinocerebellar ataxia 2 |
| *YFR006W* | PEPD | Prolidase deficiency |

Each of the human homologs identified for the yeast Psk1 interactome were screened for their association with human diseases using the Human Protein Reference Database (HPRD). The columns indicate the original yeast gene retrieved in the Psk1 interactome study, the gene name of its human homolog and the name of the associated disease. All associations retrieved are shown.

## Mapping and in vitro verification of Cbf1 phosphosites

Cbf1/USF1 became the focus of this study due to its ability to be phosphorylated in vitro by Psk1 and its association with the two major mammalian PAS kinase phenotypes (namely, lipid biosynthesis and mitochondrial metabolism). Cbf1 was first identified as a centromere-binding factor (Bram and Kornberg, 1987; Baker et al., 1989; Cai and Davis, 1990) and has since been shown to regulate the expression of genes involved in methionine biosynthesis (Cai and Davis, 1990; Thomas et al., 1992; Kuras and Thomas, 1995; Kuras et al., 1996, 1997), phosphate

metabolism (O'Connell and Baker, 1992; Zhou and O'Shea, 2011; Aow et al., 2013), and lipid biosynthesis (Kolaczkowski et al., 2004). Recent evidence suggests that Cbf1 is also a major player in controlling the expression of genes involved in mitochondrial respiration (Petti et al., 2012; Haynes et al., 2013; Lin et al., 2013).

A putative protein kinase substrate is often validated by several approaches, including phosphosite mapping and mutation, followed by genetic epistasis experiments (Johnson and Hunter, 2005). The Psk1-dependent Cbf1 phosphorylation sites were mapped by in vitro kinase assays, followed by mass spectrometry. Five phosphorylation sites were detected with confidence (Figure 2.4A). The five putative phosphosites were mutated to alanine (T211A/T212A and T154A/S156A in combination and T138A singly), and proteins were reassessed for Psk1-dependent phosphorylation via in vitro kinase assays (Figure 2.4B). The T211A/T212A protein displayed a dramatic decrease in Psk1-dependent phosphorylation. The relevance of these Cbf1 phosphorylation sites requires in vivo analysis and is assessed later by determining the effects of phosphorylation on Cbf1 activity. The other phosphosites (T138, T154, and S156) are most likely secondary sites that get phosphorylated after the primary site and may be artifacts of in vitro phosphorylation.

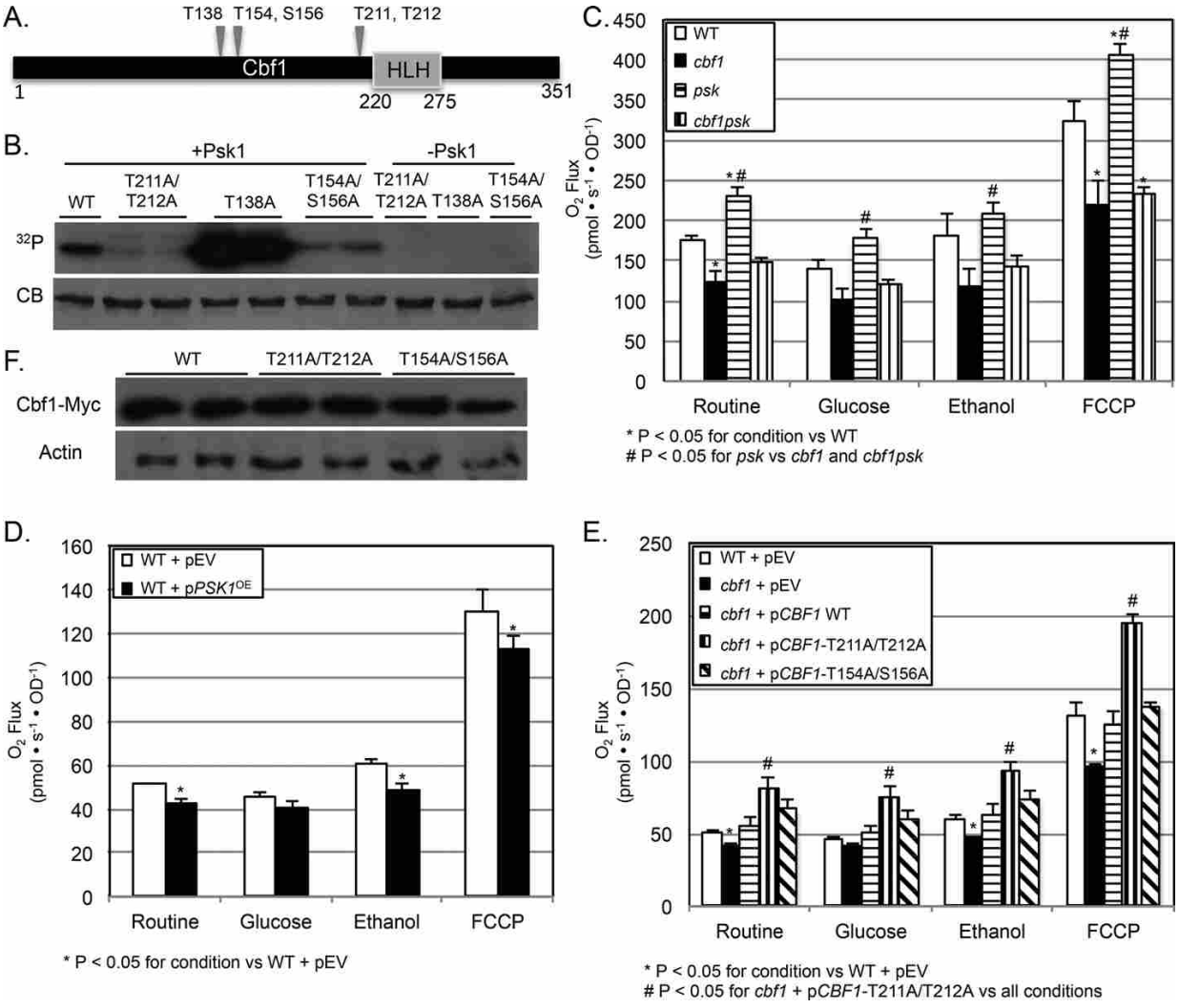


FIGURE 2.4. In vitro and in vivo evidence for the Psk1-dependent phosphorylation of Cbf1 at T211/T212. (A) Mass spectrometry of Cbf1 phosphorylated in vitro revealed five Psk1-dependent phosphorylation sites (T138, T154, S156, T211, and T212) that are indicated on a diagram, along with the conserved helix-loop-helix (HLH) domain. (B) In vitro kinase assays using purified wild type and mutant Cbf1 (T211A/T212A, T138A, and T154A/S156A) reveal T211/T212 as necessary sites for Psk1-dependent phosphorylation. Kinase assays were run with radiolabeled ATP ($^{32}$P), visualized on 12% SDS–PAGE gels, stained with Coomassie brilliant blue (CB; bottom), and exposed on x-ray film (top). (C–F) In vivo evidence for Psk1-dependent respiratory inhibition through the phosphorylation and inactivation of Cbf1. (C) *PSK*-deficient yeast (JGY1244) display increased respiration rates, whereas *CBF1*-deficient (JGY1227) or *CBF1PSK*-deficient (JGY1261) yeast display decreased rates. (D) Overexpression of *PSK1* (JGY1241) causes a significant decrease in respiration rates. (E) Yeast harboring Cbf1-T211A/T212A (JGY1263) display dramatically increased respiration rates compared with yeast harboring wild type (JGY1265) or Cbf1-T154A/S156A (JGY1264). Routine respiration (R) was determined by measuring $O_2$ consumption using an Oroboros $O_2$K Oxygraph in the absence of substrate and then with glucose (20 mM), ethanol (2%), or in the presence of the uncoupler carbonyl cyanide p-(trifluoro-methoxy) phenylhydrazine (FCCP; 70 μM). $OD_{600}$ was taken to ensure equal growth among strains. (F) Phosphosite mutants were expressed in yeast and analyzed by Western blot to ensure equal expression.

Evidence for Psk1-dependent respiratory inhibition through the phosphorylation and inactivation of Cbf1

To determine the effects of Cbf1 and Psk1-dependent phosphorylation on yeast respiration rates, mitochondrial function was assessed in *CBF1*- and/or *PSK*- deficient yeast. Yeast have two PAS kinase homologs that are both able to phosphorylate Ugp1, and hence respiration rates were determined in the double knockout (*psk1psk2* or *PSK*-deficient yeast) to abolish any overlapping function. As predicted, *CBF1*-deficient yeast displayed a significant decrease in respiration, whereas *PSK*-deficient yeast displayed a dramatic increase (Figure 2.4C). To our knowledge, this is the first demonstration of the effects of *CBF1* or *PSK1* on respiration rates. To test whether the respiratory stimulation seen in *PSK*-deficient yeast was dependent on the phosphorylation and inhibition of Cbf1, respiration was also assessed in *CBF1PSK*-deficient yeast. The *cbf1* mutant was epistatic to the *psk1psk2* mutant, in that the respiration rates of *CBF1PSK*-deficient yeast mirrored those of *CBF1*-deficient yeast. These results support the *PSK1*-dependent regulation of respiration through the phosphorylation and inhibition of Cbf1. As further evidence, overexpressing *PSK1* results in a significant inhibition of respiration (Figure 2.4D).

To assess the in vivo significance of the T211/T212 phosphorylation sites, respiration rates were determined for *CBF1*-deficient yeast expressing either wild type or Cbf1-T211A/T212A. Yeast expressing Cbf1-T211A/T212A display a dramatic increase in respiration (Figure 2.4E), consistent with the disruption of both phosphorylation and subsequent inhibition by Psk1. In contrast, yeast expressing Cbf1-T154A/S156A had rates similar to wild type, supporting in vitro evidence that these sites are either secondary phosphorylation sites or in vitro artifacts. Each strain bearing a phosphosite mutant was analyzed by Western blot to ensure equal growth among strains (Figure 2.4F). Phosphomimetic mutants (in which the phosphorylated

threonine residue was replaced with either a glutamic [T211E/T212E] or aspartic acid residue [T211D/T212D]) were constructed and assayed in an otherwise *cbf1* strain; however, they behaved like the wild type protein (unpublished data). This inability to mimic the phosphorylation state was also previously observed for Ugp1 (Rutter et al., 2002).

## DISCUSSION

Despite the clear importance of PAS kinase in eukaryotic glucose homeostasis, only one substrate has been well-characterized in yeast (Ugp1; Rutter et al., 2002; Smith and Rutter, 2007; Grose et al., 2007) and five putative substrates reported in mammalian cells: glycogen synthase (Wilson et al., 2005), PDX-1 (An et al., 2006), S6 (Schlafli et al., 2011), GSK3β (Semache et al., 2013), and elongation factor 1 (Eckhardt et al., 2007). This study describes the first global interactome for PAS kinase, identifying 93 novel putative binding partners and expanding the role of PAS kinase in glucose homeostasis, including new pathways involved in mitochondrial metabolism. In addition, the interactome suggests novel roles for PAS kinase in cell growth (gene/protein expression, replication/cell division, and protein modification and degradation), vacuole function, and stress tolerance. The Psk1 interactome could contain Psk1 substrates, regulators of its function, or proteins belonging to a larger complex that were present in the copurification. Each putative binding partner will require subsequent characterization to determine its relationship to Psk1. In this study the interactome was validated by the identification of proteins already known to be related to Psk1, the verification of four putative binding partners as in vitro substrates, and the detailed in vivo and in vitro characterization of one substrate, Cbf1.

The interactome is supported by enrichment of binding partners previously associated

with *PSK1*. FunSpec (Robinson et al., 2002) analysis revealed significant enrichment of several GO processes in which Snf1 is a player (Figure 2.3). Snf1 protein kinase is necessary and sufficient for Psk1 activation by carbon sources that stimulate respiration (Grose et al., 2007). This evidence of a protein–protein interaction between Psk1, Snf1, Gal83, and Sip2 implies direct phosphorylation and activation by Snf1, which is the subject of a research article in preparation. In addition, several processes were enriched that are linked to glycogen and cell wall biosynthesis. PAS kinase–deficient yeast display decreased β-1,6 glucan levels, increased sensitivity to cell wall–disturbing agents (Smith and Rutter, 2007), and increased glycogen accumulation (Rutter et al., 2002). This phenotype is dependent on the lack of PAS kinase–dependent phosphorylation of Ugp1; however, the results from this study suggest involvement of additional proteins in a concerted effort to shunt glucose toward cell wall biosynthesis. Another binding partner identified in our study, Ssd1, has been shown to interact with phospho-Ugp1 in order to suppress TOR2 deficiency (Cardon and Rutter, 2012). Because TOR2 is involved in regulating cell growth in response to nutrients (for a recent review see Loewith and Hall, 2011), this suppression posits a progrowth role for yeast PAS kinase, which has been shown to be a positive regulator of protein synthesis (Rutter et al., 2002). Many of the Psk1 binding partners identified in this study are involved in cell growth and division, predicting key targets for future study.

In addition to bioinformatic verification, in vitro kinase assays using 25 random binding partners suggests that 16% of the interactome represent substrates of Psk1. Four of the 25 proteins displayed clear, Psk1-dependent phosphorylation (Cbf1, Utr1, Mot3, and Zds1). This estimate may be low since proteins overexpressed and purified from bacteria may misfold, accessory proteins may be missing, or assay conditions may not be optimal. In fact, previous

kinase substrates have been shown to only be phosphorylated when truncated, as reported for Psk2 and its putative substrate Sro9 (Rutter et al., 2002). Such truncations may trap the protein in a conformation found in vivo. In vitro artifacts such as these mean that in vitro substrates must be confirmed through in vivo methods. Further study of Cbf1 provided in vivo confirmation of the interactome.

Bioinformatic analysis of the protein interactome (Figure 2.3 and Table 2.4), combined with the hypermetabolic and hyperlipidomic phenotypes of PAS kinase-deficient mice, suggested a focus on Cbf1. Further investigation showed that *CBF1*-deficient yeast display decreased respiration rates, whereas *PSK*-deficient yeast display increased rates (Figure 2.4). In addition, *cbf1* appears to be epistatic to *psk*. These results are consistent with direct phosphorylation and inhibition of Cbf1 by Psk1. Further evidence is provided for the direct in vitro phosphorylation of Cbf1 at T211/T212, as well as the dramatic increase in the respiration rates of yeast expressing an unphosphorylatable mutant, Cbf1-T211A/T212A. Although Cbf1 had been reported to increase the expression of genes involved in respiratory metabolism (Lin et al., 2013; Petti et al., 2012; Haynes et al., 2013), to our knowledge this study is the first to demonstrate its effects on respiration rates. Because PAS kinase–deficient mice have a higher rate of $O_2$ consumption and $CO_2$ production (Hao et al., 2007) and there is a conserved *CBF1* homolog in mammals (USF1), these results may shed valuable insight into the mechanisms of mammalian respiratory regulation. Although no role in respiration has been reported for USF1, USF1 plays a major role in regulating lipid biosynthesis in mammals (Pajukanta et al., 2004; Naukkarinen et al., 2006; Auer et al., 2012). The phosphorylation of USF1 by PAS kinase may also explain the decreased hepatic lipid accumulation seen in PAS kinase–deficient mice (Hao et al., 2007).

The findings from this study support a model in which yeast PAS kinase is regulating multiple pathways in order to direct glucose metabolites toward the biosynthesis of structural components necessary for cell growth (Figure 2.5). PAS kinase has been shown to phosphorylate Ugp1 to direct UDP-glucose utilization away from glycogen biosynthesis and toward the biosynthesis of structural carbohydrates such as β-glucans (Rutter et al., 2002; Smith and Rutter, 2007; Grose et al., 2007, 2009). At the same time, the inhibitory Psk1-dependent phosphorylation of Cbf1 would decrease respiration, leading to a further diversion of glucose toward structural carbohydrates necessary for growth.

The results of this study provide insight into the cellular mechanisms for regulating glucose allocation in eukaryotic cells. In addition to expanding our knowledge of yeast PAS kinase, the Psk1 interactome may be used to identify novel substrates for the mammalian homolog. Approximately 73% of the interactome is conserved from yeast to humans, including proteins involved in glucose homeostasis, a process known to be regulated by PAS kinase in mice (Hao et al., 2007) and humans (da Silva Xavier et al., 2011; MacDonald and Rorsman, 2011; Semplici et al., 2011). Because human PAS kinase is a putative therapeutic target, identifying and characterizing PAS kinase binding partners may yield more narrow therapeutic strategies, as well as predict unknown cellular effects.

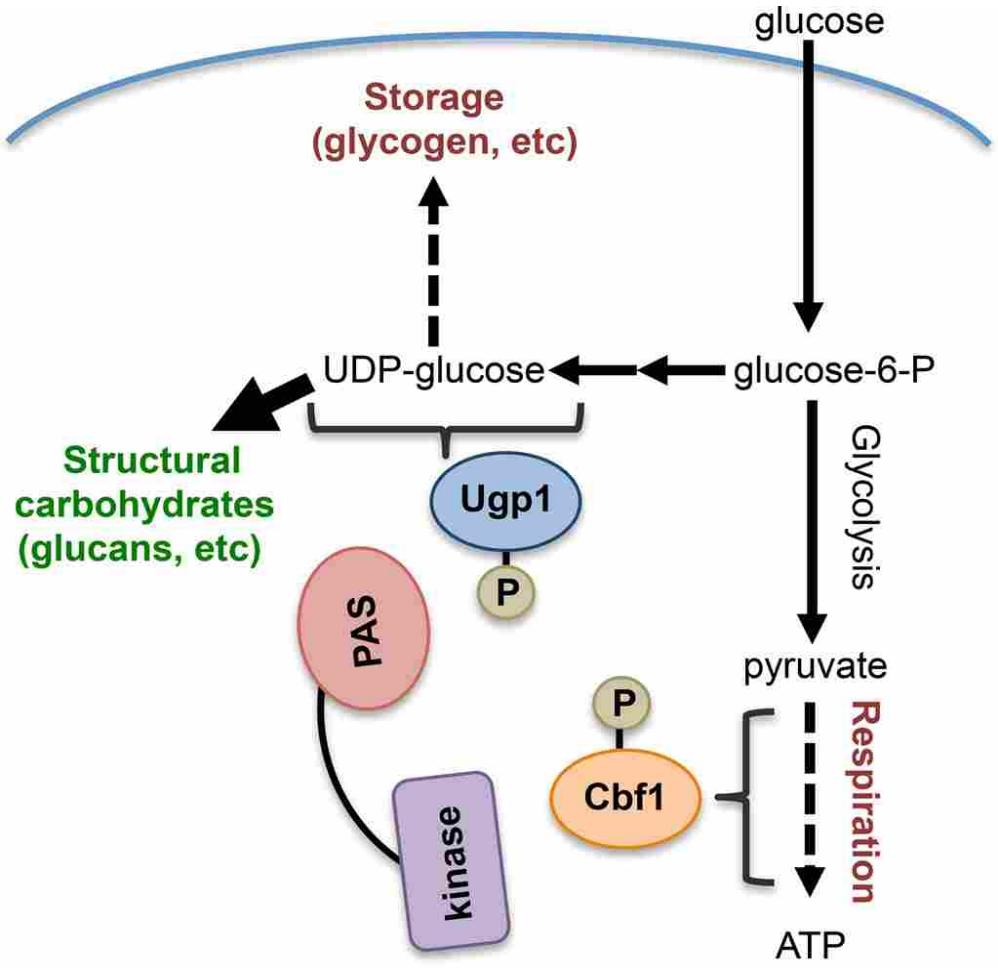


FIGURE 2.5. A model for the role of PAS kinase in regulating glucose allocation. The PAS kinase–dependent phosphorylation of Ugp1 directs UDP-glucose utilization away from glycogen biosynthesis and toward the biosynthesis of structural carbohydrates such as β-glucans (Rutter et al., 2002; Smith and Rutter, 2007; Grose et al., 2007, 2009). The inhibitory phosphorylation of Psk1 on Cbf1 decreases respiration, which may lead to a further diversion of glucose toward structural carbohydrates necessary for growth. Dashed lines indicate inhibition of a pathway, and thick lines indicate activation.

## MATERIALS AND METHODS

### Yeast cells, plasmids, and culture media

A list of strains, plasmids, and primers used in this study is given in Table 2.5. All restriction enzymes were purchased from New England Biolabs (NEB, Ipswich, MA). Deletion mutant and chromosomal-integrated epitope-tagged strains were created by standard PCR-based homologous recombination methods (Longtine et al., 1998). Psk1 Y2H bait plasmids were

constructed by PCR amplification of Psk1 truncations previously isolated (Grose et al., 2009) and subsequent cloning into the EcoRI/PstI sites of pGBDC2 (pJG425). The plasmid for overexpression and purification of HIS-tagged yeast Psk1 (pJG858) was made by PCR amplifying the GAL1-10 promoter with primers JG2894 and JG2895, then transforming the product into yeast along with SpeI-digested pJG232 to replace the Psk1 promoter through homologous recombination. The empty HIS-tagged vector (pJG859) was constructed by annealing primers JG2901 and JG2902 and transforming into yeast along with EcoRI/XhoI-digested pJG858. Myc-tagged yeast expression vectors (pJG1181 and pJG1183) were made by PCR amplifying the Myc tag with primers JG3422 and JG3423, digesting, and cloning into pJG858 and pJG859 (XhoI/SphI) to replace the HIS tag. FLAG-tagged yeast expression vectors (pJG1217 and pJG1218) were made by annealing overlapping primers JG3522 and JG3523 and ligating into the XhoI/SphI sites of pJG858 and pJG859 to replace the HIS tag.

Plasmids for HIS-tagged expression in bacteria were constructed by expanding the multiple cloning site of pET15b (Novagen, Darmstadt, Germany). This pET15b derivative (pJG1009) was made by annealing overlapping primers JG3173 and JG3174 and ligating into NdeI/BamHI digested pET15b. For cloning putative substrates, the first 22–28 coding nucleotides were used as a forward primer and the last 22–28 coding nucleotides, including the STOP codon, as a reverse (along with the desired restriction sites). Inserts were amplified using Phusion polymerase (NEB), and either the NdeI/XhoI, BamHI/XhoI, or EcoRI/XhoI restriction sites were used based on the gene sequences (SalI was substituted for XhoI in a few cases when necessary).

The Psk1 kinase-dead and Cbf1 phosphosite mutants were produced by site-directed mutagenesis using Stratagene's QuikChange Lightening Site-directed Mutagenesis Kit (Agilent

Technologies, Santa Clara, CA). The Psk1-D1230A was made by using pJG232 as template with primers JG2228 and JG2229 to create pJG410. It was then subcloned into pJG858 (BglII/XhoI) for GAL1-10 expression (pJG1170). For Cbf1 phosphosite mutants, pJG1031 was used as template with primers JG3356 and JG3357 for the T138A mutant(pJG1112), primers JG3375 and JG3376 for the T154A/S156A mutant (pJG1113), and primers JG3380 and JG3381 for the T211A/ T212A mutant (pJG1111). For medium expression of Cbf1 constructs in yeast, Cbf1 was subcloned from pJG1031, pJG1111, and pJG1113 into a plasmid (pJG725) for expression under the ADH promoter. Yeast were transformed by the lithium acetate method and grown at 30°C in synthetic (SD) medium (0.67% yeast nitrogen base, 2% glucose) with appropriate amino acids or 1% yeast extract, 2% peptone, 2% glucose, and 0.03% adenine (YPAD) and appropriate antibiotics. Alternate carbon sources (galactose or raffinose) were used at 2%. X-α-Gal was used at 20 μg/ml according to manufacturer's directions (Clontech, Mountain View, CA).

Growth assays

Growth assays were performed using saturated overnights serially diluted 1:5 in water. Diluted samples were spotted onto synthetic minimal medium lacking the appropriate amino acid(s) for Y2H selection (SD-Leu-Trp-His-Ade + X-α-Gal). Plates were then incubated at the indicated temperature for 3–7 d. Growth experiments were replicated three to six times, and control spot plates on nonselective media (SD- Leu-Trp) were always grown to ensure even dilution and spotting.

Y2H library generation

For cDNA library construction, yeast strain JGY8 (WT) was grown in either YPAD or YPAGal to stationary phase or mid log, respectively. RNA was extracted using Qiagen's RNeasy Mini Kit (Valencia, CA) followed by removal of Genomic DNA using Turbo rDNase. Full-length cDNA was generated using Clontech's Make Your Own "Mate & Plate" Library System, which uses SMART cDNA synthesis technology, and cloned into pGADT7 recombination vector (pJG549). JGY8 was chosen for library generation due to the wild type *SSD1* genotype (Cardon and Rutter, 2012).

Y2H screens

For genomic library screens, the Y2HGold (Clontech) strain (JGY1031) bearing pJG598 (ΔN692Psk1) was transformed with genomic libraries (pJG427, pJG428, or pJG429) obtained from David Stillman, University of Utah (James et al., 1996). For cDNA library screens, yeast harboring a cDNA Y2H prey library (JGY1074 or JGY1098) were mated to yeast harboring pJG598 (JGY1099) using the standard Matchmaker mating protocol (Clontech). More than 26 million matings were performed and ~14 million transformations. Colonies that arose on Y2H selection plates (SD-Leu-Trp-His-Ade) were patched to alternate Y2H selection plates (SD-Leu-Trp-His-Ade + X-α-Gal) for phenotype validation using the His, Ade, and Mel1 reporters. The library plasmid inserts were identified by colony PCR with subsequent sequencing (Brigham Young University DNA Sequencing Center) and National Center for Biotechnology Information (NCBI) BLAST analysis (an unambiguous hit with e-value of $\geq 10e^{-30}$). For verification and elimination of false positives, library plasmids were purified from yeast (Amberg et al., 2005), amplified in *Escherichia coli* (GenElute Plasmid Mini-prep Kit, Sigma-Aldrich, St. Louis, MO),

and transformed into naive yeast harboring the bait plasmid (pJG598) or the empty bait plasmid (pJG425). Colonies arising on the SD-Leu-Trp transformation plates were streaked to SD or SGal synthetic media (-Leu-Trp-His-Ade + X-α-Gal) in duplicate and allowed to grow for 3–5 d to test for Psk1 dependence.

HIS, Myc, and FLAG epitope protein purification

Yeast containing a plasmid for HIS-tagged protein expression were grown for 10–12 h in SD-Ura, pelleted, and resuspended in SGal-Ura for 36 h to induce expression from the GAL1-10 promoter. Pelleted yeast were then resuspended in lysis buffer (50 mM 4-(2-hydroxyethyl)-1-piperazineethanesulfonic acid [HEPES], 300 mM NaCl, 20 mM imidazole, 10 mM KCl, 1 mM β-mercaptoethanol, and 1:300 of Sigma-Aldrich Mammalian PICS or Roche (Indianapolis, IN) cOmplete Protease Inhibitor Cocktail Tablet, pH 7.8, with phosphatase inhibitors [50 mM NaF and glycerophosphate when appropriate]) and lysed using the Microfluidics (Westwood, MA) M-110L homogenizer. Cell debris was pelleted at 12,000 rpm for 30 min. Supernates were incubated with 200 µl of nickel-nitriloacetic acid (Ni-NTA) agarose (Qiagen) for 3 h, and beads were washed twice with 15 ml of lysis buffer and then transferred to a column to be washed with 50 ml of lysis buffer. Protein was eluted with 0.3 ml of lysis buffer containing 250 mM imidazole and 100 mM NaCl but lacking protease and phosphatase inhibitor cocktails. Full-length (pJG858) and truncated Psk1 (pJG960) proteins were expressed in JGY1 along with an empty vector control (pJG859) for mass spectrometry analysis. Yeast containing plasmids for FLAG- or Myc-tagged protein expression were prepared similar to the HIS-tagged samples with the following exceptions: FLAG lysis buffer (1x phosphate-buffered saline buffer, 1 mM β-mercaptoethanol, cOmplete Protease Inhibitor Cocktail Tablet, pH 7.4) and Myc lysis buffer (20

mM HEPES, 10 mM KCl, 1 mM EDTA, 1 mM ethylene glycol tetraacetic acid [EGTA], 50 mM NaCl, 10% glycerol, 1 mM β-mercaptoethanol, and cOmplete Protease Inhibitor Cocktail Tablet, pH 7.4). For Myc purification, 50 µl of Myc-tag Sepharose bead conjugate (Cell Signaling, Danvers, MA) was used. For FLAG purification, 50 µl of Protein G Dynabeads (Life Technologies, Grand Island, NY) incubated with monoclonal anti-FLAG antibody (Sigma-Aldrich) was used. Columns were not used for the Myc and FLAG washing steps. The beads were pelleted at 1000 rpm in a centrifuge tube and washed seven times before eluting. Proteins were eluted with 60 µl of trifluoroethanol and then boiled for 5 min for Myc purification and 100 µl of FLAG-peptide diluted in the wash buffer for FLAG purification. Full-length Psk1-FLAG (pJG1217) and Psk1-Myc (pJG1181) were expressed in JGY1 along with their respective empty vector controls (pJG1218 and pJG1183) for mass spectrometry analysis.

Bacterial plasmids containing 38 of the Y2H and copurification hits were cloned into a derivative of pET15b (Novagen) with an altered multiple cloning site to provide diverse restriction enzymes (pJG1009). The resulting pET15b plasmids were sequence verified and transformed into BL21 DE3 cells (Novagen) for expression. Overnights were grown in LB-AMP (lysis buffer with 100 µg/ml ampicilin; Sigma-Aldrich), diluted 1:100 in 500 ml of LB-AMP, and grown at 37°C for 3 h before induction with 0.5 mM isopropyl-β-D-thiogalactoside. Cells were pelleted after 5 h of induction, and proteins were purified using Ni-NTA agarose as described. In some cases these growth conditions inhibited growth or gave high degradation of the protein, in which case lower temperature (30°C) and lower aeration (rpm 80) were required for expression (Cbf1, Hap2, Zds1, Erg9).

Quantitative mass spectrometry

HIS-epitope Psk1 copurification samples were prepared for mass spectrometry using a modified filter-aided sample preparation technique (FASP; Wisniewski et al., 2009). Samples were digested in 30–40 µl of 50 mM ammonium bicarbonate (ReagentPlus Grade; Sigma-Aldrich) with 0.1–2.0 µg of modified sequence-grade trypsin (Promega, Madison, WI) for 4–7 h or overnight at 37°C on the filters. Samples within each replicate were digested with equal quantities of trypsin for equal amounts of time. Samples were acidified to ~1% formic acid (Optima LC-MS Grade from Fisher Scientific, Pittsburgh, PA) before LC-MS. To increase protein recovery, FLAG- and Myc-tagged *PSK1* coimmunoprecipitations were prepared without a filter. Briefly, samples were suspended in 50% 2,2,2-trifluoroethanol (Acros; 99.8%) 25 or 50 mM ammonium bicarbonate (Acros; 99%), reduced with dithiothreitol (Acros; 99%, or Sigma-Aldrich), alkylated with iodoacetamide, dried on a SpeedVac, resuspended in 25 mM ammonium bicarbonate (Acros; 99%), and digested with ~0.1 µg of trypsin (Promega Sequencing Grade or Pierce MS grade) at 37°C for 6–7 h or overnight. Digestions were quenched with formic acid or phenylmethanesulfonyl fluoride (MP Biomedicals, Santa Ana, CA) trypsin inhibitor. Samples were dried on a SpeedVac and resuspended in 3% acetonitrile/0.1% formic acid. All replicate experiments received the same preparation.

Mass spectral analysis was performed on the Thermo LTQ Orbitrap XL mass spectrometer coupled with the Eksigent NanoLC Ultra. Peptides were eluted from a Waters Peptide Separation Technology C18 column over 90 (for Myc, FLAG, and HIS epitope samples) or 150 min (for one set of HIS replicates) using an acetonitrile/$H_2O$ 0.1% formic acid gradient (Optima LC-MS Grade from Fischer Scientific) flowing at 325 nl/min. Peptides were ionized using a nanospray source. MS scans were performed in the Orbitrap at a resolution of

60,000 at 400 m/z. The top 5 or top 10 most abundant species were fragmented in the LTQ with collision-induced dissociation (CID) with a dynamic exclusion repeat count of 1. Charge state screening was enabled, rejecting charge state 1 and unassigned charge states with monoisotopic precursor selection. Samples within each replicate were analyzed with the same LC-MS parameters.

For phosphosite mapping, Cbf1 underwent similar FASP preparation and mass spectral analysis, with a few exceptions. Samples were digested in 50 mM ammonium bicarbonate with 0.1 μg of trypsin overnight. MS data were collected at a resolution of 30,000 at 400 m/z in the Orbitrap, and the top 10 most abundant species underwent pseudo MS (Perkins et al., 1999) multistage CID in the LTQ with phosphate neutral losses at 32.66, 48.99, and 97.97 Da (Schroeder et al., 2004).

Data analysis was performed with Mascot (Perkins et al., 1999) using Proteome Discover Software versions 1.3 and 1.4. Spectra were searched against the uni_yeast database. Mass deviation in the Orbitrap and ion trap were set to ±10 ppm and ±0.8 Da, respectively. The search allowed two or three maximum missed trypsin cleavages, with the following dynamic modifications: Carbamidomethyl (C), Oxidation (M), Phospho (ST), and Phospho (Y). Peptide confidence was set using the Proteome Discoverer 1.3 or 1.4 medium peptide confidence filter, which decided using percolator (Käll et al., 2007) or the Mascot significance threshold.

Bioinformatic analysis

FunSpec was used to access enrichment of both cellular localization patterns or GO processes in the Psk1 interactome (Robinson et al., 2002). Identification of human homologs was done through searches on NCBI HomoloGene (www.ncbi.nlm.nih.gov/homologene), NCBI

protein BLAST (Johnson et al., 2008), and the MIT Isobase database (Park et al., 2011). Our criteria for determining human homologs were as follows: 1) a clear hit in Isobase or NCBI HomoloGene database, 2) an NCBI Blast hit of $e^{-30}$ or a hit of less homology ($e^{-10}$) that was small, such as a conserved domain of function, and 3) any questionable Isobase hit had to have some limited homology.

In vitro kinase assays

Purified protein was assayed for in vitro phosphorylation by PAS kinase using radiolabeled ATP ($^{32}$P; 1–5 μCi) in 30 μl of reaction buffer containing 1x kinase buffer, 0.2 mM ATP, ~0.5 μg of purified substrate, and ~0.1 μg of purified full-length Psk1 (pJG858), ΔN931Psk1 (pJG1000), or Psk1-D1230A (pJG1170). Both full-length and ΔN931Psk1 were purified from JGY1, and Psk1-D1230A was purified from JGY4. Assays were run at 30°C for 12 min and were started by the addition of Psk1 and stopped with SDS–PAGE sample buffer. Samples were run on 8 or 12% SDS–PAGE, depending on the size of the protein, stained with Coomassie brilliant blue, and imaged. Gels were then dried and imaged on x-ray film.

Mitochondrial respiration assays

Yeast not under selection were grown overnight in YPAD and then diluted 1:50 and allowed to grow in YPAraffinose for 4 h. Yeast harboring a plasmid were grown in minimal SD-Ura overnight, pelleted, and resuspended in SGal-Ura for 20–24 h, diluted 1:50, and allowed to grow in SGal-Ura for 4 h. The $OD_{600}$ was taken to ensure equal growth among strains. High-resolution $O_2$ consumption was determined at 37°C using the Oroboros (Innsbruck, Austria) $O_2$K Oxygraph. Before addition of sample into respiration chambers, a baseline respiration rate was

determined. Samples were centrifuged at 1000 x g for 10 min and resuspended in warm mitochondrial respiration buffer 05 (MiR05; 0.5 mM EGTA, 10 mM $KH_2PO_4$, 3 mM $MgCl_2$–6 $H_2O$, 60 mM K-lactobionate, 20 mM HEPES, 110 mM sucrose, 1 mg/ml fatty acid–free bovine serum albumin, pH 7.1). After addition of sample, the chambers were hyperoxygenated to ~350 nmol/ml. After this, routine respiration was determined by measuring $O_2$ consumption in the absence of any substrate (R). Next, glucose (Glc; 20 mM) and then ethanol (EtOH; 2%) was added to the respiration chambers to determine substrate-specific respiration. After this, the uncoupler carbonyl cyanide p-(trifluoro-methoxy)phenylhydrazine (70 μM) was added to determine noncoupled respiration as a measure of maximal electron transport system capacity (E). Finally, respiration was inhibited by the addition of the cytochrome c oxidase inhibitor azide (20 mM), eliciting a state of residual oxygen consumption (ROX), which provided a control for all values. Each strain was grown in triplicate, and respiration rates were averaged.

ACKNOWLEDGMENTS

We thank Brigham Young University undergraduates Andrew Gessel, Eliza Lawrence, Katie Harris, Colby Haines, Serena Loeb, Lauren Faucer, and Raul Hererra for their contributions to the Y2H screen. This work was supported by National Institutes of Health Grant R15 GM100376-01, a Brigham Young University Mentoring Environmental Grant, and the Brigham Young University Department of Microbiology and Molecular Biology.

TABLE 2.5. Strains, plasmids, and primers

| Strain | BGD | Genotype | Abbreviation | a/α | Ref |
|---|---|---|---|---|---|
| JGY1 | W303 | ade2-1 can1-100 his3-11,15 leu2-3,112 trp1-1 ura3-1 | WT | a | 1 |
| JGY4 | W303 | *psk1*::his3 *psk2*::kan-MX4 leu2, lys2, met15, trp1, ura3 | *psk1psk2* | a | 2 |
| JGY8 | JK9 | leu2-3,112 ura3-52 rme1 trp1 his4 GAL+ HMLa | WT | a | 3 |
| JGY43 | BY4741 | His3D1 leu2D0 met15D0 ura3D0 | WT | a | 4 |
| Y2H Gold | | LYS2::GAL1UAS-GAL1TATA-His3 GAL2UAS-Gal2TATA-Ade2 | Y2H Gold | a | 5 |

| | | | | | |
|---|---|---|---|---|---|
| (JGY1031) | | URA3::MEL1UAS-MEL1TATA, AUR1-CMEL1, ura3-52, his3-200, ade2-101, trp1-901, leu2-3, 112, gal4del, gal80del, met-, | | | |
| JGY1241 | BY4741 | pJG858 into JGY43 | *PSK1*$^{OE}$ | a | 6 |
| JGY1242 | BY4741 | pJG859 into JGY43 | EV | a | 6 |
| Y187 (JGY1073) | | URA3::GAL1-GAL1-LacZ, MEL1, ura3-52, his3-200, ade2-101, trp1-901, leu2-3, 112, gal4del, gal80del, met-, | Y187 | α | 5 |
| JGY1074 | | pGADT7 Mate and Plate stationary phase YPAD library in JGY1073 | YPAD library | α | 6 |
| JGY1098 | | pGADT7 Mate and Plate mid-log YPAGal library in JGY1073 | YPAGal library | α | 6 |
| JGY1099 | | pJG598 (ΔN692Psk1) in JGY1031 (Y2H Gold) | ΔN692Psk1 | a | 6 |
| JGY1227 | BY4741 | *cbf1*::kan-MX4 his3-1, leu2-0, met15-0, ura3-0 | *cbf1* | a | 4 |
| JGY1261 | BY4741 | *psk2*::nat-MX4 *psk1*::hph-MX4 *cbf1*::kan-MX4 his3-1, leu2, met15, ura3 | *psk1psk2cbf1* | a | 6 |
| JGY1262 | BY4741 | pJG725 (EV) into JGY1227 | *cbf1* pEV | a | 6 |
| JGY1263 | BY4741 | pJG1122 (*CBF1*-T211A/T212A into JGY1227 | p*CBF1*-T211A/T212A | a | 6 |
| JGY1264 | BY4741 | pJG1123 (*CBF1*-T154A/S156A) into JGY1227 | p*CBF1*-T154A/S156A | a | 6 |
| JGY1265 | BY4741 | pJG1125 (*CBF1*) transformed into JGY1227 | p*CBF1* | a | 6 |
| JHG504 | BL21DE3 | $F^-$ *ompT hsdS*B($rB^-mB^-$) *gal dcm* (DE3) | BL21 | | 7 |

| Plasmid | Gene | Description | Backbone | YO | Selection | Ref |
|---|---|---|---|---|---|---|
| pJG232 | *PSK1* | C-terminal HIS/HA-tagged *PSK1* | pRS426 | 2u | URA | 8 |
| pJG410 | *PSK1*-D1230A | *PSK1*-D1230A in pJG232 | pRS426 | 2u | URA | 6 |
| pJG421 | EV | pGAD-C1 empty Y2H prey vector | YEp-GAD | 2u | LEU | 9 |
| pJG422 | EV | pGAD-C2 empty Y2H prey vector | YEp-GAD | 2u | LEU | 9 |
| pJG423 | EV | pGAD-C3 empty Y2H prey vector | YEp-GAD | 2u | LEU | 9 |
| pJG425 | EV | pGBD-C2 empty Y2H bait vector | YEp-GAD | 2u | TRP | 9 |
| pJG427 | Library | pGAD-C1 genomic library | YEp-GAD | 2u | LEU | 9 |
| pJG428 | Library | pGAD-C2 genomic library | YEp-GAD | 2u | LEU | 9 |
| pJG429 | Library | pGAD-C3 genomic library | YEp-GAD | 2u | LEU | 9 |
| pJG441 | *PSK1* | Full-length *PSK1* in pJG425 | YEp-GBD | 2u | TRP | 6 |
| pJG549 | EV | pGADT7 empty Y2H prey vector | pGADT7 | 2u | LEU | 5 |
| pJG568 | *PSK1* | ΔN931Psk1 in pJG425 | YEp-GBD | 2u | TRP | 6 |
| pJG598 | *PSK1* | ΔN692Psk1 in pJG425 | YEp-GBD | 2u | TRP | 6 |
| pJG725 | EV | pAdh-myc | pRS416 | CEN | URA | 6 |
| pJG858 | *PSK1* | pGAL1-10, *PSK1*-HIS/HA | pRS426 | 2u | URA | 6 |
| pJG859 | EV | pGAL1-10, HIS/HA | pRS426 | 2u | URA | 6 |
| pJG960 | *PSK1* | ΔN692Psk1-HIS/HA in pJG858 | pRS426 | 2u | URA | 6 |
| pJG1000 | *PSK1* | ΔN931Psk1-HIS/HA in pJG858 | pRS426 | 2u | URA | 6 |
| pJG1001 | *PBP1* | ΔN355Pbp1 from library pJG427 | YEp-GAD | 2u | LEU | 6 |
| pJG1005 | *PSK1* | ΔN477Psk1 in pJG425 | YEp-GBD | 2u | TRP | 6 |
| pJG1006 | *PSK1* | ΔN694Psk1 in pJG425 | YEp-GBD | 2u | TRP | 6 |
| pJG1009 | EV | pET15b with James Y2H MCS | pET15b | | AMP | 6 |
| pJG1012 | *GLK1* | *GLK1* into pET15b (pJG1009) | pET15b | | AMP | 6 |
| pJG1013 | *GND1* | *GND1* into pET15b (pJG1009) | pET15b | | AMP | 6 |
| pJG1014 | *AHP1* | *AHP1* into pET15b (pJG1009) | pET15b | | AMP | 6 |
| pJG1015 | *PBP1* | *PBP1* into pET15b (pJG1009) | pET15b | | AMP | 6 |
| pJG1017 | *UTR1* | *UTR1* into pET15b (pJG1009) | pET15b | | AMP | 6 |
| pJG1021 | *CYS3* | *CYS3* into pET15b (pJG1009) | pET15b | | AMP | 6 |
| pJG1022 | *GCD14* | *GCD14* into pET15b (pJG1009) | pET15b | | AMP | 6 |
| pJG1023 | *SAP30* | *SAP30* into pET15b (pJG1009) | pET15b | | AMP | 6 |
| pJG1024 | *STD1* | *STD1* into pET15b (pJG1009) | pET15b | | AMP | 6 |
| pJG1025 | *IPP1* | *IPP1* into pET15b (pJG1009) | pET15b | | AMP | 6 |
| pJG1026 | *MTH1* | *MTH1* into pET15b (pJG1009) | pET15b | | AMP | 6 |
| pJG1030 | *HAP2* | *HAP2* into pET15b (pJG1009) | pET15b | | AMP | 6 |
| pJG1031 | *CBF1* | *CBF1* into pET15b (pJG1009) | pET15b | | AMP | 6 |
| pJG1032 | *ZDS1* | *ZDS1* into pET15b (pJG1009) | pET15b | | AMP | 6 |
| pJG1033 | *MOT3* | *MOT3* into pET15b (pJG1009) | pET15b | | AMP | 6 |
| pJG1035 | *NOB1* | *NOB1* into pET15b (pJG1009) | pET15b | | AMP | 6 |
| pJG1041 | *YAP6* | *YAP6* into pET15b (pJG1009) | pET15b | | AMP | 6 |
| pJG1054 | *OSH7* | *OSH7* into pET15b (pJG1009) | pET15b | | AMP | 6 |
| pJG1057 | *CAR2* | *CAR2* into pET15b (pJG1009) | pET15b | | AMP | 6 |
| pJG1059 | *ERG9* | *ERG9* into pET15b (pJG1009) | pET15b | | AMP | 6 |
| pJG1063 | *PRB1* | *PRB1* into pET15b (pJG1009) | pET15b | | AMP | 6 |
| pJG1074 | *ATP2* | *ATP2* into pET15b (pJG1009) | pET15b | | AMP | 6 |
| pJG1078 | *MRM1* | *MRM1* into pET15b (pJG1009) | pET15b | | AMP | 6 |
| pJG1079 | *HXK2* | *HXK2* into pET15b (pJG1009) | pET15b | | AMP | 6 |
| pJG1081 | *PAB1* | *PAB1* into pET15b (pJG1009) | pET15b | | AMP | 6 |
| pJG1111 | *CBF1*-T211A/T212A | *CBF1*-T211A/T212A in pET15b | pET15b | | AMP | 6 |
| pJG1112 | *CBF1*-T138A | *CBF1*-T138A in pET15b | pET15b | | AMP | 6 |

| | | | | | | |
|---|---|---|---|---|---|---|
| pJG1113 | *CBF1*-T154A/S156A | *CBF1*-T154A/S156A in pET15b | pET15b | | AMP | 6 |
| pJG1122 | *CBF1*-T211A/T212A | pAdh-Myc-*CBF1*-T211A/T212A | pRS416 | CEN | URA | 6 |
| pJG1123 | *CBF1*-T154A/S156A | pAdh-Myc-*CBF1*-T154A/S156A | pRS416 | CEN | URA | 6 |
| pJG1170 | *PSK1*-D1230A | pGAL1-10-*PSK1*-D1230A-HIS/HA | pRS426 | 2u | URA | 6 |
| pJG1181 | *PSK1* | pGAL1-10-*PSK1*-Myc | pRS426 | 2u | URA | 6 |
| pJG1183 | *EV* | pGAL1-10-Myc | pRS426 | 2u | URA | 6 |
| pJG1217 | *PSK1* | pGAL1-10-*PSK1*-FLAG | pRS426 | 2u | URA | 6 |
| pJG1218 | *EV* | pGAL1-10-FLAG | pRS426 | 2u | URA | 6 |
| Primer | Sequence | | | | | |
| JG2228 | CCAGGGTATTGTTCACAGAGCTATCAAGGATGAGAATGTTA | | | | | |
| JG2229 | TAACATTCTCATCCTTGATAGCTCTGTGAACAATACCCTGG | | | | | |
| JG2894 | CAAGCGCGCAATTAACCCTCACTAAAGGGAACAAAAGCTGGAGCTCCACCGCGGTGGCGGCCGCTCTAGAACTAC AATTCGACAGGTTATCAGCAAC | | | | | |
| JG2895 | CTTTAACGTCAAGGAGAAAAAACCCGAATTCATGCCCTACATCGGTGCTTCCAACCTCTCAGAACATTCATTTGTTAA TTTGAAGGAAAAACATGCGAT | | | | | |
| JG2901 | TTAATATACCTCTATACTTTAACGTCAAGGAGAAAAAACCCGAATTCATGCCTCGAGGATCCCACCACCATCATCATC ACGGATACCCGTATGATGTTCC | | | | | |
| JG2902 | GGAACATCATACGGGTATCCGTGATGATGATGGTGGTGGGATCCTCGAGGCATGAATTCGGGTTTTTTCTCCTTGA CGTTAAAGTATAGAGGTATATTAA | | | | | |
| JG3173 | TATGGAATTCCCCGGGGGATCCATCGATGT | | | | | |
| JG3174 | AATTTCAGTCAGTCAAGATCTCTGCAGGTCGACATCGATGGATCCCCCGGGGAATTCCA | | | | | |
| JG3356 | GACTCCTTCATTTGATGGGGCTATGGCTCTTTCCCC | | | | | |
| JG3357 | GGGGAAAGAGCCATAGCCCCATCAAATGAAGGAGTC | | | | | |
| JG3375 | GTAGATTCCATTGGTGGCAGACGCCATTCCCTCCAGGGAGG | | | | | |
| JG3376 | CCTCCCTGGAGGGGAATGGCGTCTGCACCAATGGAATCTAC | | | | | |
| JG3422 | GGCCTCGAGGTGGTGGAGGAGGTGAACAAAAGCTAATCTCCGAGGAAGAC | | | | | |
| JG3423 | GGCGCATGCTTAGTGATTGATTAATTTTTGTTCACCGTTC | | | | | |
| JG3522 | TCGAGGTGATTACAAGGATGACGATGACAAGTAAGCATG | | | | | |
| JG3523 | CTTACTTGTCATCGTCATCCTTGTAATCACC | | | | | |
| JG3380 | GTCGTGGAAGAAAACCTGCTGCTTTGGCCACAACAGACG | | | | | |
| JG3381 | CGTCTGTTGTGGCCAAAGCAGCAGGTTTTCTTCCACGAC | | | | | |

Abbreviations include BGD for background and YO for yeast origin. References= [1]David Stillman, [2](Grose et al., 2007), [3]Michael Hall, [4](Winzeler et al., 1999), [5]Clontech, [6]This study, [7]Novagen, [8]Jared Rutter, [9](James et al., 1996).

REFERENCES

Amberg, D.C., Burke, D., Strathern, J.N., Burke, D., and Cold Spring Harbor Laboratory. (2005). Methods in yeast genetics : a Cold Spring Harbor Laboratory course manual, 2005 edn (Cold Spring Harbor, N.Y., Cold Spring Harbor Laboratory Press).

An, R., da Silva Xavier, G., Hao, H.X., Semplici, F., Rutter, J., and Rutter, G.A. (2006). Regulation by Per-Arnt-Sim (PAS) kinase of pancreatic duodenal homeobox-1 nuclear import in pancreatic beta-cells. Biochem Soc Trans *34*, 791-793.

Aow, J.S., Xue, X., Run, J.Q., Lim, G.F., Goh, W.S., and Clarke, N.D. (2013). Differential binding of the related transcription factors Pho4 and Cbf1 can tune the sensitivity of promoters to different levels of an induction signal. Nucleic acids research *41*, 4877-4887.

Auer, S., Hahne, P., Soyal, S.M., Felder, T., Miller, K., Paulmichl, M., Krempler, F., Oberkofler, H., and Patsch, W. (2012). Potential role of upstream stimulatory factor 1 gene variant in familial combined hyperlipidemia and related disorders. Arterioscler Thromb Vasc Biol *32*, 1535-1544.

Baker, R.E., Fitzgerald-Hayes, M., and O'Brien, T.C. (1989). Purification of the yeast centromere binding protein CP1 and a mutational analysis of its binding site. The Journal of biological chemistry *264*, 10843-10850.

Bram, R.J., and Kornberg, R.D. (1987). Isolation of a Saccharomyces cerevisiae centromere DNA-binding protein, its human homolog, and its possible role as a transcription factor. Molecular and cellular biology *7*, 403-409.

Breitkreutz, A., Choi, H., Sharom, J.R., Boucher, L., Neduva, V., Larsen, B., Lin, Z.Y., Breitkreutz, B.J., Stark, C., Liu, G.*, et al.* (2010). A global protein kinase and phosphatase interaction network in yeast. Science *328*, 1043-1046.

Cai, M., and Davis, R.W. (1990). Yeast centromere binding protein CBF1, of the helix-loop-helix protein family, is required for chromosome stability and methionine prototrophy. Cell *61*, 437-446.

Cardon, C.M., and Rutter, J. (2012a). PAS kinase: integrating nutrient sensing with nutrient partitioning. Seminars in cell & developmental biology *23*, 626-630.

Cardon, C.M., and Rutter, J. (2012b). PAS kinase: Integrating nutrient sensing with nutrient partitioning. Semin Cell Dev Biol.

Chvojka, A., Barlas, M., Ruis, H., Padrao, G.R., Panek, A.D., and Mattoon, J.R. (1981). A regulatory mutation in yeast which affects catalase T formation and metabolism of carbohydrate reserves. Curr Genet *4*, 47-50.

da Silva Xavier, G., Farhan, H., Kim, H., Caxaria, S., Johnson, P., Hughes, S., Bugliani, M., Marselli, L., Marchetti, P., Birzele, F.*, et al.* (2011). Per-arnt-sim (PAS) domain-containing protein kinase is downregulated in human islets in type 2 diabetes and regulates glucagon secretion. Diabetologia *54*, 819-827.

da Silva Xavier, G., Rutter, J., and Rutter, G.A. (2004). Involvement of Per-Arnt-Sim (PAS) kinase in the stimulation of preproinsulin and pancreatic duodenum homeobox 1 gene expression by glucose. Proc Natl Acad Sci U S A *101*, 8319-8324.

DeMille, D., and Grose, J.H. (2013). PAS kinase: a nutrient sensing regulator of glucose homeostasis. IUBMB Life *65*, 921-929.

Dunham, W.H., Mullin, M., and Gingras, A.C. (2012). Affinity-purification coupled to mass spectrometry: basic principles and strategies. Proteomics *12*, 1576-1590.

Eckhardt, K., Troger, J., Reissmann, J., Katschinski, D.M., Wagner, K.F., Stengel, P., Paasch, U., Hunziker, P., Borter, E., Barth, S.*, et al.* (2007). Male germ cell expression of the PAS domain kinase PASKIN and its novel target eukaryotic translation elongation factor eEF1A1. Cellular physiology and biochemistry : international journal of experimental cellular physiology, biochemistry, and pharmacology *20*, 227-240.

Eglen, R., and Reisine, T. (2011). Drug discovery and the human kinome: recent trends. Pharmacology & therapeutics *130*, 144-156.

Endicott, J.A., Noble, M.E., and Johnson, L.N. (2012). The structural basis for control of eukaryotic protein kinases. Annu Rev Biochem *81*, 587-613.

Fang, Z., Grutter, C., and Rauh, D. (2013). Strategies for the selective regulation of kinases with allosteric modulators: exploiting exclusive structural features. ACS chemical biology *8*, 58-70.

Fields, S., and Song, O. (1989). A novel genetic system to detect protein-protein interactions. Nature *340*, 245-246.

Fontes, G., Semache, M., Hagman, D.K., Tremblay, C., Shah, R., Rhodes, C.J., Rutter, J., and Poitout, V. (2009). Involvement of Per-Arnt-Sim Kinase and extracellular-regulated kinases-1/2 in palmitate inhibition of insulin gene expression in pancreatic beta-cells. Diabetes *58*, 2048-2058.

Gallinetti, J., Harputlugil, E., and Mitchell, J.R. (2013). Amino acid sensing in dietary-restriction-mediated longevity: roles of signal-transducing kinases GCN2 and TOR. The Biochemical journal *449*, 1-10.

Graves, L.M., Duncan, J.S., Whittle, M.C., and Johnson, G.L. (2013). The dynamic nature of the kinome. The Biochemical journal *450*, 1-8.

Grose, J.H., and Rutter, J. (2010). The role of PAS kinase in PASsing the glucose signal. Sensors (Basel) *10*, 5668-5682.

Grose, J.H., Smith, T.L., Sabic, H., and Rutter, J. (2007). Yeast PAS kinase coordinates glucose partitioning in response to metabolic and cell integrity signaling. EMBO J *26*, 4824-4830.

Grose, J.H., Sundwall, E., and Rutter, J. (2009). Regulation and function of yeast PAS kinase: a role in the maintenance of cellular integrity. Cell Cycle *8*, 1824-1832.

Hao, H.X., Cardon, C.M., Swiatek, W., Cooksey, R.C., Smith, T.L., Wilde, J., Boudina, S., Abel, E.D., McClain, D.A., and Rutter, J. (2007). PAS kinase is required for normal cellular energy balance. Proc Natl Acad Sci U S A *104*, 15466-15471.

Hao, H.X., and Rutter, J. (2008). The role of PAS kinase in regulating energy metabolism. IUBMB Life *60*, 204-209.

Hardie, D.G. (2007). AMP-activated/SNF1 protein kinases: conserved guardians of cellular energy. Nature reviews Molecular cell biology *8*, 774-785.

Haynes, B.C., Maier, E.J., Kramer, M.H., Wang, P.I., Brown, H., and Brent, M.R. (2013). Mapping functional transcription factor networks from gene expression data. Genome research *23*, 1319-1328.

Hedbacker, K., and Carlson, M. (2008). SNF1/AMPK pathways in yeast. Frontiers in bioscience : a journal and virtual library *13*, 2408-2420.

James, P., Halladay, J., and Craig, E.A. (1996). Genomic libraries and a host strain designed for highly efficient two-hybrid selection in yeast. Genetics *144*, 1425-1436.

Jessulat, M., Pitre, S., Gui, Y., Hooshyar, M., Omidi, K., Samanfar, B., Tan le, H., Alamgir, M., Green, J., Dehne, F.*, et al.* (2011). Recent advances in protein-protein interaction prediction: experimental and computational methods. Expert opinion on drug discovery *6*, 921-935.

Johnson, M., Zaretskaya, I., Raytselis, Y., Merezhuk, Y., McGinnis, S., and Madden, T.L. (2008). NCBI BLAST: a better web interface. Nucleic acids research *36*, W5-9.
Johnson, S.A., and Hunter, T. (2005). Kinomics: methods for deciphering the kinome. Nature methods *2*, 17-25.

Käll, L., Canterbury, J.D., Weston, J., Noble, W.S., and MacCoss, M.J. (2007). Semi-supervised learning for peptide identification from shotgun proteomics datasets. Nature Methods *4*, 923-925.

Kean, M.J., Couzens, A.L., and Gingras, A.C. (2012). Mass spectrometry approaches to study mammalian kinase and phosphatase associated proteins. Methods *57*, 400-408.

Knight, J.D., Pawson, T., and Gingras, A.C. (2012). Profiling the kinome: Current capabilities and future challenges. Journal of proteomics.

Kolaczkowski, M., Kolaczkowska, A., Gaigg, B., Schneiter, R., and Moye-Rowley, W.S. (2004). Differential regulation of ceramide synthase components LAC1 and LAG1 in Saccharomyces cerevisiae. Eukaryot Cell *3*, 880-892.

Kuras, L., Barbey, R., and Thomas, D. (1997). Assembly of a bZIP-bHLH transcription activation complex: formation of the yeast Cbf1-Met4-Met28 complex is regulated through Met28 stimulation of Cbf1 DNA binding. The EMBO journal *16*, 2441-2451.

Kuras, L., Cherest, H., Surdin-Kerjan, Y., and Thomas, D. (1996). A heteromeric complex containing the centromere binding factor 1 and two basic leucine zipper factors, Met4 and Met28, mediates the transcription activation of yeast sulfur metabolism. The EMBO journal *15*, 2519-2529.

Kuras, L., and Thomas, D. (1995). Identification of the yeast methionine biosynthetic genes that require the centromere binding factor 1 for their transcriptional activation. FEBS letters *367*, 15-18.

Lal, H., Kolaja, K.L., and Force, T. (2013). Cancer genetics and the cardiotoxicity of the therapeutics. Journal of the American College of Cardiology *61*, 267-274.

Lin, Z., Wang, T.Y., Tsai, B.S., Wu, F.T., Yu, F.J., Tseng, Y.J., Sung, H.M., and Li, W.H. (2013). Identifying cis-regulatory changes involved in the evolution of aerobic fermentation in yeasts. Genome biology and evolution *5*, 1065-1078.

Loewith, R., and Hall, M.N. (2011). Target of rapamycin (TOR) in nutrient signaling and growth control. Genetics *189*, 1177-1201.

Longtine, M.S., McKenzie, A., 3rd, Demarini, D.J., Shah, N.G., Wach, A., Brachat, A., Philippsen, P., and Pringle, J.R. (1998). Additional modules for versatile and economical PCR-based gene deletion and modification in Saccharomyces cerevisiae. Yeast *14*, 953-961.

MacDonald, P.E., and Rorsman, P. (2011). Per-arnt-sim (PAS) domain kinase (PASK) as a regulator of glucagon secretion. Diabetologia *54*, 719-721.

Makino, T., and McLysaght, A. (2012). Positionally biased gene loss after whole genome duplication: evidence from human, yeast, and plant. Genome Res *22*, 2427-2435.

Marcilla, M., and Albar, J.P. (2013). Quantitative proteomics: A strategic ally to map protein interaction networks. IUBMB life *65*, 9-16.

Mok, J., Zhu, X., and Snyder, M. (2011). Dissecting phosphorylation networks: lessons learned from yeast. Expert review of proteomics *8*, 775-786.

Naukkarinen, J., Ehnholm, C., and Peltonen, L. (2006). Genetics of familial combined hyperlipidemia. Curr Opin Lipidol *17*, 285-290.

O'Connell, K.F., and Baker, R.E. (1992). Possible cross-regulation of phosphate and sulfate metabolism in Saccharomyces cerevisiae. Genetics *132*, 63-73.

Pajukanta, P., Lilja, H.E., Sinsheimer, J.S., Cantor, R.M., Lusis, A.J., Gentile, M., Duan, X.J., Soro-Paavonen, A., Naukkarinen, J., Saarela, J.*, et al.* (2004). Familial combined hyperlipidemia is associated with upstream transcription factor 1 (USF1). Nat Genet *36*, 371-376.

Park, D., Singh, R., Baym, M., Liao, C.S., and Berger, B. (2011). IsoBase: a database of functionally related proteins across PPI networks. Nucleic acids research *39*, D295-300.

Perkins, D.N., Pappin, D.J., Creasy, D.M., and Cottrell, J.S. (1999). Probability-based protein identification by searching sequence databases using mass spectrometry data. Electrophoresis *20*, 3551-3567.

Petti, A.A., McIsaac, R.S., Ho-Shing, O., Bussemaker, H.J., and Botstein, D. (2012). Combinatorial control of diverse metabolic and physiological functions by transcriptional regulators of the yeast sulfur assimilation pathway. Mol Biol Cell *23*, 3008-3024.

Rajagopala, S.V., Sikorski, P., Caufield, J.H., Tovchigrechko, A., and Uetz, P. (2012). Studying protein complexes by the yeast two-hybrid system. Methods *58*, 392-399.

Robinson, M.D., Grigull, J., Mohammad, N., and Hughes, T.R. (2002). FunSpec: a web-based cluster interpreter for yeast. BMC Bioinformatics *3*, 35.

Rutter, J., Probst, B.L., and McKnight, S.L. (2002). Coordinate regulation of sugar flux and translation by PAS kinase. Cell *111*, 17-28.

Schlafli, P., Troger, J., Eckhardt, K., Borter, E., Spielmann, P., and Wenger, R.H. (2011). Substrate preference and phosphatidylinositol monophosphate inhibition of the catalytic domain of the Per-Arnt-Sim domain kinase PASKIN. The FEBS journal *278*, 1757-1768.

Schroeder, M.J., Shabanowitz, J., Schwartz, J.C., Hunt, D.F., and Coon, J.J. (2004). A neutral loss activation method for improved phosphopeptide sequence analysis by quadrupole ion trap mass spectrometry. Anal Chem *76*, 3590-3598.

Semache, M., Zarrouki, B., Fontes, G., Fogarty, S., Kikani, C., Chawki, M.B., Rutter, J., and Poitout, V. (2013). Per-Arnt-Sim kinase regulates pancreatic duodenal homeobox-1 protein stability via phosphorylation of glycogen synthase kinase 3beta in pancreatic beta-cells. J Biol Chem *288*, 24825-24833.

Semplici, F., Vaxillaire, M., Fogarty, S., Semache, M., Bonnefond, A., Fontes, G., Philippe, J., Meur, G., Diraison, F., Sessions, R.B.*, et al.* (2011). Human Mutation within Per-Arnt-Sim (PAS) Domain-containing Protein Kinase (PASK) Causes Basal Insulin Hypersecretion. J Biol Chem *286*, 44005-44014.

Smith, T.L., and Rutter, J. (2007). Regulation of glucose partitioning by PAS kinase and Ugp1 phosphorylation. Mol Cell *26*, 491-499.

Sopko, R., and Andrews, B.J. (2008). Linking the kinome and phosphorylome--a comprehensive review of approaches to find kinase targets. Molecular bioSystems *4*, 920-933.

Taylor, S.S., Yang, J., Wu, J., Haste, N.M., Radzio-Andzelm, E., and Anand, G. (2004). PKA: a portrait of protein kinase dynamics. Biochimica et biophysica acta *1697*, 259-269.

Thomas, D., Jacquemin, I., and Surdin-Kerjan, Y. (1992). MET4, a leucine zipper protein, and centromere-binding factor 1 are both required for transcriptional activation of sulfur metabolism in Saccharomyces cerevisiae. Mol Cell Biol *12*, 1719-1727.

Wilson, W.A., Skurat, A.V., Probst, B., de Paoli-Roach, A., Roach, P.J., and Rutter, J. (2005). Control of mammalian glycogen synthase by PAS kinase. Proc Natl Acad Sci U S A *102*, 16596-16601.

Winzeler, E.A., Shoemaker, D.D., Astromoff, A., Liang, H., Anderson, K., Andre, B., Bangham, R., Benito, R., Boeke, J.D., Bussey, H.*, et al.* (1999). Functional characterization of the S. cerevisiae genome by gene deletion and parallel analysis. Science *285*, 901-906.

Wisniewski, J.R., Zougman, A., Nagaraj, N., and Mann, M. (2009). Universal sample preparation method for proteome analysis. Nat Methods *6*, 359-362.

Zhang, L., and Daly, R.J. (2012). Targeting the human kinome for cancer therapy: current perspectives. Critical reviews in oncogenesis *17*, 233-246.

Zhou, X., and O'Shea, E.K. (2011). Integrated approaches reveal determinants of genome-wide binding and function of the transcription factor Pho4. Molecular cell *42*, 826-836.

# CHAPTER 3: PAS kinase is activated by direct SNF1-dependent phosphorylation and mediates inhibition of TORC1 through the phosphorylation and activation of Pbp1

Desiree DeMille[a], Bryan D. Badal[a], J. Brady Evans[a], Andrew D. Mathis[b], Joseph F. Anderson[a], and Julianne H. Grose[a]

[a]Department of Microbiology and Molecular Biology and [b]Department of Chemistry, Brigham Young University, Provo, UT 84602

*Address correspondence to:

Julianne H. Grose
Department of Microbiology and Molecular Biology
Brigham Young University, Provo, UT 84602
E-mail: julianne_grose@byu.edu

ABSTRACT

We describe the interplay between three sensory protein kinases in yeast: AMP-regulated kinase (AMPK, or SNF1 in yeast), PAS kinase 1 (Psk1 in yeast), and the target of rapamycin complex 1 (TORC1). This signaling cascade occurs through the SNF1-dependent phosphorylation and activation of Psk1, which phosphorylates and activates poly(A)-binding protein binding protein 1 (Pbp1), which then inhibits TORC1 through sequestration at stress granules. The SNF1-dependent phosphorylation of Psk1 appears to be direct, in that Snf1 is necessary and sufficient for Psk1 activation by alternate carbon sources, is required for altered Psk1 protein mobility, is able to phosphorylate Psk1 in vitro, and binds Psk1 via its substrate-targeting subunit Gal83. Evidence for the direct phosphorylation and activation of Pbp1 by Psk1 is also provided by in vitro and in vivo kinase assays, including the reduction of Pbp1 localization at distinct cytoplasmic foci and subsequent rescue of TORC1 inhibition in PAS kinase–deficient yeast. In support of this signaling cascade, Snf1-deficient cells display increased TORC1 activity, whereas cells containing hyperactive Snf1 display a PAS kinase–dependent decrease in TORC1 activity. This interplay between yeast SNF1, Psk1, and TORC1 allows for proper glucose allocation during nutrient depletion, reducing cell growth and proliferation when energy is low.

INTRODUCTION

Nutrient-sensing kinases maintain metabolic homeostasis by allocating cellular resources in response to nutrient status. Their ability to control multiple central metabolic pathways has made them the target of many therapeutic approaches, including treatments for cancer and diabetes (Eglen and Reisine, 2011; Zhang and Daly, 2012; Fang et al., 2013; Lal et al., 2013;

Rosilio et al., 2014). This study focuses on the interplay between three evolutionarily conserved nutrient kinases—target of rapamycin complex 1 (TORC1), AMP-regulated kinase (AMPK, known as SNF1 in yeast), and PAS kinase (PASK, or Psk1 in yeast)—which all play critical roles in maintaining cellular homeostasis. TOR forms two distinct complexes in yeast and mammalian cells, TOR complex 1 (TORC1) and 2 (TORC2), and regulates cell growth and proliferation in response to a variety of signals, including nitrogen, amino acids, insulin, growth factors, and stress factors (due to the immense literature, only recent reviews are provided: Laplante and Sabatini, 2012; Porta et al., 2014; Shimobayashi and Hall, 2014). AMPK/SNF1 regulates energy production and consumption pathways in response to the cellular AMP:ATP ratio. High AMP levels, which indicates low cellular energy, activate AMPK to stimulate energy production pathways and down-regulate energy consumption pathways (for recent reviews, see Ghillebert et al., 2011; Broach, 2012; Hardie, 2013; Liu and Jiang, 2013; Burkewitz et al., 2014; Rosilio et al., 2014; Ye et al., 2014). Mammalian PAS kinase is regulated by glucose levels and is essential for glucose homeostasis, specifically through the control of metabolic rate, insulin/glucagon secretion, and lipid/glycogen storage (da Silva Xavier et al., 2004, 2011; Wilson et al., 2005; An et al., 2006; Hao et al., 2007; Semplici et al., 2011; Wu et al., 2014). In yeast, there are two PAS kinase homologs, Psk1 and Psk2, which play a conserved role in the regulation of respiration and glycogen storage (Rutter et al., 2002; Grose et al., 2007, 2009; Smith and Rutter, 2007; DeMille et al., 2014). These kinases coordinate cellular energy and nutrient availability with central metabolism, making cross-talk between these pathways essential for optimal cellular health.

The interplay between AMPK/SNF1 and TORC1 is documented in several studies. In mammals, activated AMPK inhibits TOR function through direct phosphorylation of the TORC1

subunit RAPTOR (Bolster et al., 2002; Kimura et al., 2003; Cheng et al., 2004; Reiter et al., 2005), as well as the phosphorylation and stabilization of tuberous sclerosis complex 2 (TSC2), a negative regulator of TORC1 (Inoki et al., 2003a,b). This inhibition of TORC1 by AMPK appears to be conserved in yeast, in which glucose starvation has recently been shown to inhibit TORC1 in a SNF1-dependent manner (Hughes Hallett et al., 2014).

There are also reported connections between PAS kinase, AMPK, and TORC1/2 in both mammalian and yeast cells. The TORC1 inhibitor TSC2 is activated by glycogen synthase kinase 3 (GSK3; Inoki et al., 2003b, 2006), and GSK3 is in turn inhibited by PAS kinase–dependent phosphorylation (Semache et al., 2013). These results suggest that PAS kinase may act as a progrowth signal in mammalian cells through the activation of TORC1. In support of this pro-growth association, PAS kinase overexpression suppresses a temperature-sensitive mutation of TOR2 in yeast (*tor2*$^{ts}$; Cardon et al., 2012). In addition, PAS kinase was recently shown to be required for proper activation of AMPK and mTOR in the hypothalamus, where AMPK activation by nutrient depletion and TORC1 activation by refeeding are both blunted in PASK-/- mice (Hurtado-Carneiro et al., 2013, 2014). The converse association is found in yeast, in which AMPK/SNF1 is required for the activation of PAS kinase by non-glucose carbon sources (Grose et al., 2007). These studies solidify communication between AMPK, PAS kinase, and TORC1/2 and highlight the many overlapping complexities. Such overlap is expected to be extensive and complex, given the various mechanisms by which each kinase is activated and the importance of coordinating cellular energy and growth.

Here we provide molecular evidence for the Psk1-dependent interplay between AMPK/SNF1 and TORC1 in yeast. Both in vivo and in vitro assays support the direct phosphorylation and activation of Psk1 by Snf1. Once activated, Psk1 may phosphorylate

poly(A)-binding protein binding protein 1 (Pab1 binding protein, or Pbp1), which is known to stimulate stress granule formation and inhibit TORC1 through sequestration (Takahara and Maeda, 2012). This phosphorylation is seen through direct in vitro phosphorylation assays, as well as in vivo phosphostate and phenotypic analysis. Finally, evidence is provided for the entire cascade, with SNF1 inhibiting TORC1 in a Psk1-dependent manner. Together these results support PAS kinase as a link between energy status and cell growth/proliferation, being activated by AMPK/SNF1 under nutrient/energy depletion and inhibiting cell growth/proliferation through the phosphorylation of Pbp1.

## RESULTS

### Evidence for in vivo phosphorylation and activation of Psk1 by SNF1

As mentioned, SNF1 is the master and commander of the fermentation/respiration switch in yeast and is required for the activation of Psk1 by non-glucose carbon sources (Grose et al., 2007). We recently retrieved Snf1 and two of its subunits (Gal83 and Sip2) from a large-scale screen for Psk1 binding partners (DeMille et al., 2014), suggesting that this activation is direct. To test for direct phosphorylation, in vivo Psk1 activity and phosphorylation state were monitored in response to SNF1 activation or depletion.

If this SNF1-dependent activation is due to direct phosphorylation rather than transcriptional regulation, the time required to activate Psk1 should be minimal. In support of direct in vivo phosphorylation, Psk1 was activated within 1 min of shifting cells from glucose to raffinose (Figure 3.1A), as determined by monitoring in vivo phosphorylation of the well-characterized substrate UDP-glucose pyrophosphorylase (Ugp1; Rutter et al., 2002; Smith and Rutter, 2007; Grose et al., 2009; Cardon et al., 2012). To provide further in vivo evidence, Psk1

was purified from wild type (WT), Snf1-deficient (*snf1*), and SNF1-hyperactive (*reg1*) yeast grown in galactose (to induce expression of Psk1 from the GAL1-10 promoter due to low endogenous levels), and analyzed by SDS–PAGE electrophoretic mobility shift assay (EMSA; Figure 3.1B). Reg1 is an inhibitor of SNF1 that promotes dephosphorylation by protein phosphatase 1 (Ludin et al., 1998), making SNF1 constitutively active in Reg1-deficient yeast. An obvious mobility shift was observed between samples, indicating a SNF1-dependent protein modification. The shift is dramatic for such a large protein, suggesting a modification other than a single phosphorylation event. Mass spectrometry confirmed multisite phosphorylation. Samples from the WT, *reg1*, and *snf1* cells were submitted for mass spectrometry analysis and 17 phosphorylation sites were identified that appeared to be Snf1-dependent (S10, S101, S185, S202, S255, S307, T453, T496, T717, T919, S953, S992, S996, S1020, T1021, S1035, S1094). No other modifications were detected.

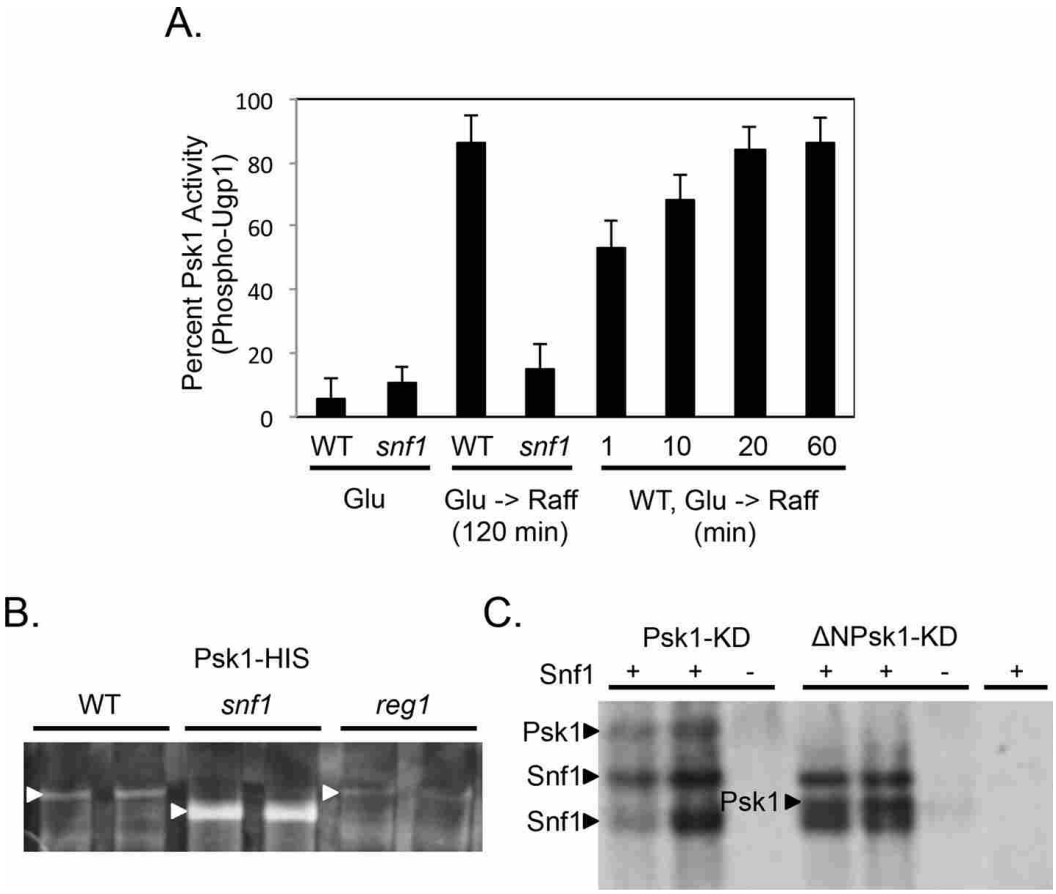


FIGURE 3.1. (A, B) In vivo and (C) in vitro evidence for Psk1 phosphorylation and activation by Snf1. (A) Psk1 is activated quickly by a nonfermenting carbon source in a Snf1-dependent manner. Yeast (*PSK1psk2*, JGY3) growing in YPAD (Glu) were transferred to a nonfermenting carbon source (YPAraffinose, Raff) for the indicated time (minutes). Psk1 activity was measured by assessing Ugp1 phosphorylation in crude yeast extracts by a monoQ fractionation as previously described (Smith and Rutter, 2007). (B) Psk1 protein displays a gel shift when purified from cells expressing Snf1. HIS-HA epitope-tagged Psk1 was purified from WT, Snf1-deficient (*snf1*), and SNF1-hyperactive (*reg1*) cells grown in galactose, analyzed by 8% SDS–PAGE, and visualized by silver stain. (C) Snf1 directly phosphorylates Psk1 in vitro. Full-length (Psk1-KD [D1230A]) and truncated (ΔN931Psk1-KD [D1230A]) kinase-dead Psk1 were incubated with Snf1 and $^{32}$P-ATP. Autoradiograms of SDS–PAGE gels are shown, and Snf1-dependent incorporation of $^{32}$P-ATP is seen in both Psk1 constructs. Kinase-dead Psk1 was used to prevent autophosphorylation. Coomassie blue–stained gels are not shown due to low protein expression, making it difficult to visualize by staining, but all proteins are the expected size.

Evidence for direct phosphorylation and activation of Psk1 by Snf1

To determine whether the phosphorylation and activation of Psk1 is direct, we performed in vitro phosphorylation assays. Kinase-dead Psk1 (D1230A; DeMille et al., 2014) was purified and subjected to in vitro kinase assays with purified Snf1. PAS kinase is known to auto-

phosphorylate in vitro (Rutter et al., 2001), making the kinase-dead mutant vital to ensure Snf1-dependent phosphorylation. Snf1-dependent Psk1 phosphorylation was seen in these in vitro assays (Figure 3.1C). These results confirm direct phosphorylation of Psk1 by Snf1.

PAS kinase contains a sensory N-terminal PAS domain and the C-terminal canonical serine/threonine kinase domain. In the model for PAS kinase regulation, the PAS domain binds and inhibits the kinase domain (Amezcua et al., 2002). Phosphorylation of the PAS or kinase domain may disrupt such binding, activating the kinase. To determine domains necessary for Snf1-depedent phosphorylation, we used a truncated Psk1 bearing the kinase-only domain (ΔN931Psk1-KD [D1230A]; Figure 3.1C). Snf1 was able to phosphorylate even this kinase-only construct, suggesting that Snf1 phosphorylates Psk1 in the kinase domain. However, due to the large number of phosphorylation sites identified in the kinase domain (seven total), mapping the critical phosphorylation site(s) will require further study.

Evidence for an in vivo interaction between Psk1 and Snf1

As mentioned, Snf1 and two of its three β-subunits (Gal83 and Sip2) were retrieved as in vivo binding partners of Psk1 through copurification liquid chromatography–electrospray tandem mass spectrometry (LC–MS/MS) studies (DeMille et al., 2014). An active SNF1 complex consists of three subunits: one of the three β-subunits (Gal83, Sip2, or Sip1), the Snf1 catalytic subunit, and the regulatory Snf4 subunit. Because copurification can retrieve large protein complexes, direct interaction between Psk1 and Snf1, Gal83, or Sip2 was examined via the yeast two-hybrid (Y2H) system. All three proteins were cloned into both the Y2H prey and bait plasmids (James et al., 1996) and tested for interaction using a Psk1 bait or prey plasmid, respectively (Figure 3.2A). The Y2HGold strain was used, which harbors four different

reporters (ADE2, HIS3, AUR1-C, MEL1) under three different Gal4-responsive promoters (Clontech), and transformed yeast were spotted onto selective media for protein–protein interactions, as well as for plasmid maintenance (media lacking histidine and adenine, as well as tryptophan and leucine, respectively). Note that all constructs were tested with their corresponding empty vector control and were negative. A direct interaction was detected between Psk1 and Gal83 but not Sip2 or Snf1. These results are not surprising, given that the Gal83 and Sip2 β-subunits of Snf1 are each responsible for binding a subset of its targets (Vincent and Carlson, 1999; Schmidt and McCartney, 2000). Whereas a strong interaction was seen between Psk1 and Gal83 when Gal83 was used as the bait, no interaction was observed when Gal83 was used as the prey, suggesting a nonfunctional construct. The Psk1/Gal83 interaction was also strong when using either full-length Psk1 or a truncation removing the PAS domain (ΔN692Psk1). This interaction supports the in vitro phosphorylation of the kinase-only Psk1 construct observed in Figure 3.1C.

Previous Y2H interactions of Psk1 with its substrates were detected using the ΔN692Psk1 but not the full-length Psk1 construct (DeMille et al., 2014). The Psk1/Gal83 interaction is different, in that both full-length and truncated Psk1 bound Gal83. This finding lends additional support for Psk1 being a substrate of SNF1 rather than an upstream kinase.

The Gal83 protein was then truncated to determine the regions required for interaction with Psk1 (Figure 3.2, B and C). Gal83 has three main regions: an N-terminal region containing a glycogen-binding domain (amino acids [aa] 1–141), which has been shown to mediate the interaction between Snf1 and Reg1 (Momcilovic et al., 2008); a “Snf1-binding domain” (aa 141–343); and a C-terminal “Snf4-interacting domain” (aa 343–417; Jiang and Carlson, 1997). The Gal83 Snf1-binding domain was clearly necessary for the Gal83 Psk1 interaction (Figure 3.2C).

This direct in vivo interaction, combined with the foregoing in vivo and in vitro phosphorylation and activation assays, affords strong evidence for the direct phosphorylation and activation of Psk1 by Snf1.

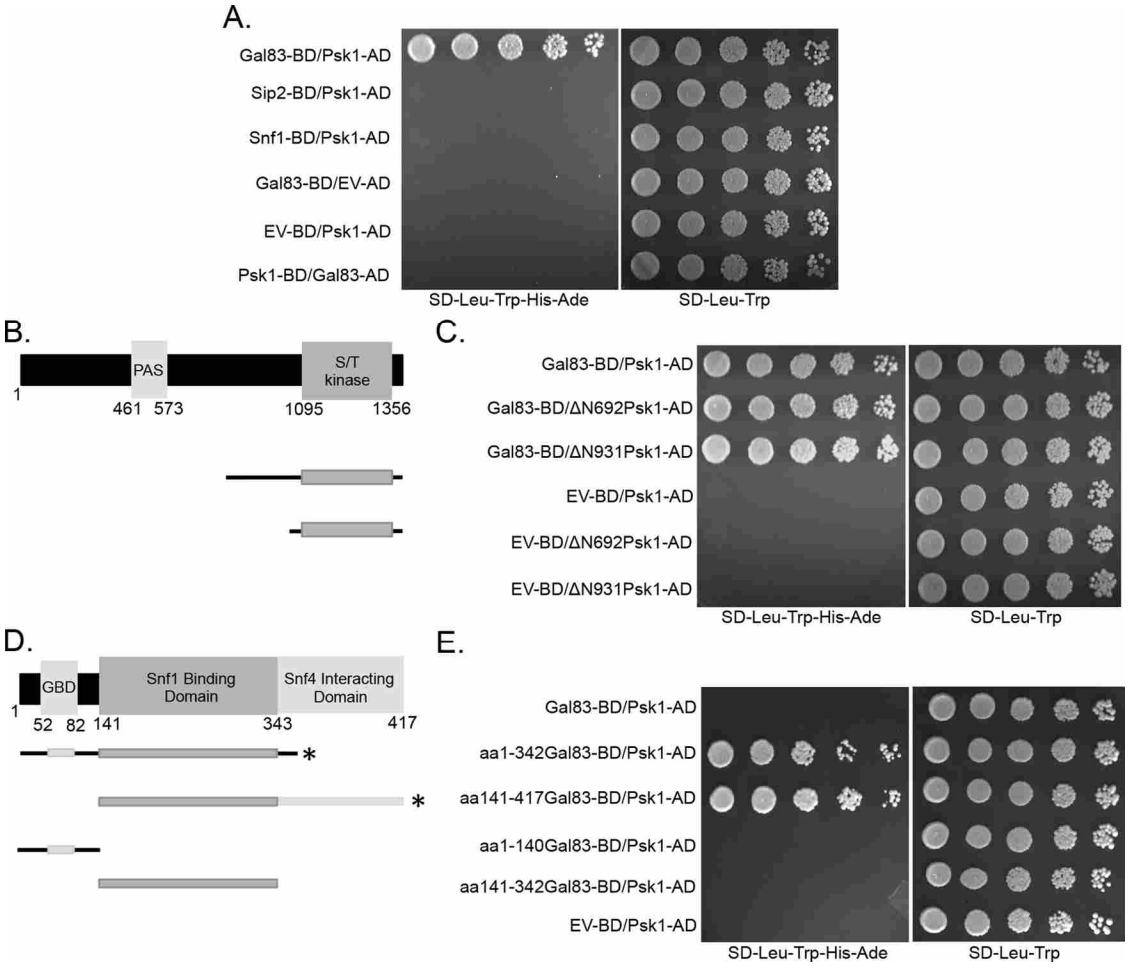


FIGURE 3.2. Yeast two-hybrid assays reveal an interaction between the Gal83 Snf1-binding domain and the Psk1 kinase domain. (A) The SNF1 complex subunit Gal83, but not Sip2 or Snf1, interacts with full-length Psk1. Y2HGold cells (Clontech) containing the Gal83 (pJG1236 or pJG1237), Sip2 (pJG1238 or pJG1239), and Snf1 (pJG1240 or pJG1241) bait (BD) and prey (AD) plasmids, respectively, were cotransformed with bait and prey plasmids harboring full-length Psk1 (pJG441 or pJG442) or empty vector (pJG424 or pJG421). Only representative interactions are shown (all other combinations of bait and prey were negative). (B) Psk1 truncations used to screen for interactions with Gal83 are diagrammed. (C) Gal83 interacts with truncated versions of Psk1 that harbor the kinase domain. Y2HGold cells were cotransformed with bait plasmids harboring either Gal83 (pJG1236) or the empty vector (pJG424), and prey plasmids harboring truncations of Psk1 (ΔN692Psk1 [pJG709] or ΔN931Psk1 [pJG1276]). (D) The Snf1-binding domain is necessary for interaction with Psk1. Truncations used to screen for the Gal83 domains necessary for Psk1 binding are diagrammed. Constructs are marked with an asterisk if any binding to Psk1 was detected in the Y2H assays shown in E. (E) Y2HGold cells containing the Psk1 prey

plasmid (pJG442) were cotransformed with bait plasmids harboring full-length Gal83 (pJG1236), truncated Gal83 (aa 1–342 [pJG1258], 141–417 [pJG1260], 1–140 [pJG1262], 141–342 [pJG1264]), or empty vector (pJG424). Overnight samples were grown in SD-Leu-Trp for plasmid maintenance, diluted fivefold serially, and plated on Y2H selective medium (SD-Leu-Trp-His-Ade), as well as on a control plate (SD-Leu-Trp). Plates were incubated at 30°C for 3–4 d.

Evidence for direct phosphorylation of Pbp1 by Psk1

In addition to Snf1 and its subunits, Pbp1 was recently identified as a Psk1 binding partner (DeMille et al., 2014). Although Pbp1 was retrieved from both yeast two-hybrid and copurification screens, we did not observe phosphorylation of full-length Pbp1 when purified from bacteria (DeMille et al., 2014) or yeast (unpublished data). However, the Y2H retrieved two truncations of Pbp1 (ΔN196Pbp1 and ΔN355Pbp1), and when a further truncated (ΔN419Pbp1) Pbp1 was used in the in vitro kinase assays, a strong phosphorylation was observed (Figure 3.3A). The ability of Psk1 to phosphorylate the truncated but not full-length Pbp1 suggests that Pbp1 may adopt different conformations regulated by its N-terminal end.

Pbp1 contains three regions: the Sm domain, the LSmAD domain, and the self-interaction region (Figure 3.3B). The Sm (Sm-ATX or LSm) domain is required for interaction with other proteins, namely Lsm12, Pbp4, and Rpl12a. The LSmAD domain is usually associated with Sm domains and enhances protein binding, and the self-interaction region is required for binding Pab1 and itself (Mangus et al., 2004; Kimura et al., 2013). To map the Pbp1 regions necessary for Psk1 interaction, we tested several Pbp1 truncations via the Y2H assay (Figures 3.3, B and C; note that all constructs were tested with their corresponding empty vector control and were negative). The results mirrored the in vitro kinase assays, in that Psk1 was not able to bind the full-length Pbp1 protein but bound truncated constructs in which the N-terminal 196 amino acids were removed. Larger N-terminal truncations were made to further characterize the minimal region necessary for interaction. Removal of the N-terminal 419 amino acids still allowed for a

Psk1 interaction, whereas removal of the N-terminal 469 amino acids did not. Further attempts to narrow in on the essential interaction region of Pbp1 by creating C-terminal truncations in the self-interaction domain (removing aa 420-722, 566–722, 581–722, or 661– 722) did not result in constructs that interact, even when the N-terminus was also removed. Thus the Pbp1 self-interaction region (aa 420–722) is necessary for in vivo association with Psk1, whereas the N-terminal Sm region (aa 1–197) of Pbp1 appears to inhibit interaction. Because this C-terminal region is involved in enhancing protein binding (Mangus et al., 2004; Kimura et al., 2013), the phosphorylation of Pbp1 by Psk1 may either enhance or inhibit its activity.

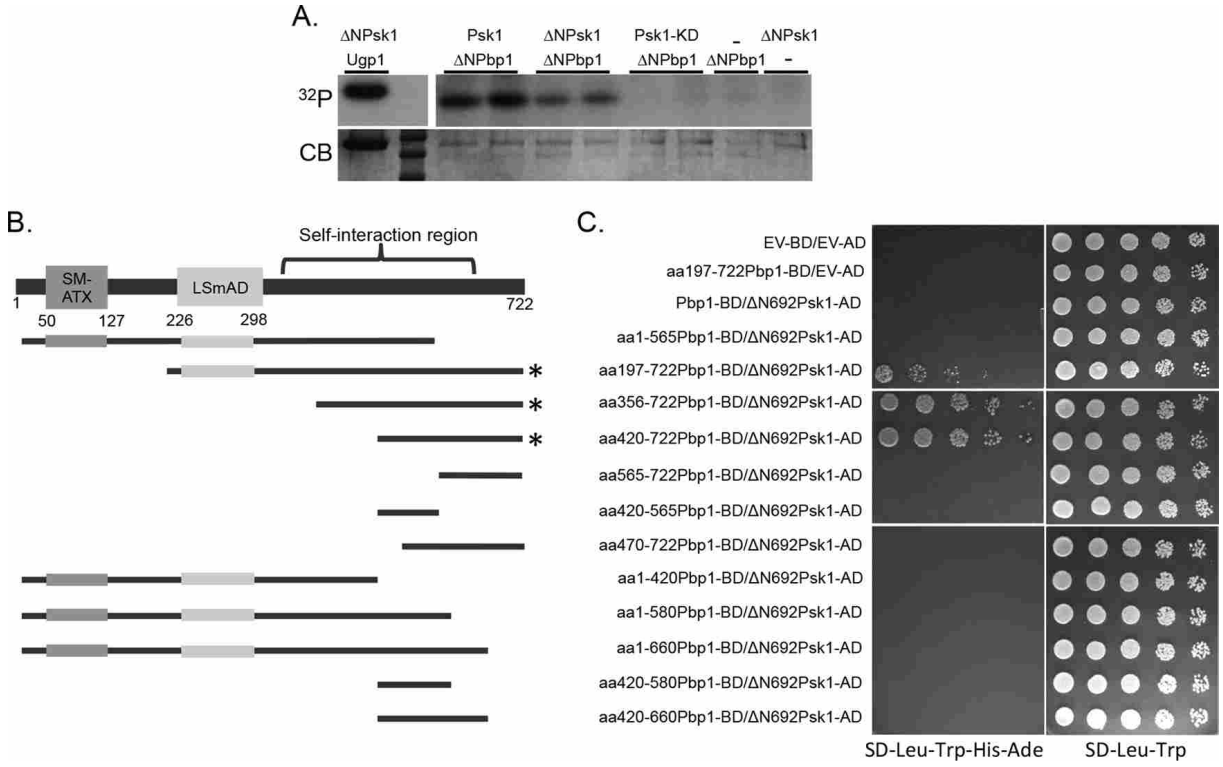


FIGURE 3.3. Evidence for direct phosphorylation of Pbp1 by Psk1. (A) Truncated Pbp1 (ΔN419Pbp1, aa 420–722, pJG1250) was shown to be phosphorylated in vitro when incubated in the presence of either full-length (pJG1181) or truncated (ΔN931Psk1, pJG1216) Psk1 but not with the kinase-dead mutant (Psk1-KD, pJG1215). In vitro kinase assays using purified Pbp1 protein incubated with radiolabeled ATP ($^{32}$P) in the presence or absence of purified Psk1. Reactions were visualized on 15% SDS–PAGE gels, stained with Coomassie brilliant blue (CB; bottom), and exposed on x-ray film ($^{32}$P; top). Ugp1 (a positive control) and Pbp1 were run on the same gel, but the film was developed differently due to varying signal strength. (B) A diagram of the Pbp1 protein, including the conserved domains. The C-

terminal portion of the protein is known as the self-interaction region. The Pbp1 truncations tested in the yeast two-hybrid are diagrammed, and those that interacted with Psk1 are marked with an asterisk. (C) Mapping the Psk1-binding region of Pbp1 reveals an inhibitory N-terminus and a required C-terminal region between aa 420 and 722. The Y2H prey vector containing full-length Pbp1 (pJG1008), Pbp1 truncations (aa 1–565 Pbp1 [pJG1168], 197–722 Pbp1 [pJG1002], 356–722 Pbp1 [pJG1001], 420–722 Pbp1 [pJG1003], 565–722 Pbp1 [pJG1004], 420–565 Pbp1 [pJG1169], 470–722 Pbp1 [pJG1195], 1–420 Pbp1 [pJG1196], 1–580 Pbp1 [pJG1197], 1–660 Pbp1 [pJG1198], 420–580 Pbp1 [pJG1230], and 420–660 Pbp1 [pJG1231]) or empty vector (EV, pJG423) were expressed in yeast (JGY1031) along with the empty vector (EV, pJG425) or ΔN692Psk1 (pJG598) bait plasmid. Overnight samples were grown in SD-Leu-Trp for plasmid maintenance, diluted fivefold serially, and plated on Y2H selective medium (SD-Leu-Trp-His-Ade), as well as on a control plate (SD-Leu-Trp). Plates were grown at 30°C for 2–5 d.

Evidence for in vivo phosphorylation and activation of Pbp1 by Psk1

The combined evidence of in vivo protein–protein interaction with in vitro kinase assays makes Pbp1 a high-confidence cellular Psk1 substrate. To determine whether Pbp1 is phosphorylated by Psk1 in vivo, we monitored the Psk1-dependent phosphorylation of Pbp1 through nonspecific PhosphoThreonine (Cell Signaling Technology) or PhosphoSerine (Q5; Qiagen) antibodies (Figure 3.4A). HIS-HA epitope-tagged Pbp1 was purified from yeast grown on galactose, and a Western blot revealed Psk1-dependent phosphorylation of at least one threonine residue, whereas phosphoserine presence was independent of Psk1. Phosphorylation state was assessed in cells deficient in both Psk1 and Psk2 (*PSK1PSK2* deficient) as compared with WT because both Psk1 and Psk2 phosphorylate the well-characterized PAS kinase substrate Ugp1. Psk2 is unlikely to phosphorylate Pbp1 in this study, however, because Psk2 is not expressed on carbon sources other than glucose, and is thus not activated by Snf1 (Grose et al., 2007). Therefore phosphorylation of Pbp1 grown in galactose is attributed to Psk1 activity.

To determine the effects of this phosphorylation on Pbp1 function, Pbp1-dependent caffeine sensitivity was assessed in WT and *PSK1PSK2*-deficient yeast. Pbp1 has been shown to inhibit TORC1 through its sequestration to stress granules (Takahara and Maeda, 2012), suggesting a role for PAS kinase in TORC1 regulation. This sequestration and inactivation of

TORC1 produces a caffeine sensitive phenotype. *PSK1PSK2* deficiency alleviates the caffeine sensitivity of cells overexpressing *PBP1*, consistent with Psk1-dependent activation of Pbp1 (Figure 3.4B). Combined these results suggest that Psk1 phosphorylates Pbp1 at a threonine residue, which activates Pbp1, inducing stress granule formation and subsequent TORC1 sequestration.

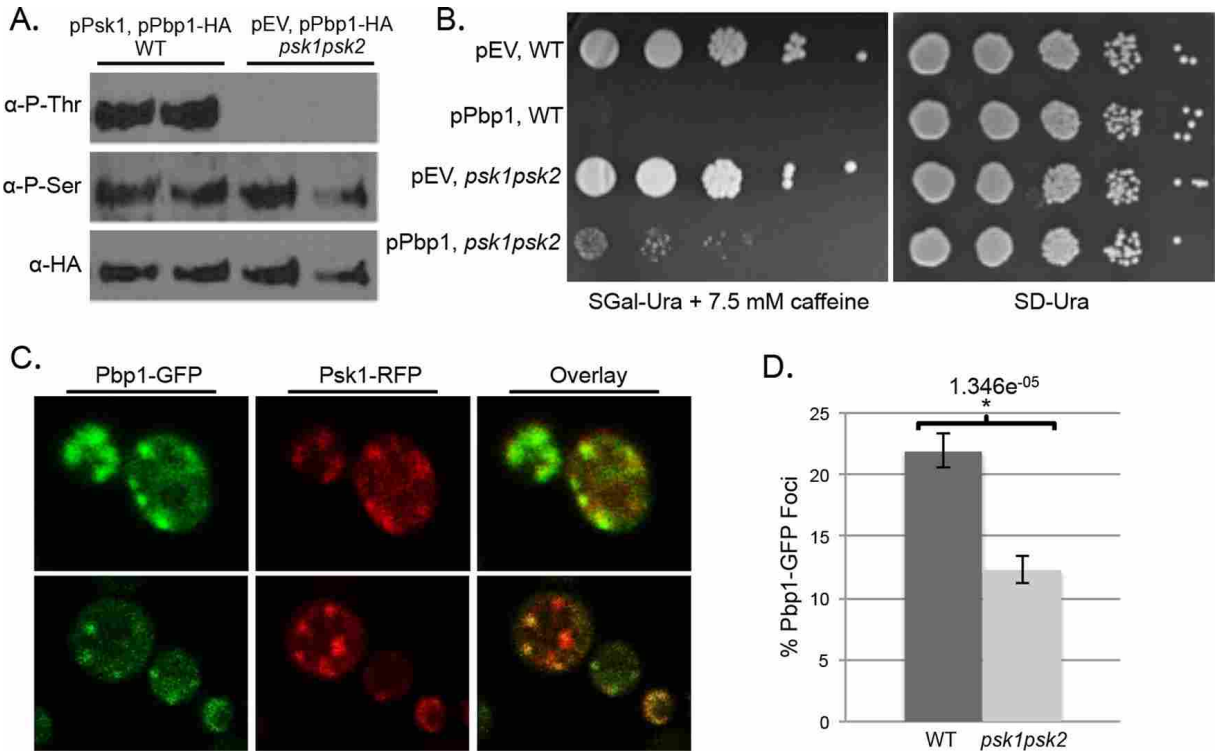


FIGURE 3.4. In vivo evidence for the activation of Pbp1 by Psk1. (A) Monitoring the in vivo phosphorylation state of Pbp1 reveals Psk1-dependent threonine phosphorylation. Purified HIS-HA epitope-tagged Pbp1 protein from WT cells (JGY1) overexpressing full-length Psk1 (pJG9) was compared with purified Pbp1 from *PSK1PSK2*-deficient cells (*psk1psk2*, JGY4) using anti-PhosphoThreonine (Cell Signaling Technology) and anti-PhosphoSerine antibodies (Q5; Qiagen). Anti-HA antibody (Roche) was used as a control for total Pbp1 protein. (B) *PSK1PSK2* deficiency ameliorates caffeine toxicity due to Pbp1 overexpression. Wild type (JGY299) or *psk1psk2* yeast (JGY1161) was transformed with an empty vector (EV, pJG859) or a plasmid overexpressing Pbp1 (pJG925), grown in SD-Ura, serially diluted 1:10, and spotted on SGal-Ura + 7.5 mM caffeine plates, as well as on a control SD-Ura plate. Plates were incubated at 30°C for 7–10 d until colonies were apparent. (C) Colocalization of Psk1 and Pbp1 to stress granules. Pbp1-GFP fusion yeast (Invitrogen) was transformed with Psk1-RFP (pJG1119), grown under glucose deprivation (SC medium lacking a carbon source), and imaged using an Olympus Fluoview confocal microscope. (D) Pbp1-GFP foci decrease significantly in *psk1psk2* (JGY1160) yeast compared with WT (JGY1144). For percentage of Pbp1-GFP foci, 1199 cells for WT and 782 for *psk1psk2* were counted. SEM was used for error bars, and Student's t test was used in statistical significance calculations.

Psk1 increases Pbp1 localization at cytoplasmic foci

The Pbp1-dependent localization of TORC1 to stress granules was previously shown by Takahara and Maeda (2012). To determine whether Psk1 also localizes to the same distinct cytoplasmic foci as Pbp1, red fluorescent protein (RFP)–tagged Psk1 was transformed into yeast containing Pbp1–green fluorescent protein (GFP). Cytoplasmic foci were induced by glucose deprivation, a condition known to induce both P-body and stress granule formation. Psk1 colocalized to distinct cytoplasmic foci with Pbp1 in ~74% of cells in which Pbp1-GFP foci were visible (Figure 3.4C).

The effect of PAS kinase on Pbp1 localization to distinct foci was then assessed. Pbp1-GFP foci were significantly reduced in the *psk1psk2* yeast when compared with WT (Figure 3.4D), suggesting that PAS kinase activates Pbp1 by increasing localization to stress granules or P-bodies.

Snf1 inhibits TORC1 phosphorylation of Sch9

We provided evidence for the Snf1-dependent phosphorylation and activation of Psk1, which then leads to the phosphorylation and activation of Pbp1, inhibiting TORC1. To further support this model, we monitored TORC1 activity in response to both Snf1 and PAS kinase. TORC1 activity was assessed through the in vivo phosphostate of the S6 kinase, Sch9, commonly used as a readout of TORC1 activity (Kingsbury et al., 2014; Urban et al., 2007). Sch9 is phosphorylated on glucose, and Snf1 is necessary and sufficient for its dephosphorylation, as shown through the increased phosphorylation seen in the Snf1-deficient strain (*snf1*) and the dramatic decrease seen in the hyperactive Snf1 strain (*reg1*; Figure 3.5). In addition, PAS kinase was shown to be essential for this apparent inhibition of TORC1, as seen

by dramatic increase in phosphorylation in *reg1* or *reg1snf1* yeast that are also Psk1Psk2 deficient.

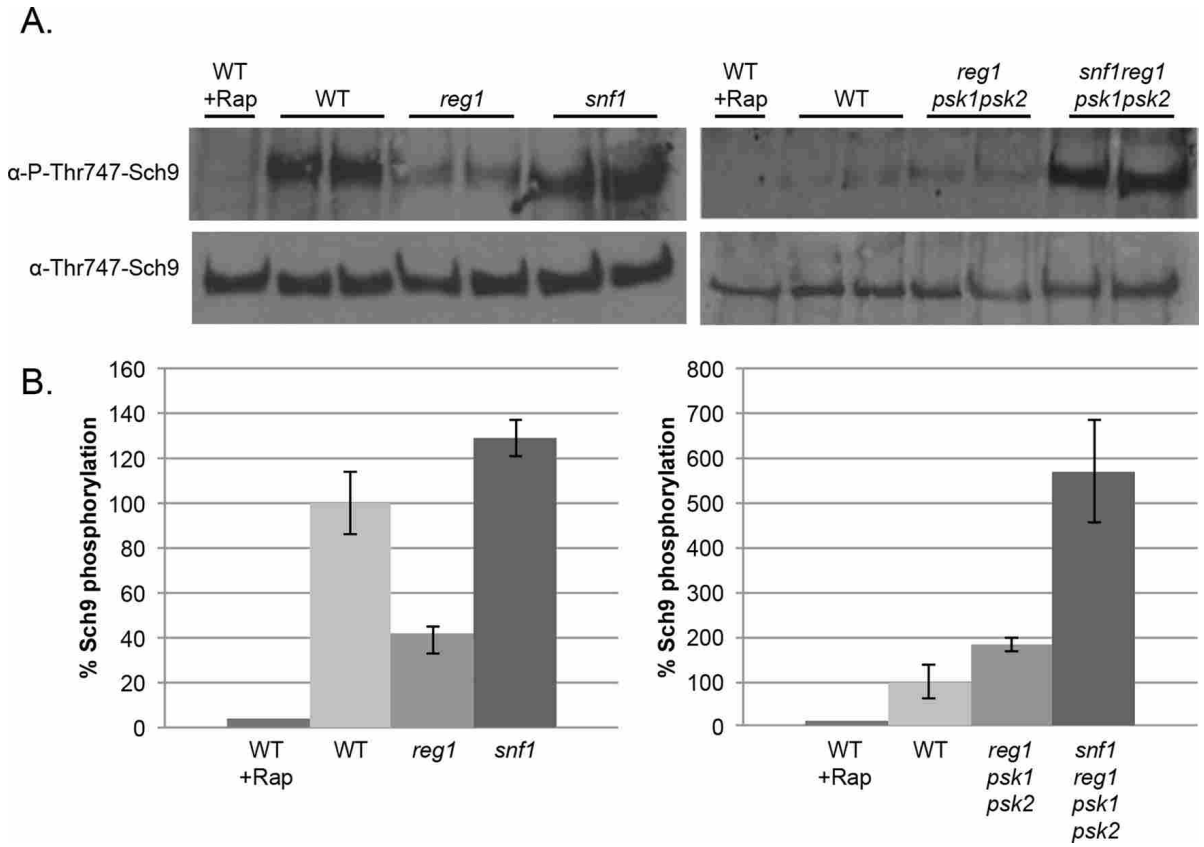


FIGURE 3.5. SNF1 inhibits TORC1 phosphorylation of Sch9 through PAS kinase. (A) Western blots of phospho-Sch9 and total Sch9. (B) Quantification of band intensities in A. A plasmid expressing Sch9 under the yeast ADH promoter was transformed into yeast (WT [JGY1], *reg1* [JGY95], *snf1* [JGY91], *reg1psk1psk2* [JGY283], *reg1snf1psk1psk2* [JGY280]). Yeast were grown in YPAD until $OD_{600}$ ~1.0. Preparation of Sch9 protein extract was performed as described by Miller-Fleming et al. (2014). Samples were normalized and loaded on 8% SDS–PAGE, transferred to nitrocellulose membrane, and incubated overnight with anti–phospho-Thr737-Sch9 and anti–Thr737-Sch9 antibodies (Kingsbury et al., 2014). Intensity signals were quantified using ImageJ. Phosphorylation was determined in duplicate. Error bars represent SEM.

## DISCUSSION

The nutrient-sensing protein kinases TOR (which forms the TORC1 and TORC2 complexes) and AMPK/SNF1 are essential regulators of growth/proliferation and cellular energy, respectively. Several studies have shown the interplay between these kinases, including

the direct phosphorylation and inhibition of mammalian TORC1 by AMPK (Bolster et al., 2002; Kimura et al., 2003; Cheng et al., 2004; Reiter et al., 2005). This study provides evidence for PAS kinase as a mediator in the inhibition of TORC1 by Snf1 in yeast (Figure 3.6).

In yeast, Psk1 is activated in a SNF1-dependent manner in response to energy/nutrient deprivation (Grose et al., 2007). This study expands these findings by providing in vivo and in vitro evidence for the direct phosphorylation and subsequent activation of Psk1 by Snf1 (Figure 3.1). Phosphorylation may activate PAS kinase by interfering with inhibitory binding of the PAS domain. Once activated, Psk1 phosphorylates Pbp1 (Figures 3.3 and 3.4), which sequesters TORC1 to stress granules, inhibiting cell growth (Takahara and Maeda, 2012). Caffeine sensitivity is associated with inhibition of TORC1, and Psk1Psk2 deficiency can rescue the caffeine sensitivity of cells overexpressing Pbp1 (Figure 3.4B), suggesting that phosphorylation of Pbp1 by Psk1 is activating. In support of this finding, Psk1Psk2 deficiency reduces the amount of Pbp1 localized to distinct cytoplasmic foci (Figure 3.4D).

This model for the PAS kinase–dependent interplay between SNF1 and TORC1 was further supported by monitoring the in vivo phosphorylation state of Sch9, a TORC1 substrate. Sch9 was fully phosphorylated in WT yeast grown on glucose. This phosphorylation was increased in *snf1* yeast and inhibited in *reg1* yeast, in which Snf1 is constitutively active (Figure 3.5). In addition, PAS kinase was necessary for this inhibition. During the revision of the manuscript, an article was published validating the Snf1-dependent inhibition of TORC1 signaling on alternate carbon sources (Hughes Hallett et al., 2014). Our results describe the molecular pathways underlying this observation.

The present article describes the second recent connection between yeast PAS kinase and TOR. In yeast, two TOR paralogues exist, Tor1 (which is a subunit of TORC1) and Tor2 (which

can function in both TORC1 and TORC2 complexes). TORC1 primarily controls growth in response to nutrients through the regulation of transcription, translation, ribosome biogenesis, nutrient transport, and autophagy; TORC2 controls cell cycle–dependent polarization of the actin cytoskeleton (for a review, see Loewith and Hall, 2011). Overexpression of yeast *PSK1* or *PSK2* suppresses a $tor2^{ts}$ mutation (Cardon et al., 2012; Cardon and Rutter, 2012), suggesting rescue of the TORC2 complex, since TORC1 is still functional in this background. In contrast, Psk1 appears to be a negative regulator of TORC1 activity (Figures 3.4 and 3.5). These findings are consistent with the cellular selection for two differentially controlled TOR complexes that regulate separate pathways involved in cell growth and proliferation.

In a cell's adaptation to its environment, there cannot simply be one "progrowth" pathway, but instead alternate pathways, such as those allowing for growth with or without division. Not only are there separate TOR complexes, but these complexes regulate different pathways in response to different stimuli. This complexity is necessary due to the multiple metabolic inputs and outputs the cell must sense (e.g., energy, amino acids, nitrogen, carbon source, etc.). It remains to be determined whether PAS kinase inhibits only the phosphorylation of Sch9, a progrowth kinase stimulating many pathways including protein synthesis, or whether other TORC1 pathways are also affected. The PAS kinase–dependent interplay between SNF1 and TORC1 would allow for an additional regulatory input, rather than just direct SNF1-dependent phosphorylation of TORC1. The complexity of these pathways is further demonstrated by comparing different cell types. Although the direct inhibition of TORC1 by AMPK reported in mammalian cells (Bolster et al., 2002; Kimura et al., 2003; Cheng et al., 2004; Reiter et al., 2005) is consistent with the overall pathway mediated by PAS kinase described here, PAS kinase is predicted to activate TORC1 in mammalian cells through the

inhibition of GSK3 (Inoki et al., 2003b, 2006; Semache et al., 2013). This alternate role for PAS kinase may be due to the differential metabolic responses of different cell types. For example, yeast ferment when glucose is high and respire on poor carbon sources, whereas mammalian cells activate respiration in response to nutrient-rich conditions (high glucose). These differences are reflected in AMPK/SNF1 activity, which is stimulated by alternate carbon sources in yeast and high glucose in mammalian cells (Ghillebert et al., 2011; Broach, 2012; Hardie, 2013; Liu and Jiang, 2013; Burkewitz et al., 2014; Ye et al., 2014). Whether PAS kinase also mediates inhibition of TORC1 through the mammalian Pbp1 homolog, ataxin-2, remains to be seen.

These findings may provide valuable insight into the function of PAS kinase in mammalian cells, in that all of the proteins in this pathway have conserved homologs. The human homolog of Pbp1, ataxin-2, is associated with neurodegenerative disease. This study provides both in vitro and in vivo evidence for the direct, Psk1-dependent phosphorylation of Pbp1 and the inhibition of phosphorylation by the Pbp1 N-terminal domain (Figure 3.3). This N-terminal truncation may trap Pbp1 into a conformation that is naturally obtained under certain in vivo conditions because WT Pbp1 copurifies with Psk1 (DeMille et al., 2014) and is phosphorylated in a Psk1-dependent manner within cells (Figure 3.4A). The N-terminus of Pbp1, which inhibits Psk1-dependent phosphorylation, also harbors the ataxin-2 domain, a conserved domain required for localization to P-bodies and stress granules and for promoting their formation (Mangus et al., 1998; Nonhoff et al., 2007; Swisher and Parker, 2010; Kaehler et al., 2012). The conservation of this N-terminal domain suggests that this regulatory role may also be conserved. Because mutations in ataxin-2 are associated with cerebral ataxia (SCA2), amyotrophic lateral sclerosis (ALS), and Parkinsonism (for recent reviews, see Magana et al.,

2013; Borza, 2014), understanding the regulation of this protein may provide key therapeutic targets for disease treatment.

The cross-talk between AMPK/SNF1, PAS kinase, and TOR seems vital for appropriate metabolic regulation, linking energy production to growth in response to a wide variation in available nutrients. These pathways are central to understanding a cell's basic metabolism. In addition, both AMPK and TOR are key therapeutic targets for the treatment of a variety of diseases, including obesity, diabetes, and cancer (for recent reviews, see Khan et al., 2013; Quinn et al., 2013). As a nonessential protein, PAS kinase may prove to be a safer target for therapeutic treatment of metabolic disease.

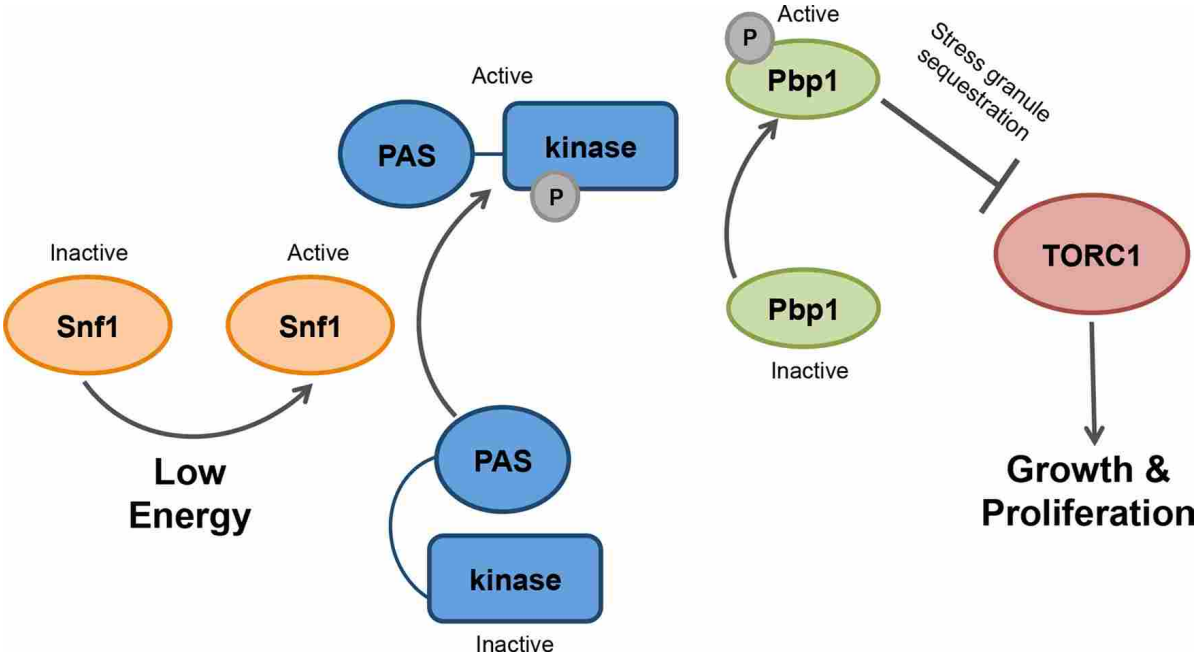


FIGURE 3.6. A model for the cross-talk between the nutrient-sensing kinases SNF1, TORC1, and Psk1 proposed in this study. SNF1 becomes activated when cellular energy levels are low (such as in conditions of glucose deprivation) and phosphorylates PAS kinase (Psk1). This phosphorylation leads to a disruption of the inhibitory binding of the PAS domain, leading to activation of the kinase. Once active, Psk1 phosphorylates Pbp1, which inhibits TORC1 by sequestering it to stress granules. The inhibition of TORC1 inactivates the S6 kinase, Sch9, and possibly other pathways that control cellular growth and proliferation.

## MATERIALS AND METHODS

### Growth assays

Lists of strains, plasmids, and primers used in this study are provided in Table 3.1. For plasmid construction, standard PCR-based cloning methods were used. All restriction enzymes were purchased from New England BioLabs (Ipswich, MA). Yeast two-hybrid bait and prey plasmids were made by PCR amplification and subsequent cloning into the EcoRI/SalI sites of pJG424 (pJG1236 [JG3199/3200], pJG1238 [JG3245/3246], pJG1240 [JG3274/3275], pJG1258 [JG3199/3532], pJG1260 [JG3531/3200], pJG1262 [JG3199/3530], pJG1264 [JG3531/3532]) or the EcoRI/SalI sites of pJG421 (pJG1003 [JG3136/3138], pJG1004 [JG3137/3138], pJG1008 [JG2916/2917], pJG1168 [JG2917/3418], pJG1169 [JG3419/3418], pJG1195 [JG3460/3138], pJG1196 [JG2917/3461], pJG1197 [JG2917/3462], pJG1198 [JG2917/3463], pJG1230 [JG3136/3462], pJG1231 [JG3136/3463], pJG1237 [JG3199/3200], pJG1239 [JG3245/3246], pJG1241 [JG3274/3275], pJG1259 [JG3199/3532], pJG1261 [JG3531/3200], pJG1262 [3530/3199], pJG1263 [JG3199/3530], pJG1265 [JG3531/3532], pJG1276 [2454/2458]). Two constructs were retrieved from an earlier Y2H screen and were not made by PCR (pJG1001 and pJG1002; DeMille et al., 2014). Yeast two-hybrid Gold cells (Clontech, Mountain View, CA) were used to transform in bait and prey plasmids for interaction studies.

For yeast-two hybrid spot dilutions, overnight samples were grown in selective SD-Leu-Trp media, serially diluted 1:5 in water and spotted to SD-Leu-Trp-His-Ade or SD-Leu-Trp plates as a control, and incubated at 30°C for 2–5 d until colonies were apparent. For caffeine sensitivity assays, spot dilutions were performed by growing overnight samples in SD-Ura media, diluting saturated overnights 1:10 in water, and spotting on SGal-Ura media with 7.5 mM caffeine or SD-Ura as a control. Plates were incubated at 30°C for 7–10 d.

Histidine- and Myc-tagged protein purification

Yeast harboring plasmids for histidine (HIS)- or Myc-tagged protein expression were grown in SD-Ura media overnight, diluted 1:100-fold into 100 or 500 ml of SD-Ura, and grown for 10–12 h, pelleted, and resuspended in SGal-Ura for 36 h to induce expression under the GAL1-10 promoter. Yeast were pelleted and resuspended in lysis buffer for HIS purification (50 mM 4-(2-hydroxyethyl)piperazine-1-ethanesulfonic acid [HEPES], 300 mM NaCl, 20 mM imidazole, 10 mM KCl, 1 mM β-mercaptoethanol, and 1:300 mammalian protease inhibitor cocktail [Sigma-Aldrich, St. Louis, MO] or cOmplete Protease Inhibitor Cocktail Tablet [Roche], pH 7.8, with phosphatase inhibitors, 50 mM NaF, and glycerophosphate when necessary) or for Myc purification (20 mM HEPES, 10 mM KCl, 1 mM EDTA, 1 mM ethylene glycol tetraacetic acid [EGTA], 50 mM NaCl, 10% glycerol, 1 mM β-mercaptoethanol, cOmplete Protease Inhibitor Cocktail Tablet, pH 7.4, with phosphatase inhibitors when necessary). Resuspended cultures were lysed using the Microfluidics M-110P homogenizer (Microfluidics, Westwood, MA [for 500-ml cultures]) or bead blasted for 1 min, followed by 1 min on ice repeated three times using 0.2-mm glass beads (for 100-ml cultures). Cell debris was then pelleted at 12,000 rpm for 20–30 min. Supernates were transferred to new tubes and incubated with 200 μl of nickel-nitrilotriacetic acid (Ni-NTA) agarose beads (Qiagen, Valencia, CA [for 500-ml HIS purification]) or 5–10 μl of Myc-conjugated magnetic beads (Cell Signaling, Danvers, MA [for 100-ml Myc purification]) for 2–3 h at 4°C. For HIS-epitope purification, beads were washed twice with 15 ml of lysis buffer and then transferred to a polypropylene column and washed with 30–50 ml of lysis buffer. For Myc-protein purification, beads were separated using magnetic force and washed four times with 500 μl of lysis buffer lacking the protease inhibitor. HIS-tagged proteins were eluted three times with 0.3 ml of lysis

buffer containing 250 mM imidazole and 100 mM NaCl but lacking protease and phosphatase inhibitors. Beads containing Myc-tagged proteins were used directly for in vitro kinase assays without eluting.

Quantification of in vivo phosphorylation of Ugp1

As a measure of Psk1 activity, the amount of Ugp1 phosphorylated in vivo was assessed. Briefly, an overnight sample of Psk2-deficient cells (*PSK1psk2*, JGY3) was diluted 1:100 in yeast extract/peptone/dextrose/adenine (YPAD) and grown for 3–4 h at 30°C to an $OD_{600}$ of 0.5. Medium was then changed by filtering with a 0.2-μm filter and resuspending in YPAraffinose (2%). Cells were harvested at various time points by filtering and flash freezing at -80°C. Percentage Ugp1 phosphorylated was assayed as previously described (Smith and Rutter, 2007). Briefly, cells were lysed by bead blast, and the supernatant was fractionated on a monoQ column, which separates the phosphorylated and unphosphorylated forms of Ugp1. The activity of Ugp1 in each fraction was assessed, and the percentage of phosphorylated Ugp1 was calculated by fitting the sum of two Gaussians to the curves to determine the area under the peak using KaleidaGraph (Synergy Software, Reading, PA).

In vivo Psk1 EMSA

HIS-HA epitope-tagged Psk1 (pJG858) was purified from WT (JGY1), *snf1* (JGY91), and *reg1* (JGY95) yeast grown in galactose, run on 8% SDS–PAGE, and silver stained to visualize any electrophoretic mobility shift.

In vitro kinase assays

Constructs of Psk1-Myc and Pbp1-Myc epitope-tagged plasmids were made as follows: full-length Pbp1 (pJG1251) was constructed by PCR amplification using primers JG2916/2917 and cloning into the EcoRI/XhoI sites of pJG1183. ΔN419Pbp1 (pJG1250) was constructed by PCR amplification using primers JG3384/2916 and cloning into the EcoRI/XhoI sites of pJG1183. ΔN931Psk1 (pJG1216) was constructed by PCR amplification using primers JG3140/1158 and cloning into the EcoRI/XhoI sites of pJG1181. Full-length Psk1-D1230A (kinase dead) (pJG1215) was constructed by digesting pJG410 and subcloning into BglII/XhoI sites of pJG1181. ΔN931Psk1-D1230A (pJG1281) was constructed by PCR amplification of pJG1170 using primers JG3140/1158 and cloning into the EcoRI/XhoI sites of pJG1181. Full-length Psk1 (pJG1181) was made previously (DeMille et al., 2014).

Full-length Psk1 and ΔN931Psk1 were purified from WT yeast (JGY1), and kinase-dead Psk1 and both Pbp1 constructs were purified from *psk1psk2* yeast (JGY4). Purified full-length and ΔN419Pbp1-Myc–tagged proteins were assayed for PAS kinase–dependent phosphorylation by incubating purified protein in 30 µl of reaction buffer containing 1x Psk1 kinase buffer (0.4 M HEPES, 0.1 M KCl, 5 mM $MgCl_2$, pH 7.0), 0.2 mM ATP, $^{32}$P-ATP [5 µCi; MP Biomedicals, Santa Ana, CA]) in the presence or absence of purified full-length Psk1, truncated ΔN931Psk1, or kinase-dead Psk1-D1230A. Kinase assays were started with the addition of Psk1 and stopped with SDS–PAGE sample buffer. Reactions were incubated for 12 min at 30°C. For in vitro kinase assays of Snf1 (pJG1193) and Psk1-D1230A (pJG1215) or ΔN931Psk1-D1230A (pJG1281), reaction conditions were similar, except the following changes: 1x Snf1 kinase buffer (50 mM Tris-HCl, 10 mM $MgCl_2$, 1 mM dithiothreitol [DTT], pH 7.5), 10 µM ATP, and 7.5 µCi of $^{32}$P-ATP, and reactions were incubated for 35 min.

In vivo Pbp1 phosphostate analysis

Pbp1-HIS expressed under the GAL1-10 promoter (pJG925) was made by PCR amplifying Pbp1 with primers JG2916/2917 and cloning into the EcoRI/XhoI sites of pJG859. HIS-tagged Pbp1 (pJG925) was expressed in JGY1 (WT) overexpressing full-length Psk1 on a plasmid (pJG9) or in JGY4 (*psk1psk2*) containing an empty vector (pJG124). Proteins were grown in duplicate in SD-Ura overnight, induced with SGal-Ura for 36 h, and purified on Ni-NTA as described. Eluates were run on 8% SDS–PAGE, transferred to nitrocellulose membrane, and incubated overnight with nonspecific PhosphoThreonine (Cell Signaling Technology) antibody. Blots were imaged, stripped, and then incubated overnight with PhosphoSerine (Q5; Qiagen) antibody. Total Pbp1 was assessed by stripping the membrane once more, incubating overnight with hemagglutinin (HA) antibody (Roche), and imaging.

Microscopy

Pbp1-GFP fusion yeast (JGY1144) was obtained from the Invitrogen yeast-GFP clone collection (Invitrogen, Grand Island, NY) and transformed with Psk1-RFP (pJG1119) for colocalization analysis. pJG1119 was made by PCR amplification of dsRED using JG3334/3352 and BBa_J04450 (iGEM registry plasmid) as DNA template and cloned into the XhoI/SphI sites of pJG858 to replace the HISHA tag with the RFP fusion. Overnight samples were grown in SD-Ura medium, and then yeast were pelleted and resuspended in SGal-Ura medium to induce expression of Psk1-RFP. Cultures were grown in SGal-Ura for 3–5 d, cells were pelleted, washed once with synthetic complete (SC) medium lacking a carbon source, and resuspended in fresh SC medium. Cultures were incubated at 30°C for an additional 1 h to allow them to grow under glucose deprivation conditions. Images were then captured using a FluoView FV1000

confocal laser-scanning microscope (Olympus, Tokyo, Japan) with 60x magnification lens and the appropriate filter sets (GFP, dsRED). For percentage of Pbp1-GFP foci in WT (JGY1144) and *psk1psk2* (JGY1160) yeast, strains were grown in SD complete medium for 4 d and then washed, resuspended in SC lacking a carbon source, incubated, and imaged as described. For percentage of Psk1 and Pbp1 colocalization, 50 cells (96 distinct cytoplasmic foci) were counted. For percentage of Pbp1-GFP foci, 1199 cells for WT and 782 for *psk1psk2* were counted. SEM was used for error bars, and Student's t test was used for statistical significance calculations.

Sch9 phosphorylation assays

A plasmid expressing Sch9 under the ADH1 promoter (pJG1288) was made by amplifying Sch9-HIS using primers JG3330 and JG3331 and cloning into pJG1285. This Sch9 plasmid was transformed into yeast (WT [JGY1], *reg1* [JGY95], *snf1* [JGY91], *reg1psk1psk2* [JGY283], *reg1snf1psk1psk2* [JGY280]), grown in SD-Trp overnight, and then diluted 1:100 into YPAD and grown until $OD_{600}$ ~1.0. For rapamycin controls, 100 nM rapamycin (Research Products International, Mount Prospect, IL) was added 1 h before harvesting cells. Preparation of Sch9 protein extract was performed as described by Miller-Fleming et al. (2014). Samples were normalized and loaded on 8% SDS–PAGE, transferred to nitrocellulose membrane, and incubated overnight with anti–phospho-Thr737-Sch9 and anti–Thr737-Sch9 antibodies (Kingsbury et al., 2014). Intensity signals were quantified using ImageJ (National Institutes of Health, Bethesda, MD).

Mass spectrometry

Psk1 samples were prepared using a modified version of filter-aided sample preparation

(Wisniewski et al., 2009). Briefly, samples were placed on filters, denatured by adding 8 M urea (Molecular Biology Grade; EMD Chemicals, Gibbstown, NJ), reduced with dithiothreitol (DTT, Sigma-Aldrich), alkylated with iodoacetamide (BioUltra Grade; Sigma-Aldrich), and digested with trypsin (Sequencing Grade Modified; Promega, Madison, WI). Digested protein was analyzed by LC-MS using the Eksigent NanoLC Ultra coupled with the LTQ Orbitrap XL mass spectrometer. Peptides were separated on a Waters Peptide Separation Technology c18 column with a water/acetonitrile gradient containing 0.1% formic acid (Optima LC-MS Grade, Fisher Scientific, Pittsburgh, PA). MS scans were collected in the Orbitrap. Fragmentation scans were collected in the LTQ, excluding charge state 1 and unassigned charge states using collision induced dissociation (CID). $MS^2$ multistage activation or $MS^3$ CID (Kall et al., 2007) was used, with neutral losses corresponding to phosphate groups (32.66, 48.99, and 97.97 m/z) in some cases (Schroeder et al., 2004).

Data were analyzed using Mascot, Sequest, and/or Sequest HT with or without Percolator (Perkins et al., 1999; Tabb et al., 2001; Kall et al., 2007). The Proteome Discoverer Package was also used on some samples. Search settings included dynamic modifications: phosphorylation (STY) and oxidation (M). Carbamidomethyl (C) was set as a dynamic or static modification. Searches were performed against the uni_yeast database or a modified uni_yeast database containing 6x HIS-tagged Psk1 (UniProt, 2014).

ACKNOWLEDGMENTS

We thank Mark Johnston (University of Colorado School of Medicine, Aurora, CO) for the generous gift of a functional Snf1-Myc construct and Maria Cardenas (Duke University, Durham, NC) for the generous gift of anti–phospho-Thr737-Sch9 and anti–Thr737-Sch9

antibodies. We also thank John T. Prince (Brigham Young University, Provo, UT) for aid with the mass spectrometry experiments. This work was supported by National Institutes of Health Grant R15 GM100376-01, a Brigham Young University Mentoring Environmental Grant to J.H.G., Brigham Young University Cancer Research Center Fellowships to B.D.B. and J.F.A., and the Brigham Young University Department of Microbiology and Molecular Biology and College of Life Sciences.

TABLE 3.1. Strains, plasmids, and primers used in this study

| Strain | Background | Genotype | Abbreviation | a/α | Reference or source |
|---|---|---|---|---|---|
| JGY1 | W303 | *ade2-1 can1-100 his3-11,15 leu2-3,112 trp1-1 ura3-1* | WT | a | David Stillman University of Utah |
| JGY3 | W303 | *psk2*::kan-MX4 *ade2-1 can1-100 his3-11,15 leu2-3,112 trp1-1 ura3-1* | *PSK1psk2* | a | Grose *et al*. (2007) |
| JGY4 | W303 | *psk1*::*his3 psk2*::kan-MX4 *ade2-1 can1-100 his3-11,15 leu2-3,112 trp1-1 ura3-1* | *psk1psk2* | a | Grose *et al*. (2007) |
| JGY91 | W303 | *snf1*::hphMX4 *ade2-1 can1-100 his3-11,15 leu2-3,112 trp1-1 ura3-1* | *snf1* | a | Grose *et al*. (2007) |
| JGY95 | W303 | *reg1*::hphMX4 *ade2-1 can1-100 his3-11,15 leu2-3,112 trp1-1 ura3-1* | *reg1* | a | Grose *et al*. (2007) |
| JGY299 | S288C | *PSK2*-TAPtag::kanMX *ura3-0 trp1-0 SUC2 mal mel gal2 CUP1 flo1 flo8-1* | WT | α | Jared Rutter University of Utah |
| Y2H Gold (JGY1031) | | *LYS2*::*GAL1*UAS-*GAL1*TATA-His3, *GAL2*UAS-Gal2TATA-Ade2 *URA3*::*MEL1*UAS-*MEL1*TATA, *AUR1*-C*MEL1*, *ura3-52 his3-200 ade2-101 trp1-901 leu2-3, 112 gal4del gal80del met-* | Y2H Gold | a | Clontech |
| JGY1144 | BY4741 | Chromosomally-tagged Pbp1-GFP::*HIS3* from Invitrogen *his3-1 leu2-0 met15-0 ura3-0* | WT | a | Invitrogen |
| JGY1160 | BY4741 | Pbp1-GFP::*HIS3*, *psk1*::hygro, *psk2*::NAT *his3-1 leu2-0 met15-0 ura3-0* | *psk1psk2* | a | This study |
| JGY1161 | S288C | *psk1*::hygro *psk2*::NAT *ura3-0 trp1-0 SUC2 mal mel gal2 CUP1 flo1 flo8-1* | *psk1psk2* | α | This study |

| Plasmid | Gene | Description | Backbone | Yeast origin | Selection | Reference or source |
|---|---|---|---|---|---|---|
| pJG9 | *PSK1* | Psk1 in pRS424 | pRS424 | 2u | TRP | Jared Rutter University of Utah |
| pJG124 | EV | EV | pRS424 | 2u | TRP | Bruce Horazdovsky Mayo Clinic |
| pJG232 | *PSK1* | C-terminal HIS/HA-tagged Psk1 | pRS426 | 2u | URA | Jared Rutter University of Utah |
| pJG410 | *PSK1* | Psk1-D1230A in pJG232 | pRS426 | 2u | URA | DeMille *et al*. (2014) |
| pJG421 | EV | pGAD-C1 empty Y2H prey vector | YEp-GAD | 2u | LEU | James *et al*. (1996) |
| pJG422 | EV | pGAD-C2 empty Y2H prey vector | YEp-GAD | 2u | LEU | James *et al*. (1996) |
| pJG423 | EV | pGAD-C3 empty Y2H prey vector | YEp-GAD | 2u | LEU | James *et al*. (1996) |
| pJG424 | EV | pGBD-C1 empty Y2H bait vector | YEp-GBD | 2u | TRP | James *et al*. (1996) |
| pJG425 | EV | pGBD-C2 empty Y2H bait vector | YEp-GBD | 2u | TRP | James *et al*. (1996) |
| pJG441 | *PSK1* | Full-length Psk1 in pJG425 | YEp-GBD | 2u | TRP | DeMille *et al*. (2014) |
| pJG442 | *PSK1* | Full-length Psk1 in pJG422 | YEp-GAD | 2u | LEU | This study |
| pJG598 | *PSK1* | ΔN692Psk1 in pJG425 | YEp-GBD | 2u | TRP | DeMille *et al*. (2014) |

| | | | | | | |
|---|---|---|---|---|---|---|
| pJG709 | *PSK1* | ΔN692Psk1 in pJG422 | YEp-GAD | 2u | LEU | This study |
| pJG858 | *PSK1* | pGAL1-10, Psk1-HIS/HA | pRS426 | 2u | URA | DeMille *et al*. (2014) |
| pJG859 | EV | pGAL1-10, HIS/HA | pRS426 | 2u | URA | DeMille *et al*. (2014) |
| pJG925 | *PBP1* | Full-length Pbp1 in pJG859 | pRS426 | 2u | URA | This study |
| pJG960 | *PSK1* | ΔN692Psk1-HIS/HA in pJG858 | pRS426 | 2u | URA | DeMille *et al*. (2014) |
| pJG998 | EV | pET15b with pGADT7 MCS | pET15b | | AMP | This study |
| pJG1000 | *PSK1* | ΔN931Psk1-HIS/HA in pJG858 | pRS426 | 2u | URA | DeMille *et al*. (2014) |
| pJG1001 | *PBP1* | aa356-722Pbp1 | YEp-GAD | 2u | LEU | DeMille *et al*. (2014) |
| pJG1002 | *PBP1* | aa197-722Pbp1 | YEp-GAD | 2u | LEU | DeMille *et al*. (2014) |
| PJG1003 | *PBP1* | aa420-722Pbp1 | YEp-GAD | 2u | LEU | This study |
| pJG1004 | *PBP1* | aa565-722Pbp1 | YEp-GAD | 2u | LEU | This study |
| pJG1008 | *PBP1* | Full-length Pbp1 | YEp-GAD | 2u | LEU | This study |
| pJG1046 | *GAL83* | pGAL1-10, Gal83-HIS/HA | pRS426 | 2u | URA | This study |
| pJG1047 | *SIP2* | pGAL1-10, Sip2-HIS/HA | pRS426 | 2u | URA | This study |
| pJG1119 | *PSK1* | pGAL1-10, Psk1-RFP | pRS426 | 2u | URA | This study |
| pJG1168 | *PBP1* | aa1-565Pbp1 | YEp-GAD | 2u | LEU | This study |
| pJG1169 | *PBP1* | aa420-565Pbp1 | YEp-GAD | 2u | LEU | This study |
| pJG1170 | *PSK1* | pGAL1-10-Psk1-D1230A-HIS/HA | pRS426 | 2u | URA | DeMille *et al*. (2014) |
| pJG1181 | *PSK1* | pGAL1-10-Psk1-Myc | pRS426 | 2u | URA | DeMille *et al*. (2014) |
| pJG1183 | EV | pGAL1-10, EV-Myc | pRS426 | 2u | URA | DeMille *et al*. (2014) |
| pJG1193 | *SNF1* | Snf1-8xmyc | pRS313 | 2u | URA | Mark Johnston University of Colorado Denver |
| pJG1195 | *PBP1* | aa470-722Pbp1 | YEp-GAD | 2u | LEU | This study |
| pJG1196 | *PBP1* | aa1-420Pbp1 | YEp-GAD | 2u | LEU | This study |
| pJG1197 | *PBP1* | aa1-580Pbp1 | YEp-GAD | 2u | LEU | This study |
| pJG1198 | *PBP1* | aa1-660Pbp1 | YEp-GAD | 2u | LEU | This study |
| pJG1203 | *ROD1* | Rod1-HIS in pJG998 | pET15b | | AMP | This study |
| pJG1215 | *PSK1* | pGAL1-10-Psk1-D1230A-Myc | pRS426 | 2u | URA | This study |
| pJG1216 | *PSK1* | pGAL1-10-ΔN931Psk1-Myc | pRS426 | 2u | URA | This study |
| pJG1230 | *PBP1* | aa420-580Pbp1 | YEp-GAD | 2u | LEU | This study |
| pJG1231 | *PBP1* | aa420-660Pbp1 | YEp-GAD | 2u | LEU | This study |
| pJG1236 | *GAL83* | Gal83 in pJG424 | YEp-GBD | 2u | TRP | This study |
| pJG1237 | *GAL83* | Gal83 in pJG421 | YEp-GAD | 2u | LEU | This study |
| pJG1238 | *SIP2* | Sip2 in pJG424 | YEp-GBD | 2u | TRP | This study |
| pJG1239 | *SIP2* | Sip2 in pJG421 | YEp-GAD | 2u | LEU | This study |
| pJG1240 | *SNF1* | Snf1 in pJG424 | YEp-GBD | 2u | TRP | This study |
| pJG1241 | *SNF1* | Snf1 in pJG421 | YEp-GAD | 2u | LEU | This study |
| pJG1250 | *PBP1* | pGAL1-10, ΔN419Pbp1-Myc | pRS426 | 2u | URA | This study |
| pJG1251 | *PBP1* | pGAL1-10, Pbp1-Myc | pRS426 | 2u | URA | This study |
| pJG1258 | *GAL83* | aa1-342Gal83 in pJG424 | YEp-GBD | 2u | TRP | This study |
| pJG1259 | *GAL83* | aa1-342Gal83 in pJG421 | YEp-GAD | 2u | LEU | This study |
| pJG1260 | *GAL83* | aa141-417Gal83 in pJG424 | YEp-GBD | 2u | TRP | This study |
| pJG1261 | *GAL83* | aa141-417Gal83 in pJG421 | YEp-GAD | 2u | LEU | This study |
| pJG1262 | *GAL83* | aa1-140Gal83 in pJG424 | YEp-GBD | 2u | TRP | This study |
| pJG1263 | *GAL83* | aa1-140Gal83 in pJG421 | YEp-GAD | 2u | LEU | This study |
| pJG1264 | *GAL83* | aa141-342Gal83 in pJG424 | YEp-GBD | 2u | TRP | This study |
| pJG1265 | *GAL83* | aa141-342Gal83 in pJG421 | YEp-GAD | 2u | LEU | This study |

| Primer | Sequence |
|---|---|
| JG1158 | TCACCTAACCAACCATTTG |
| JG2916 | GCCTCGAGGTTTATGGCCACTGGTACTACTATTATGG |
| JG2917 | GGCGAATTCATGAAGGGAAACTTTAGGAAAAGAG |
| JG3136 | GGCGAATTCTCGTTGCCTCCAAAACCGATCAGC |
| JG3137 | GGCGAATTCCAACAACGCCAATTGAACTCCATGG |
| JG3138 | GGCGTCGACCTATTTATGGCCACTGGTACTAC |
| JG3140 | CCGGAATTCATGGAGGATTTGGCCCACCGAACG |
| JG3199 | GGCGAATTCATGGCTGGCGACAACCCTGAAAAC |
| JG3200 | GCCGTCGACGTTGCAATGGTGTATACAGTATTTGGGTC |
| JG3245 | GGCGAATTCATGGGTACTACGACAAGTCATCCAG |
| JG3246 | GGCGTCGACGCGAGGACTCTATGGGCGTATAAAG |
| JG3274 | GGCGAATTCATGAGCAGTAACAACAACACAAACAC |
| JG3275 | GCCTCGAGGATTGCTTTGACTGTTAACGGCTAATTCC |
| JG3334 | GGCCTCGAGTGGCTTCCTCCGAAGACGTTATCAAAG |
| JG3352 | GGCGCATGCTTAGCGATCTACACTAGCACTATCAGCG |
| JG3384 | GGCGAATTCATGTCGTTGCCTCCAAAACCGATCAGC |

| | |
|---|---|
| JG3418 | GGCGTCGACGAACCTAGTTTGAGCTTCTTGAATCG |
| JG3419 | GGCGAATTCATGTCGTTGCCTCCAAAACCGATCAGC |
| JG3432 | GGCCATATGATGTTTTCATCATCATCTCGACCTTC |
| JG3447 | GGCGAGCTCCTATGAGCGATCCCGTTTTGTGAAC |
| JG3460 | GGCGAATTCACTTCATTGAGAAGACGTAATCATGGTTCC |
| JG3461 | GGCGTCGACCGAAGAATTAGATTTTAATGTAGAGCTTG |
| JG3462 | GGCGTCGACAGCTTCTTGAATCGCCGTATCCTCATC |
| JG3463 | GGCGTCGACGCTACCCATAACTGGCATCATTTGAGGC |
| JG3530 | GGCGTCGACGGCCTTGATTTTGAAGTGAGTCAGGC |
| JG3531 | GGCGAATTCTTTCAACAGCAACAAGAACAGCAACAG |
| JG3532 | GGCGTCGACGGGCCATATTTTGGTGATTATTTTGCTGC |
| JG3533 | GGCGAATTCTGGTTGACTCCTCCACAACTGCC |

REFERENCES

An, R., da Silva Xavier, G., Hao, H.X., Semplici, F., Rutter, J., and Rutter, G.A. (2006). Regulation by Per-Arnt-Sim (PAS) kinase of pancreatic duodenal homeobox-1 nuclear import in pancreatic beta-cells. Biochem Soc Trans *34*, 791-793.

Bolster, D.R., Crozier, S.J., Kimball, S.R., and Jefferson, L.S. (2002). AMP-activated protein kinase suppresses protein synthesis in rat skeletal muscle through down-regulated mammalian target of rapamycin (mTOR) signaling. The Journal of biological chemistry *277*, 23977-23980.

Brusco, A., Gellera, C., Cagnoli, C., Saluto, A., Castucci, A., Michielotto, C., Fetoni, V., Mariotti, C., Migone, N., Di Donato, S.*, et al.* (2004). Molecular genetics of hereditary spinocerebellar ataxia: mutation analysis of spinocerebellar ataxia genes and CAG/CTG repeat expansion detection in 225 Italian families. Arch Neurol *61*, 727-733.

Burkewitz, K., Zhang, Y., and Mair, W.B. (2014). AMPK at the Nexus of Energetics and Aging. Cell metabolism.

Cardon, C.M., Beck, T., Hall, M.N., and Rutter, J. (2012). PAS kinase promotes cell survival and growth through activation of Rho1. Sci Signal *5*, ra9.

Cardon, C.M., and Rutter, J. (2012a). PAS kinase: integrating nutrient sensing with nutrient partitioning. Semin Cell Dev Biol *23*, 626-630.

Cardon, C.M., and Rutter, J. (2012b). PAS kinase: Integrating nutrient sensing with nutrient partitioning. Semin Cell Dev Biol.

Cheng, S.W., Fryer, L.G., Carling, D., and Shepherd, P.R. (2004). Thr2446 is a novel mammalian target of rapamycin (mTOR) phosphorylation site regulated by nutrient status. The Journal of biological chemistry *279*, 15719-15722.

da Silva Xavier, G., Farhan, H., Kim, H., Caxaria, S., Johnson, P., Hughes, S., Bugliani, M., Marselli, L., Marchetti, P., Birzele, F.*, et al.* (2011). Per-arnt-sim (PAS) domain-containing protein kinase is downregulated in human islets in type 2 diabetes and regulates glucagon secretion. Diabetologia *54*, 819-827.

DeMille, D., Bikman, B.T., Mathis, A.D., Prince, J.T., Mackay, J.T., Sowa, S.W., Hall, T.D., and Grose, J.H. (2014). A Comprehensive Protein-protein Interactome for Yeast PAS Kinase 1 Reveals Direct Inhibition of Respiration Through the Phosphorylation of Cbf1. Mol Biol Cell.

DeMille, D., and Grose, J.H. (2013). PAS kinase: a nutrient sensing regulator of glucose homeostasis. IUBMB life *65*, 921-929.

Eglen, R., and Reisine, T. (2011). Drug discovery and the human kinome: recent trends. Pharmacol Ther *130*, 144-156.

Fang, Z., Grutter, C., and Rauh, D. (2013). Strategies for the selective regulation of kinases with allosteric modulators: exploiting exclusive structural features. ACS Chem Biol *8*, 58-70.

Gallinetti, J., Harputlugil, E., and Mitchell, J.R. (2013). Amino acid sensing in dietary-restriction-mediated longevity: roles of signal-transducing kinases GCN2 and TOR. The Biochemical journal *449*, 1-10.

Grose, J.H., Smith, T.L., Sabic, H., and Rutter, J. (2007). Yeast PAS kinase coordinates glucose partitioning in response to metabolic and cell integrity signaling. EMBO J *26*, 4824-4830.

Grose, J.H., Sundwall, E., and Rutter, J. (2009). Regulation and function of yeast PAS kinase: a role in the maintenance of cellular integrity. Cell Cycle *8*, 1824-1832.

Hao, H.X., Cardon, C.M., Swiatek, W., Cooksey, R.C., Smith, T.L., Wilde, J., Boudina, S., Abel, E.D., McClain, D.A., and Rutter, J. (2007). PAS kinase is required for normal cellular energy balance. Proc Natl Acad Sci U S A *104*, 15466-15471.

Hardie, D.G. (2013). AMPK: a target for drugs and natural products with effects on both diabetes and cancer. Diabetes *62*, 2164-2172.

Hurtado-Carneiro, V., Roncero, I., Blazquez, E., Alvarez, E., and Sanz, C. (2013). PAS Kinase as a Nutrient Sensor in Neuroblastoma and Hypothalamic Cells Required for the Normal Expression and Activity of Other Cellular Nutrient and Energy Sensors. Mol Neurobiol *48*, 904-920.

Hurtado-Carneiro, V., Roncero, I., Egger, S.S., Wenger, R.H., Blazquez, E., Sanz, C., and Alvarez, E. (2014). PAS Kinase Is a Nutrient and Energy Sensor in Hypothalamic Areas Required for the Normal Function of AMPK and mTOR/S6K1. Molecular neurobiology.

Inoki, K., Li, Y., Xu, T., and Guan, K.L. (2003a). Rheb GTPase is a direct target of TSC2 GAP activity and regulates mTOR signaling. Genes & development *17*, 1829-1834.

Inoki, K., Ouyang, H., Zhu, T., Lindvall, C., Wang, Y., Zhang, X., Yang, Q., Bennett, C., Harada, Y., Stankunas, K.*, et al.* (2006). TSC2 integrates Wnt and energy signals via a coordinated phosphorylation by AMPK and GSK3 to regulate cell growth. Cell *126*, 955-968.

Inoki, K., Zhu, T., and Guan, K.L. (2003b). TSC2 mediates cellular energy response to control cell growth and survival. Cell *115*, 577-590.

James, P., Halladay, J., and Craig, E.A. (1996). Genomic libraries and a host strain designed for highly efficient two-hybrid selection in yeast. Genetics *144*, 1425-1436.

Jiang, R., and Carlson, M. (1997). The Snf1 protein kinase and its activating subunit, Snf4, interact with distinct domains of the Sip1/Sip2/Gal83 component in the kinase complex. Molecular and cellular biology *17*, 2099-2106.

Kaehler, C., Isensee, J., Nonhoff, U., Terrey, M., Hucho, T., Lehrach, H., and Krobitsch, S. (2012). Ataxin-2-like is a regulator of stress granules and processing bodies. PLoS One *7*, e50134.

Khan, K.H., Yap, T.A., Yan, L., and Cunningham, D. (2013). Targeting the PI3K-AKT-mTOR signaling network in cancer. Chin J Cancer *32*, 253-265.

Kim, J.M., Hong, S., Kim, G.P., Choi, Y.J., Kim, Y.K., Park, S.S., Kim, S.E., and Jeon, B.S. (2007). Importance of low-range CAG expansion and CAA interruption in SCA2 Parkinsonism. Arch Neurol *64*, 1510-1518.

Kimura, N., Tokunaga, C., Dalal, S., Richardson, C., Yoshino, K., Hara, K., Kemp, B.E., Witters, L.A., Mimura, O., and Yonezawa, K. (2003). A possible linkage between AMP-activated protein kinase (AMPK) and mammalian target of rapamycin (mTOR) signalling pathway. Genes to cells : devoted to molecular & cellular mechanisms *8*, 65-79.

Kimura, Y., Irie, K., and Irie, K. (2013). Pbp1 Is Involved in Ccr4- and Khd1-Mediated Regulation of Cell Growth through Association with Ribosomal Proteins Rpl12a and Rpl12b. Eukaryot Cell *12*, 864-874.

Lal, H., Kolaja, K.L., and Force, T. (2013). Cancer genetics and the cardiotoxicity of the therapeutics. J Am Coll Cardiol *61*, 267-274.

Laplante, M., and Sabatini, D.M. (2012). mTOR signaling in growth control and disease. Cell *149*, 274-293.

Liu, W.Y., and Jiang, R.S. (2013). Advances in the research of AMPK and its subunit genes. Pakistan journal of biological sciences: PJBS *16*, 1459-1468.

Loewith, R., and Hall, M.N. (2011). Target of rapamycin (TOR) in nutrient signaling and growth control. Genetics *189*, 1177-1201.

Ludin, K., Jiang, R., and Carlson, M. (1998). Glucose-regulated interaction of a regulatory subunit of protein phosphatase 1 with the Snf1 protein kinase in Saccharomyces cerevisiae. Proceedings of the National Academy of Sciences of the United States of America *95*, 6245-6250.

Magnuson, B., Ekim, B., and Fingar, D.C. (2012). Regulation and function of ribosomal protein S6 kinase (S6K) within mTOR signalling networks. The Biochemical journal *441*, 1-21.

Mangus, D.A., Amrani, N., and Jacobson, A. (1998). Pbp1p, a factor interacting with Saccharomyces cerevisiae poly(A)-binding protein, regulates polyadenylation. Molecular and cellular biology *18*, 7383-7396.

Mangus, D.A., Smith, M.M., McSweeney, J.M., and Jacobson, A. (2004). Identification of factors regulating poly(A) tail synthesis and maturation. Molecular and cellular biology *24*, 4196-4206.

Nonhoff, U., Ralser, M., Welzel, F., Piccini, I., Balzereit, D., Yaspo, M.L., Lehrach, H., and Krobitsch, S. (2007). Ataxin-2 interacts with the DEAD/H-box RNA helicase DDX6 and interferes with P-bodies and stress granules. Molecular biology of the cell *18*, 1385-1396.

Porta, C., Paglino, C., and Mosca, A. (2014). Targeting PI3K/Akt/mTOR Signaling in Cancer. Frontiers in oncology *4*, 64.

Quinn, B.J., Kitagawa, H., Memmott, R.M., Gills, J.J., and Dennis, P.A. (2013). Repositioning metformin for cancer prevention and treatment. Trends Endocrinol Metab *24*, 469-480.

Reiter, A.K., Bolster, D.R., Crozier, S.J., Kimball, S.R., and Jefferson, L.S. (2005). Repression of protein synthesis and mTOR signaling in rat liver mediated by the AMPK activator aminoimidazole carboxamide ribonucleoside. American journal of physiology Endocrinology and metabolism *288*, E980-988.

Rosilio, C., Ben-Sahra, I., Bost, F., and Peyron, J.F. (2014). Metformin: a metabolic disruptor and anti-diabetic drug to target human leukemia. Cancer letters *346*, 188-196.

Rutter, J., Michnoff, C.H., Harper, S.M., Gardner, K.H., and McKnight, S.L. (2001). PAS kinase: an evolutionarily conserved PAS domain-regulated serine/threonine kinase. Proceedings of the National Academy of Sciences of the United States of America *98*, 8991-8996.

Rutter, J., Probst, B.L., and McKnight, S.L. (2002). Coordinate regulation of sugar flux and translation by PAS kinase. Cell *111*, 17-28.

Sanpei, K., Takano, H., Igarashi, S., Sato, T., Oyake, M., Sasaki, H., Wakisaka, A., Tashiro, K., Ishida, Y., Ikeuchi, T.*, et al.* (1996). Identification of the spinocerebellar ataxia type 2 gene using a direct identification of repeat expansion and cloning technique, DIRECT. Nat Genet *14*, 277-284.

Schmidt, M.C., and McCartney, R.R. (2000). beta-subunits of Snf1 kinase are required for kinase function and substrate definition. EMBO J *19*, 4936-4943.

Semache, M., Fontes, G., Fogarty, S., Kikani, C., Rutter, J., and Poitout, V. (2013). PAS Kinase Regulates PDX-1 Protein Stability Via Phosphorylation of GSK3beta in Pancreatic Beta Cells. Canadian journal of diabetes *37 Suppl 4*, S59.

Semplici, F., Vaxillaire, M., Fogarty, S., Semache, M., Bonnefond, A., Fontes, G., Philippe, J., Meur, G., Diraison, F., Sessions, R.B.*, et al.* (2011). Human Mutation within Per-Arnt-Sim (PAS) Domain-containing Protein Kinase (PASK) Causes Basal Insulin Hypersecretion. J Biol Chem *286*, 44005-44014.

Shimobayashi, M., and Hall, M.N. (2014). Making new contacts: the mTOR network in metabolism and signalling crosstalk. Nature reviews Molecular cell biology *15*, 155-162.

Shinoda, J., and Kikuchi, Y. (2007). Rod1, an arrestin-related protein, is phosphorylated by Snf1-kinase in Saccharomyces cerevisiae. Biochemical and biophysical research communications *364*, 258-263.

Smith, T.L., and Rutter, J. (2007). Regulation of glucose partitioning by PAS kinase and Ugp1 phosphorylation. Mol Cell *26*, 491-499.
Socal, M.P., Emmel, V.E., Rieder, C.R., Hilbig, A., Saraiva-Pereira, M.L., and Jardim, L.B. (2009). Intrafamilial variability of Parkinson phenotype in SCAs: novel cases due to SCA2 and SCA3 expansions. Parkinsonism Relat Disord *15*, 374-378.

Swisher, K.D., and Parker, R. (2010). Localization to, and effects of Pbp1, Pbp4, Lsm12, Dhh1, and Pab1 on stress granules in Saccharomyces cerevisiae. PLoS One *5*, e10006.

Takahara, T., and Maeda, T. (2012). Transient sequestration of TORC1 into stress granules during heat stress. Mol Cell *47*, 242-252.

Vincent, O., and Carlson, M. (1999). Gal83 mediates the interaction of the Snf1 kinase complex with the transcription activator Sip4. The EMBO journal *18*, 6672-6681.

Wilson, W.A., Skurat, A.V., Probst, B., de Paoli-Roach, A., Roach, P.J., and Rutter, J. (2005). Control of mammalian glycogen synthase by PAS kinase. Proc Natl Acad Sci U S A *102*, 16596-16601.

Ye, T., Bendrioua, L., Carmena, D., Garcia-Salcedo, R., Dahl, P., Carling, D., and Hohmann, S. (2014). The mammalian AMP-activated protein kinase complex mediates glucose regulation of gene expression in the yeast Saccharomyces cerevisiae. FEBS letters *588*, 2070-2077.

Zhang, L., and Daly, R.J. (2012). Targeting the human kinome for cancer therapy: current perspectives. Crit Rev Oncog *17*, 233-246.

# CHAPTER 4: Novel molecular mechanisms behind the roles of PAS kinase and Cbf1 in regulating respiration

[1]Desiree DeMille, [1]Jenny A. Pattison, [2]Benjamin T. Bikman, and [1]Julianne H. Grose*

[1]Department of Microbiology and Molecular Biology, [2]Department of Physiology and Developmental Biology, Brigham Young University, Provo, UT 84602

*Address correspondence to:

Julianne H. Grose
Department of Microbiology and Molecular Biology
Brigham Young University, Provo, UT 84602
E-mail: julianne_grose@byu.edu

ABSTRACT

PAS kinase 1 (Psk1) is a key regulator of respiration in yeast. Psk1 regulates respiration in part through the phosphorylation and inhibition of Centromere binding factor 1 (Cbf1). Evidence is provided for the mechanisms by which PAS kinase and Cbf1 regulate respiration. First, transmission electron micrographs show an increased number of mitochondria in PAS kinase-deficient yeast. Second, PAS kinase-deficient yeast have an increase in succinate dehydrogenase (SDH) activity while Cbf1-deficient yeast have a significant decrease. Neither effect is attributable to altered SDH protein levels suggesting a post-translational effect. A high-copy suppressor screen as well as beta-galactosidase reporter assays of reported Cbf1 targets identifies novel pathways by which Cbf1 and Psk1 regulate respiration, including the identification of another protein kinase (Mck1) as well as direct transcriptional control of *ATP3*, a subunit of the mitochondrial $F_1$-ATP synthase complex. Finally, evidence that the human homolog of Cbf1, Upstream transcription factor 1 (USF1), is a conserved substrate of human PAS kinase (hPASK) is provided along with evidence that USF1 plays a key role in regulating respiration in mammals. Both Cbf1/USF1 and PAS kinase have previously been reported to affect lipid biogenesis. Combined, our data supports a model in which Cbf1/USF1 functions to partition glucose towards respiration and away from lipid biogenesis, while PAS kinase inhibits Cbf1/USF1. These results place PAS kinase and Cbf1/USF1 as central regulators of respiration and lipid metabolism, key pathways disrupted in diseases such as obesity, diabetes and cancer. In addition, they identify several novel pathways in the regulation of mitochondrial respiration.

## INTRODUCTION

Proper resource allocation is fundamental to the success of any system. For example, in cellular organisms it is crucial to sense available nutrients and decide how to properly allocate them among several pathways including growth, storage and energy metabolism. If nutrients are not properly allocated, e.g. when too many nutrients are diverted to one pathway, it comes at the expense of another important pathway and often leads to diseases such as obesity, diabetes and cancer. One of the mechanisms that cells have evolved to help coordinate resource allocation are nutrient sensing protein kinases.

PAS kinase is a highly conserved sensory kinase with both a sensory PAS (Per-ARNT-Sim) domain and a serine/threonine kinase domain (Rutter et al., 2001). It is a key player in sensing and allocating glucose in eukaryotic cells (reviewed in (DeMille and Grose, 2013)). Additionally, PAS kinase is activated both in yeast and mammalian cells under conditions that activate respiratory metabolism (da Silva Xavier et al., 2004; Grose et al., 2007). For yeast, this occurs when cells are grown under carbon sources other than glucose, whereas for mammalian cells, this occurs under conditions of high glucose.

PAS kinase is not only activated by respiratory conditions, but is also implicated in regulating respiratory metabolism itself. PAS kinase-deficient mice (PASK-/-) have a hypermetabolic phenotype in that they consume more oxygen and give off more $CO_2$ and heat (Hao et al., 2007). Additionally, these mice accumulate significantly less lipids in their liver when placed on a high fat diet. These data suggest that PAS kinase is allocating glucose away from respiration towards lipid storage in wild type mice. However, the mechanisms behind these phenotypes are largely unknown. We recently identified a novel substrate of yeast PAS kinase 1

(Psk1), Centromere binding factor 1 (Cbf1) that could be an important player in the mechanisms behind these phenotypes (DeMille et al., 2014).

Cbf1 is a general transcription factor conserved from yeast to man. Its human homolog, Upstream transcription factor 1 (USF1), is a key regulator of genes involved in lipid homeostasis (Auer et al., 2012; Naukkarinen et al., 2006; Pajukanta et al., 2004). In yeast, transcriptome data suggests that Cbf1 regulates a wide variety of genes including those involved in respiration and lipid biogenesis, as well as amino acid biosynthesis (Cai and Davis, 1990; Kolaczkowski et al., 2004; Lin et al., 2013). We recently provided evidence for the PAS kinase-dependent phosphorylation and inhibition of Cbf1, which resulted in decreased respiration rates in yeast (DeMille et al., 2014). This altered respiration could be due to many alterations within the cell, including increased total mitochondrial mass or increased electron transport chain expression or activity. Here we further characterize the mechanisms behind PAS kinase and Cbf1 function in regulating respiration in yeast. Specifically, we looked at the differences in mitochondrial mass and electron transport chain activity between wild type, Cbf1-deficient and PAS kinase-deficient yeast. In addition, a high-copy suppressor screen of Cbf1-deficiency revealed novel targets involved in mitochondrial regulation. Finally, evidence is provided for Cbf1/USF1 being a conserved substrate in humans. Combined, our data supports a model in which Cbf1/USF1 partitions glucose towards respiration at the expense of lipid biogenesis, while PAS kinase inhibits Cbf1/USF1 favoring lipid biogenesis.

## RESULTS

### Respiratory control is a specialized function of PAS kinase 1 (Psk1)

In budding yeast there are two orthologs of PAS kinase, Psk1 and Psk2 (Rutter et al., 2001), which have high sequence similarity and are partially redundant in function (Rutter et al., 2002). Duplicated genes arose from a whole-genome duplication event that occurred in an early ancestor of yeast (Byrne and Wolfe, 2007; Conant and Wolfe, 2007; Grassi et al., 2010; Maclean and Greig, 2011; Sugino and Innan, 2005). From this, duplicated proteins either gained accessory functions allowing for their selection and maintenance, or were selected against and lost. Psk1 and Psk2 being maintained suggests differential functions for these proteins, however, both proteins phosphorylate the well-characterized substrate UDP-glucose pyrophosphorylase (Ugp1). We recently showed that *psk1psk2*-deficient yeast have an increased respiration rate when compared to wild type (WT) yeast (DeMille et al., 2014). We expect this phenotype to be a specialized function of Psk1 specifically because it is activated under non-glucose carbon sources (respiratory conditions) whereas Psk2 is downregulated and inactivated by these conditions (Grose et al., 2007). To verify that respiratory control is a specialized function of Psk1 we tested respiration rates in the individual mutant yeast (*psk1* and *psk2*) compared to WT and the double mutant (*psk1psk2*) (Figure 4.1). Both *psk1psk2* and *psk1* yeast had significantly higher maximal respiration rates compared to WT. There was no significant difference between *psk2* and WT yeast. These results support that the Psk1 ortholog is primarily responsible for regulating respiration in yeast consistent with differential functions for Psk1 and Psk2. This also gives supporting evidence that the recently identified PAS kinase substrate, Cbf1, is a specific target of Psk1, at least under respiratory conditions (DeMille et al., 2014).

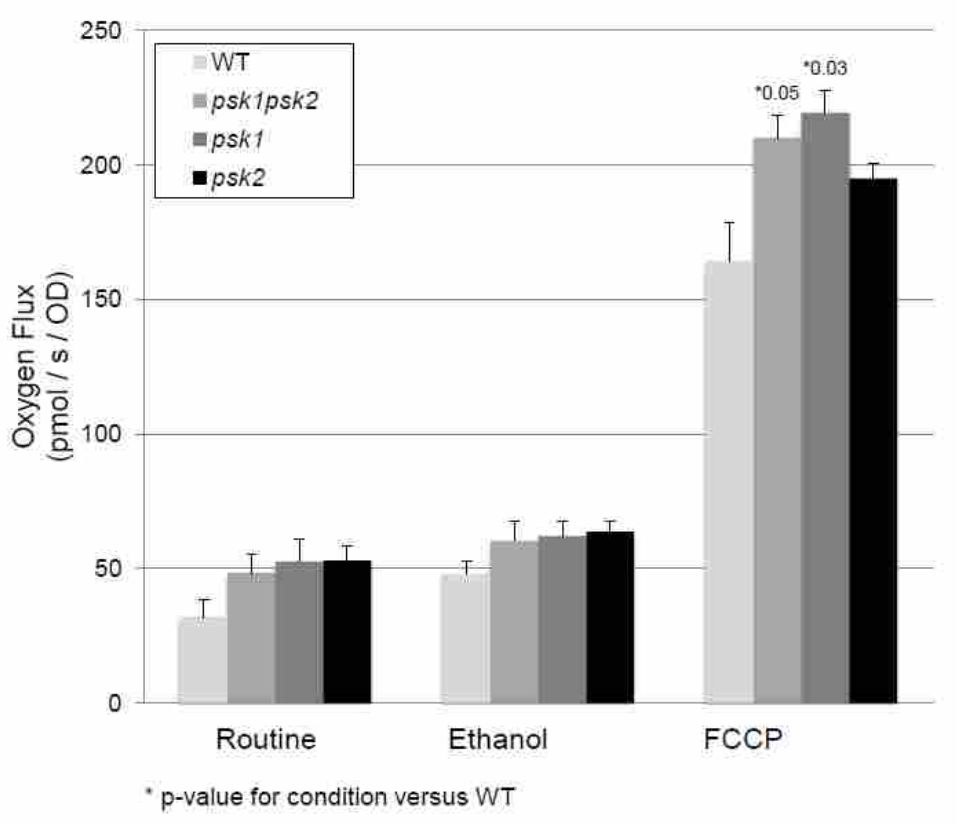


FIGURE 4.1. Respiratory control is a specialized function of Psk1 in yeast. WT, *psk1psk2*, *psk1* or *psk2* yeast were grown under YPAglycerol/EtOH conditions and respiration rates were measured using an Oroboros $O_2K$ Oxygraph. First, routine respiration was measured, then cells were supplied with ethanol, and finally, respiration was measured in the presence of an uncoupler (FCCP) to represent maximal respiration. Significant p values for strain versus WT are indicated.

Psk1 inhibits respiration through phosphorylation of Cbf1 at T211

In our recent publication, we showed that the combination of threonines 211 and 212 of Cbf1 are important for Psk1 phosphorylation and inhibition of respiration (DeMille et al., 2014). We further investigated each of these two sites individually through in vitro kinase assays with each phosphomutant protein (T211A and T212A) and found that T211 of Cbf1 is the critical site for Psk1 phosphorylation (Figure 4.2A). Additionally, T211 is the site that is critical for Psk1 inhibition of respiration in vivo (Figure 4.2B). Cbf1-deficient yeast were transformed with either an empty vector, wild type Cbf1, phosphomutants T211A and T212A, or phosphomimetics

T211D and T211E. As expected, yeast containing the unphosphorylatable T211A-Cbf1 protein had a significant increase in respiration. Both phosphomimetic forms of T211 (T211D and T211E) were not significantly different from the WT controls (data not shown), suggesting that the phosphomimetic mutations do not mimic Psk1 phosphorylation. Interestingly, the phosphomimetic form of Ugp1 also did not mimic phospho-Ugp1 (Smith and Rutter, 2007).

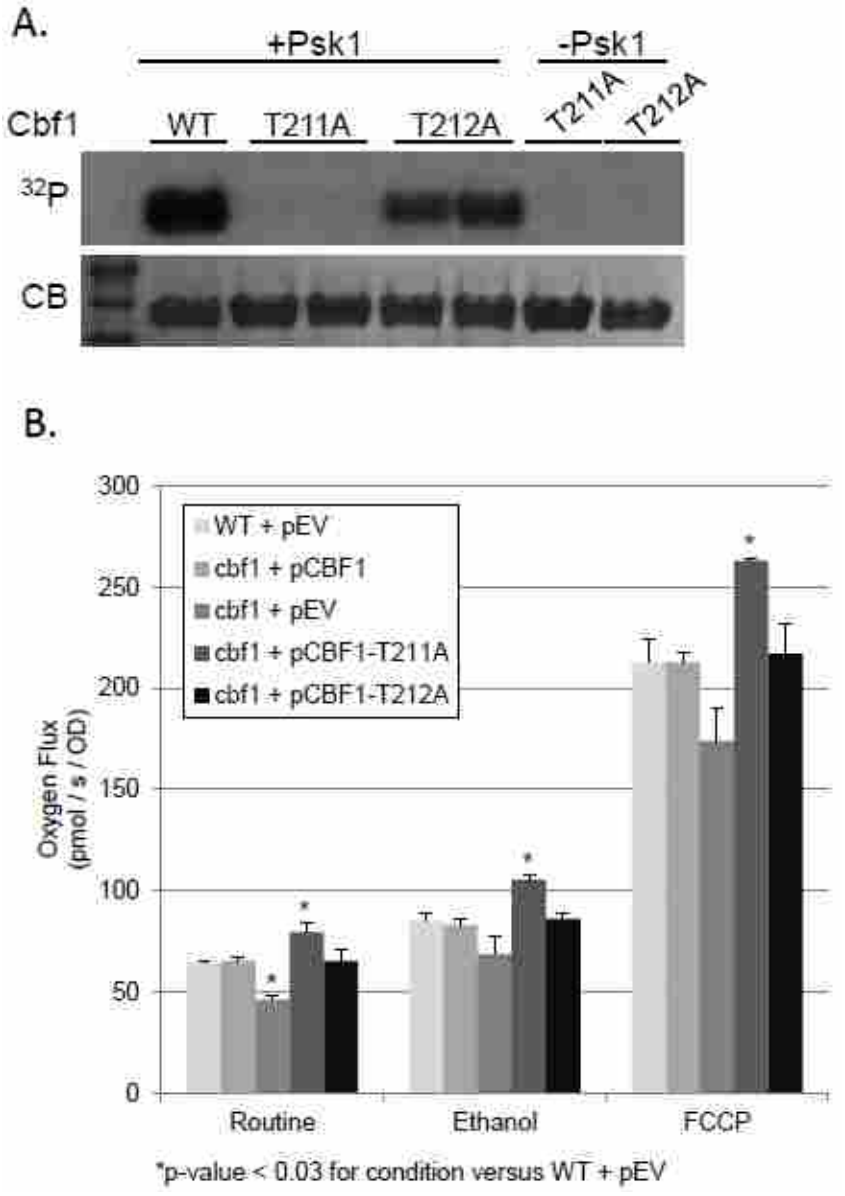


FIGURE 4.2. Threonine 211 of Cbf1 is critical for Psk1 phosphorylation and inhibition of respiration. (A) In vitro kinase assays using purified Cbf1 proteins incubated with radiolabeled-ATP were tested in the presence and absence of Psk1. Kinase reactions were run on SDS PAGE, stained with Coomassie

Brilliant Blue (CB panel) and imaged using autoradiography ($^{32}$P panel). (B) WT yeast (JGY43) transformed with an empty vector (pJG725) or Cbf1-deficient yeast (JGY1227) transformed with either the empty vector, WT Cbf1 (pJG1125), Cbf1-T211A (pJG1335) or Cbf1-T212A (pJG1336) were grown in selective synthetic glycerol/EtOH media and respiration rates were measured using an Oroboros $O_2K$ Oxygraph. Error bars represent SEM. Significant p-values for condition versus WT are shown.

PAS kinase-deficient yeast have increased mitochondrial mass

We previously provided evidence for the PAS kinase-dependent phosphorylation and inhibition of Cbf1, which causes altered respiration rates in yeast (DeMille et al., 2014). Cbf1-deficient yeast showed a significant decrease whereas PAS kinase-deficient yeast showed a significant increase in respiration that was primarily dependent on Cbf1. These effects on respiration could be due to several different alterations in the cell including increased mitochondrial mass. To test the hypothesis that Cbf1 increases respiration by upregulating mitochondrial biogenesis pathways, mitochondria were viewed by electron microscopy and both the number and total area of mitochondria were quantified in WT, *cbf1* and *psk1psk2* yeast (Figure 4.3 and Table 4.1). PAS kinase-deficient yeast showed a significant increase in both the number of mitochondria per cell as well as average mitochondrial area per total cell area. These PAS kinase affects are consistent with the respiration phenotype; however, Cbf1 appeared to have no significant effect suggesting increased electron transport activity rather than increased mitochondrial mass.

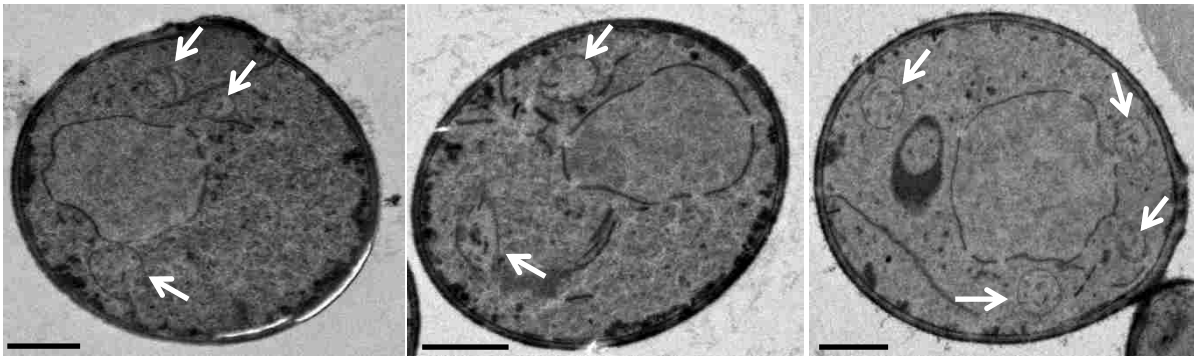


FIGURE 4.3. Representative pictures from transmission electron microscopy of WT, *cbf1* and *psk1psk2* yeast. Each yeast strain (wild type (WT, JGY43), *cbf1* (JGY1227) and *psk1psk2* (JGY1244)) were grown in duplicate, fixed according to the permanganate fixation protocol described by Perkins and McCaffrey (Perkins and McCaffery, 2007), stained with Reynold's Lead Citrate then observed in a Technai T-12 transmission electron microscope. White arrows indicate mitochondria. Scale bars= 1uM.

TABLE 4.1. PAS kinase-deficient yeast have increased mitochondrial mass

| Strain | N | Av. # mito per cell | Av. mito area/cell area |
|---|---|---|---|
| WT | 74 | 3.01 | 0.0369 |
| *cbf1* | 73 | 2.78 | 0.0399 |
| *psk1psk2* | 60 | (*p = 0.011) 3.55 | (*p = 0.002) 0.0465 |

Mitochondrial quantification of electron micrographs was determined using AxioVision Software. "N" number of images were analyzed for each strain as indicated. Both the average number of mitochondria per cell as well as average mitochondrial area per total cell area was determined. Significant p values are indicated for *psk1psk2* versus WT.

Cbf1 increases respiration by increasing electron transport chain activity

Observing no significant effect of Cbf1 on mitochondrial mass led us to investigate the effects of Cbf1 on electron transport chain activity. We looked at a common point of respiratory regulation, succinate dehydrogenase (SDH). As both a component of the citric acid cycle (TCA) and electron transport chain (ETC), SDH is the first dedicated step in respiration. The SDH activity reflected what we observed in our previous observations for yeast respiration rates

(DeMille et al., 2014). As expected, *cbf1* yeast had a significant decrease in SDH activity and PAS kinase-deficient yeast had a significant increase when compared to WT (Figure 4.4A). As a control, there was no significant difference among strains for citrate synthase activity, a TCA enzyme.

Increased activity could be due to an increase in protein amount or altered protein activity therefore we did Western blots of SDH protein levels compared to mitochondrial Vdac1 (porin) protein. We found that the decreased respiration of *cbf1* yeast was not due to decreased SDH amounts (Figure 4.4B), in fact, SDH protein levels were upregulated in both the *cbf1 and psk1psk2* yeast. These findings suggest that the decreased respiration of Cbf1-deficient yeast is most likely caused by a post-translational effect. To better understand this effect on respiration, we performed beta-galactosidase reporter assays with reported transcriptional targets of Cbf1 as well as a high-copy suppressor screen of Cbf1-deficiency to identify novel respiratory targets of Cbf1or proteins in parallel pathways.

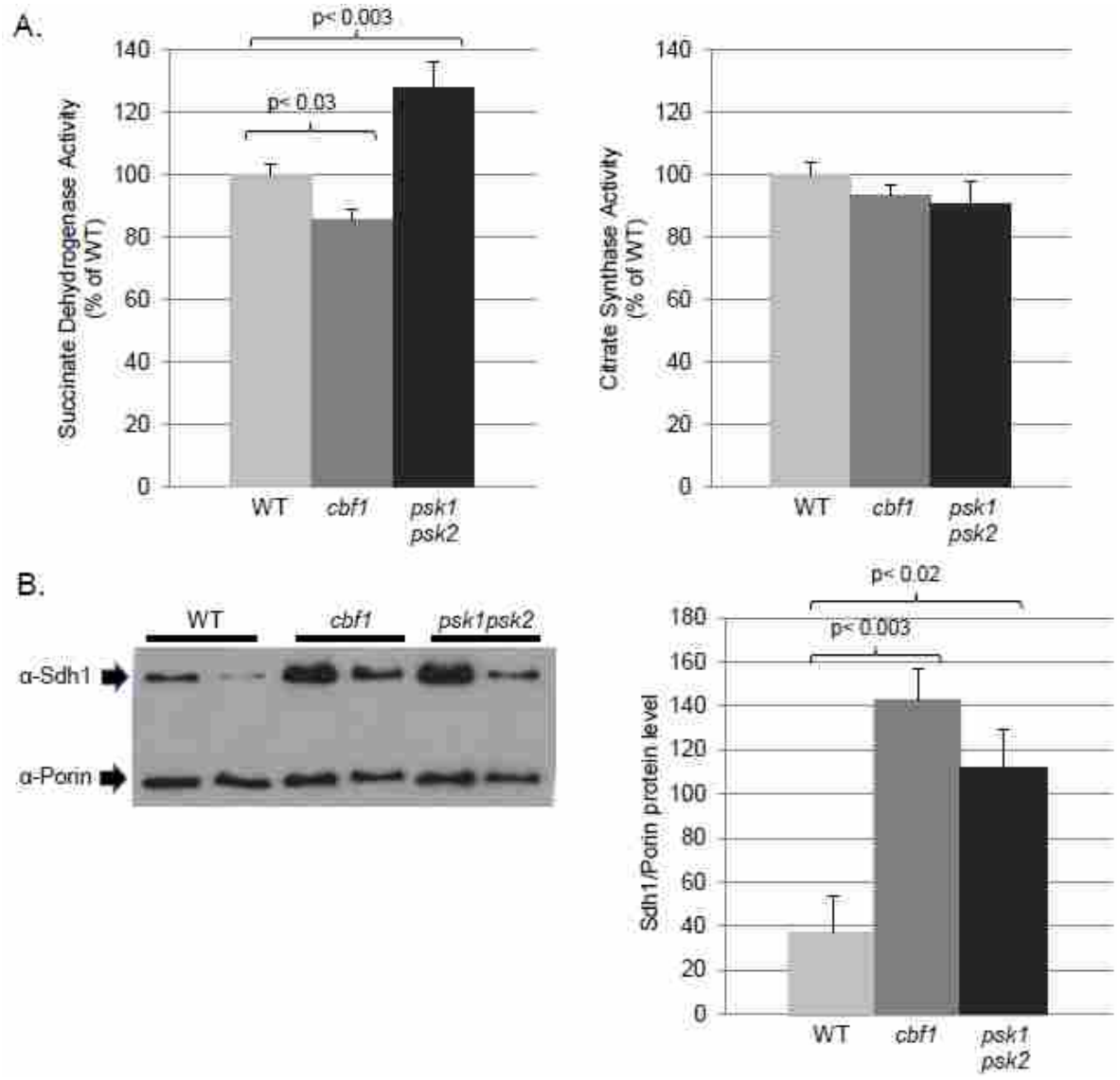


FIGURE 4.4. Cbf1 increases respiration through increased succinate dehydrogenase activity. (A) Isolated mitochondria from WT (JGY43), *cbf1* (JGY1227) and *psk1psk2* (JGY1244) yeast were assayed for succinate dehydrogenase (SDH) activity (left) as well as citrate synthase (CS) activity (right) using kits from BioVision (Milpitas, CA). (B) Purified mitochondria used in the SDH and CS assays were run on SDS PAGE, transferred to nitrocellulose paper and then probed with antibodies for Sdh1 and porin (left). Quantification of Sdh1 to porin protein amounts (right). Biological replicates were run in triplicate for SDH and CS and duplicate for Western blot. Error bars represent SEM.

*MCK1* and *COT1* rescue respiration growth defects caused by Cbf1-deficiency

Transcriptome data of Cbf1 has suggested it to be a player in respiratory control through direct transcriptional regulation of respiratory targets (Haynes et al., 2013; Lin et al., 2013;

MacIsaac et al., 2006; Petti et al., 2012). We took several respiration-associated genes reported to be upregulated by Cbf1 in large-scale transcriptome studies (*ATP3*, *COX4*, *HAP4*, *NDI1*, *QCR6*) and cloned in their promoters into a LacZ fusion plasmid to test transcriptional control in vivo. The gene encoding $F_1$-ATP synthase complex *ATP3* was the only gene from the ones tested that appeared to be upregulated by Cbf1 in our beta-galactosidase reporter assays and is shown in Figure 4.5, however, no significant difference was observed. As a control, we assayed two ceramide synthase promoters (*LAC1* and *LAG1*) that were previously shown through beta-galactosidase assays to be significantly downregulated by Cbf1. The *LAC1* and *LAG1* behaved similarly to what Kolaczkowski et al. have reported, giving support that the assays were working properly. Through these assays we were unable to identify a key respiratory regulation target of Cbf1, thus novel targets of Cbf1 were sought through a high-copy suppressor screen.

Cbf1-deficient yeast grow poorly on respiratory carbon sources such as glycerol/EtOH medium. Using this growth phenotype, we conducted high-copy suppressor screens to look for suppressors of Cbf1-deficiency. Screens were conducted by transforming Cbf1-deficient yeast with two different high-copy genomic DNA libraries and screening for rescuers of respiratory-growth deficiency on synthetic glycerol/EtOH plates. A WT Cbf1 plasmid transformed into *cbf1* yeast was used as a positive control and an empty vector was used as a negative control. Two novel genes were retrieved from these screens, the Meiotic and centromere regulatory ser, tyr-kinase (*MCK1*) as well as Cobalt Toxicity (*COT1*) (Table 4.2). Approximately 99% of the hits we retrieved were either full-length or a truncated (ΔNCbf1) form of Cbf1. Novel plasmids retrieved from the screens were isolated, retransformed into naïve *cbf1* yeast and plated via spot dilutions to confirm rescue of Cbf1-deficiency was due to the plasmids and not a chromosomal mutation in the yeast (Figure 4.6).

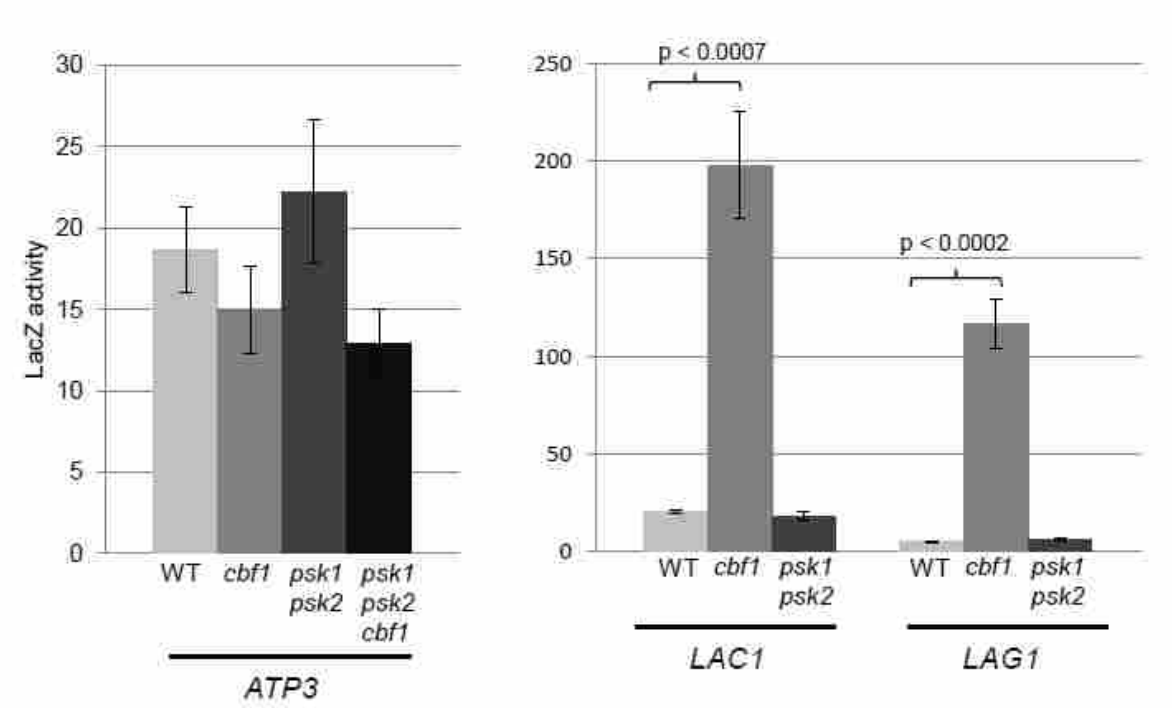


FIGURE 4.5. Beta-galactosidase reporter assays of *ATP3*, *LAC1* and *LAG1* promoters. WT, *cbf1*, *psk1psk2, psk1psk2cbf1* yeast were transformed with LacZ fusion plasmids containing the *ATP3* (pJG1315), *LAC1* (pJG1321), or *LAG1* (pJG1322) promoters. Yeast were grown in selective SD-Leu media to $OD_{600}$ ~0.5-1.0 then assayed for beta-galactosidase activity as previously described by John Strebbins, Triezenberg lab. Cell extracts were normalized by the Bradford assay to ensure equal amounts of total protein were used.

TABLE 4.2. High-copy suppressor screen of Cbf1-deficiency

| Library | # transformants | # positive hits | Cbf1 hits | Unique hits |
|---|---|---|---|---|
| 727 | ~1,332,600 | 141 | ~91% (Cbf1)<br>~9% (ΔNCbf1) | - |
| 728 | ~2,407,066 | 207 | ~85% (Cbf1)<br>~14% (ΔNCbf1) | Mck1<br>Cot1 |

High-copy plasmid yeast genomic libraries (pJG727 or pJG728) were transformed into Cbf1-deficient yeast (JGY1227), and plated to selective SD-Ura plates. Plates were allowed to grow 2 days then replica printed to synthetic glycerol/EtOH plates and grown another 2 days. Positive hits were patched, lyticased and PCR amplified to first determine full-length or truncated Cbf1 hits. Hits that were neither construct of Cbf1 were sequenced to determine the high-copy suppressor gene. The table indicates the library used, number of yeast transformants, number of positive suppressors, the percentage of hits that were either full-length or truncated Cbf1, and any unique hits identified from the screen.

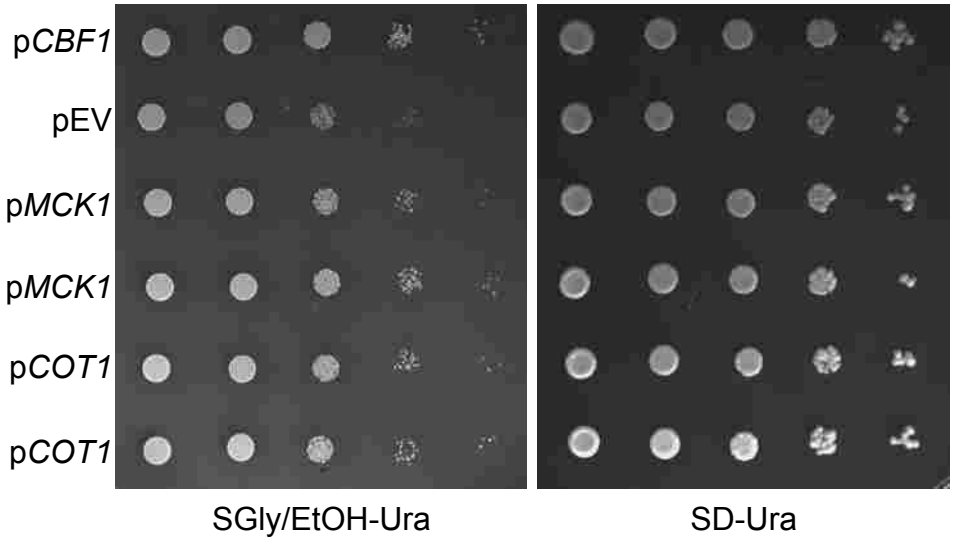


FIGURE 4.6. *MCK1* and *COT1* overexpression rescues Cbf1-deficiency. Cbf1-deficient yeast (JGY1227) transformed with plasmids containing WT Cbf1 (p*CBF1*, pJG1125), empty vector (pEV, pJG725), or plasmids isolated from our high-copy suppressor screen (p*MCK1* and p*COT1*), were grown 2 days in SD-Ura liquid media. Cultures were serially diluted (1/5, 1/5, 1/10, 1/10, 1/10) in water and spotted to both selective synthetic glycerol/EtOH (SGly/EtOH-Ura) and synthetic dextrose (SD-Ura (control)) plates and incubated for 2-3 days at 30˚C.

Human USF1 protein is a conserved substrate of PAS kinase and rescues Cbf1-deficiency in yeast

The human homolog of Cbf1, Upstream transcription factor 1 (USF1) is a major contributor to Familial Combined Hyperlipidemia (FCHL) (Auer et al., 2012; Coon et al., 2005; Di Taranto et al., 2015; Holzapfel et al., 2008; Huertas-Vazquez et al., 2005; Komulainen et al., 2006; Lee et al., 2007; Meex et al., 2008; Naukkarinen et al., 2006; Naukkarinen et al., 2005; Naukkarinen et al., 2009; Ng et al., 2005; Pajukanta et al., 2004; Plaisier et al., 2009; Reiner et al., 2007; van der Vleuten et al., 2007). Although several studies have confirmed its role in lipid homeostasis, a role in respiratory regulation has not been shown. Cbf1 and USF1 have homology in the region of the PAS kinase phosphorylation site on Cbf1 just upstream of the conserved basic helix-loop helix domain (Figure 4.7A). To determine if USF1 is a conserved substrate of the human PAS kinase protein (hPASK) we tested for phosphorylation through in

vitro kinase assays (Figure 4.7B). USF1 does get phosphorylated in a hPASK-dependent manner. Additionally, Cbf1 and USF1 alignment suggested that serine 186 of USF1 is a good candidate for a hPASK phosphorylation site, however, the mutated S186A-USF1 was still phosphorylated by hPASK in vitro (data not shown).

Next we looked to see if USF1 could have a conserved role in regulating respiration. This was tested by seeing if USF1 could rescue the decreased respiration phenotype of Cbf1-deficient yeast through both respiration chamber assays (Figure 4.8A) as well as plate assays (Figure 4.8B). The results from both assays gave supporting evidence that USF1 is able to complement the respiration phenotype of Cbf1-deficiency in yeast, suggesting that Cbf1/USF1 play a conserved role in the partitioning of glucose towards respiration.

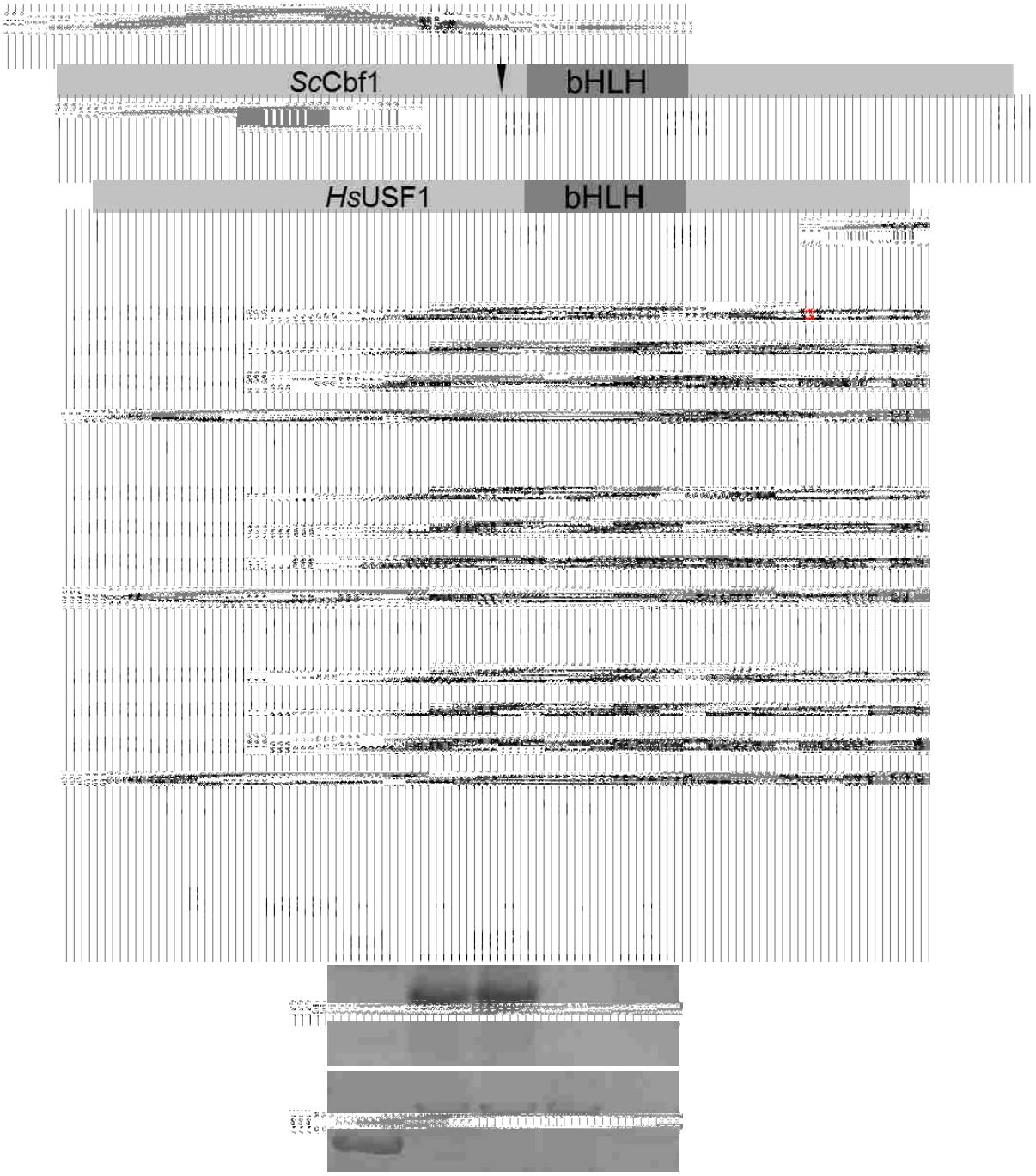


FIGURE 4.7. An alignment of Cbf1 functional orthologs and in vitro evidence of USF1 as a hPASK substrate. (A) The amino acid sequences near the bHLH domain of Cbf1orthologs (obtained from the Isobase database (MIT)) were aligned using Clustal Omega software. *S. cerevisiae* (*Sc*Cbf1), *H. sapiens* (*Hs*USF1), *M. musculus* (*Mm*USF1) and *C. elegans* (*Ce*MXL-1). (B) In vitro kinase assays using purified USF1 and hPASK proteins incubated in the presence of radiolabeled-ATP were run on SDS PAGE, stained with Coomassie Brilliant Blue (CB) and imaged using autoradiography ($^{32}$P). Ipp1 was used as a negative control to show specificity of hPASK to USF1.

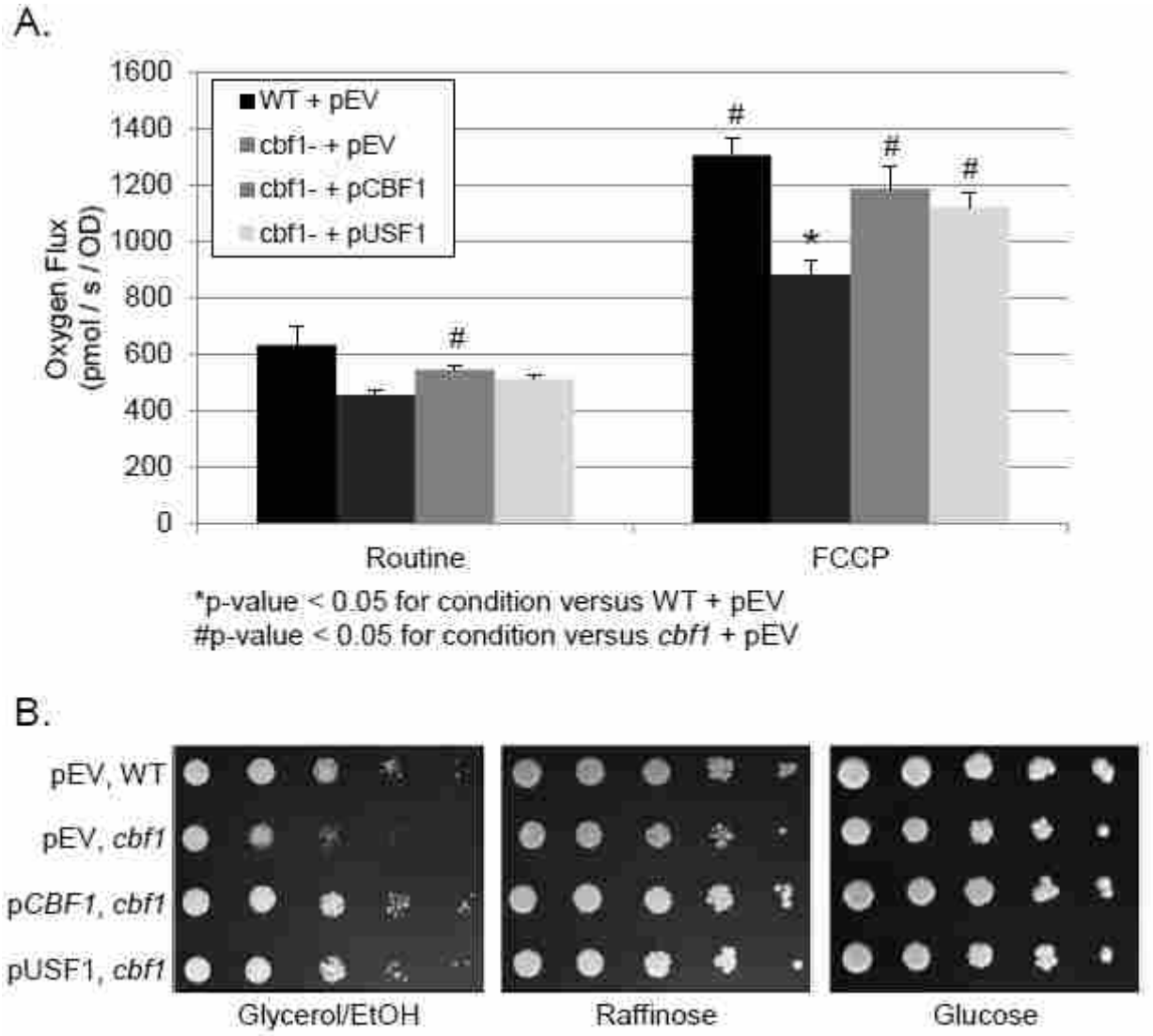


FIGURE 4.8. USF1 rescues Cbf1-deficiency in yeast. WT yeast transformed with an empty vector (pEV, pJG725), or *cbf1* yeast transformed with an empty (pEV, pJG725), Cbf1 (p*CBF1*, pJG1125) or USF1 (pUSF1, pJG1246) vector were grown in SD-Ura. (A) For respiration chamber assays, overnights in SD-Ura were switched to SGal-Ura media and respiration assays were performed on an Oroboros $O_2K$ Oxygraph. (B) For plate assays, overnights in SD-Ura were serially diluted in water (1:10) then plated to selective glycerol/EtOH, raffinose, or glucose plates and incubated for 2-3 days at 30˚C.

## DISCUSSION

As the primary source of cellular energy, the regulation of mitochondrial metabolism is key in proper glucose allocation. As such, mitochondrial dysfunction has come to the forefront of a wide variety of diseases, from diabetes and obesity to cancer, alzheimers and

neurodegenerative disease. Despite their clear importance, there is still much unknown about mitochondrial regulation. This study provides novel molecular mechanisms behind the regulation of mitochondrial metabolism by PAS kinase and Cbf1. First, PAS kinase-dependent phosphorylation of Cbf1 at the critical threonine 211 site dramatically reduces cellular respiration (Figure 4.2). The mechanisms behind this respiratory phenotype were characterized by looking at mitochondrial content and electron transport chain activity. Electron micrographs support PAS kinase-deficient yeast having increased mitochondrial mass consistent with increased respiration rates, whereas, no significant decrease was observed in the Cbf1-deficient yeast (Figure 4.3). However, Cbf1-deficient yeast did show a trend towards lower numbers of mitochondria compared to WT yeast, which may be significant if a higher sample size were used. Another possible explanation is that PAS kinase could have additional targets that may control mitochondrial biogenesis. Additional effects on morphology including fusion and fission rates would be worth further study to better understand the mitochondrial morphological effects of PAS kinase.

Although a significant decrease in mitochondrial mass was not observed as being the cause behind the decrease in respiration of Cbf1-deficient yeast, we did see a significant effect on electron transport chain activity (Figure 4.4). Cbf1-deficient yeast have decreased succinate dehydrogenase activity and PAS kinase-deficient yeast have increased when compared to WT yeast. Both phenotypes reflected what was previously seen in the respiration assays (DeMille et al., 2014). Additionally, the decrease in SDH activity of *cbf1* yeast was not due to a decrease in protein amount, which is consistent with unaltered mitochondrial mass in the electron micrographs, suggesting this regulation is caused by a post translational effect. To try to understand this effect, high copy suppressor screens were conducted to identify suppressors of

Cbf1-deficiency (Table 4.2). Two novel respiratory targets were retrieved, Mck1 (a serine/threonine protein kinase) and Cot1 (a protein involved in vacuolar zinc transport). These could be downstream targets of Cbf1 or work in parallel pathways as Cbf1 to control respiration. Further work to determine their precise mechanisms to suppress Cbf1 function will be required.

Although we were the first to show that Cbf1 directly regulates respiration, Cbf1 has previously been shown to regulate genes involved in lipid biogenesis (Kolaczkowski et al., 2004; Petti et al., 2012). In addition, human USF1 alleles have been associated with hyperlipidemia in several studies (Auer et al., 2012; Coon et al., 2005; Di Taranto et al., 2015; Holzapfel et al., 2008; Huertas-Vazquez et al., 2005; Komulainen et al., 2006; Lee et al., 2007; Meex et al., 2008; Naukkarinen et al., 2006; Naukkarinen et al., 2005; Naukkarinen et al., 2009; Ng et al., 2005; Pajukanta et al., 2004; Plaisier et al., 2009; Reiner et al., 2007; van der Vleuten et al., 2007). Combined, these results suggest that Cbf1/USF1 play a conserved role in partitioning glucose towards respiration at the expense of lipid metabolism. In support of this hypothesis, USF1 appears to regulate respiration in both yeast and mammalian cells (Figure 4.8). The role of PAS kinase in inhibiting Cbf1 also appears to be conserved, in that hPASK can phosphorylate USF1 in vitro (Figure 4.7). Thus, with the powerful tools yeast provides, we are able to identify and characterize a key substrate that may explain the most dramatic phenotypes observed in PAS kinase-deficient mice (Hao et al., 2007). Further study of how PASK is regulating the many activities of USF1 may provide further insights into the role of PAS kinase in human diseases including hyperlipidemia, obesity and diabetes. In addition, it will identify novel targets in the regulation of mitochondria which may be key targets for disease treatment.

## MATERIALS AND METHODS

### Growth assays and vector construction

A list of strains, plasmids and primers used in this study are provided in Table 4.3. All plasmids constructed for this study were made using standard polymerase chain reactions (PCR) followed by restriction digests using enzymes from New England Biolabs (Mymrikov et al.).

### In vitro kinase assays

Full-length yeast Psk1 protein (pJG1181) was purified from WT yeast (JGY1) following a previously described Myc-epitope purification protocol (DeMille et al., 2015). Cbf1 (pJG1031) and USF1 (pJG1233) were HIS purified from BL21DE3 *E. coli* (JHG504) as previously described (DeMille et al., 2015). hPASK was expressed in insect cells using the BAC-to-BAC baculovirus expression system (GIBCO/BRL) and purified as previously described (Rutter et al., 2001).

For yeast in vitro kinase assays, purified proteins were incubated with and without Psk1 in a 30 uL reaction containing 1x kinase buffer as previously described (DeMille et al., 2014). For in vitro kinase assays using purified USF1 and hPASK proteins, reactions were run similar to the yeast proteins except for the following: 1 mM ATP was used and reactions were incubated for 30 minutes. Ipp1 (pJG1025) was purified similarly as Cbf1 and USF1, and was used as a negative control to show specificity of hPASK with USF1.

### Mitochondrial respiration

Yeast strains not transformed with a plasmid (WT (JGY43), *psk1psk2* (JGY1244), *psk1* (JGY1348) and *psk2* (JGY1349)) were grow in YPAD overnight, diluted 1:100 in

YPAGly/EtOH and grown for 13 hours. Wild type yeast (JGY43) transformed with an empty vector (pJG725), or Cbf1-deficient yeast (JGY1227) transformed with either empty vector (pJG725), WT Cbf1 (pJG1125), T211A-Cbf1 (pJG1335), T212A-Cbf1 (pJG1336), or USF1 (pJG1246) were grown in selective SD-Ura media until saturated, diluted 1:100 in SGly/EtOH-Ura and grown an additional 24-26 hours. The $OD_{600}$ was taken to ensure equal growth among strains. High-resolution $O_2$ consumption was determined at 37˚C using the Oroboros $O_2K$ Oxygraph (Innsbruck, Austria). Samples were centrifuged at 5000 x g for 5 min and resuspended in warm mitochondrial respiration buffer 05 (MiR05; 0.5 mM EGTA, 10 mM KH2PO4, 3 mM MgCl2-6 $H_2O$, 60 mM K-lactobionate, 20 mM HEPES, 110 mM sucrose, 1 mg/ml fatty acid free BSA, pH 7.1). After addition of sample, the chambers were hyperoxygenated to ~350 nmol/ml. Following this, routine respiration was determined by measuring $O_2$ consumption in the absence of any substrate (routine). Next, EtOH was added, then the uncoupler carbonyl cyanide p-(trifluoromethoxy)phenylhydrazone (FCCP; 70 μM) was added to determine uncoupled respiration as a measure of maximal electron transport system capacity (E). Finally, respiration was inhibited by the addition of the cytochrome c oxidase inhibitor, azide (20 mM) eliciting a state of residual oxygen consumption (ROX), which provided a control for all values. Samples were run in triplicate and averaged.

Respiration plate assays

Wild type yeast transformed with an empty vector (pJG725) or *cbf1* yeast (JGY1227) transformed with plasmids containing WT Cbf1 (pJG1125), the empty vector, plasmids isolated from the high-copy suppressor screen (p*MCK1* and p*COT1*), or USF1 (pJG1246) were grown 2 days in SD-Ura liquid media. Cultures were serially diluted (1/10) or (1/5, 1/5, 1/10, 1/10, 1/10)

in water and spotted to both selective synthetic glycerol/EtOH, raffinose, or glucose plates (control) and incubated for 2-3 days at 30˚C.

EM imaging

Wild type (JGY43), *cbf1* (JGY1227) and *psk1psk2* (JGY1244) yeast were grown overnight in YPAD then diluted into YPAraffinose and grown until $OD_{600}$ ~0.5. Cell size was measured using a Moxi Flow micro cytometer (ORFLO Technologies, Hailey, ID). Permanganate fixation protocol described by Perkins and McCaffery (Perkins and McCaffery, 2007) was followed. Samples were sectioned at 80 nm using a RMC MTX ultramicrotome with a diamond knife then post stained with Reynold's Lead Citrate for 10 min. Cells were observed in a Tecnai T-12 transmission electron microscope and images recorded digitally.

Mitochondrial quantification was determined using AxioVision Rel 4.8 Software (Zeiss) as described by Braun et al. (Braun et al., 2006). Each strain was grown in duplicate with ≥ 60 images per yeast strain obtained with the following criteria: 1. Cells must be at least 3 uM to ensure the section includes a majority of the cell 2. Cells must bear a visible nucleus 3. Cells must have an intact cell wall and 4. Cells must be fairly uniform in shape to exclude cells that are budding.

Beta-galactosidase reporter assays

A LacZ reporter plasmid (pJG1314) was constructed by amplifying LacZ from BL21DE3 *E. coli* with primers JG3683 and JG3684, digesting with HindIII/BamHI and ligating into a similarly digested pRS415 vector (pJG121). Promoter regions (*LAC1* (JG3440/JG3441), *LAG1* (JG3442/3443), *ATP3* (JG3671/3672), *COX4* (JG3675/3676), *HAP4* (JG3669/3670), *NDI1* (JG3679/3680), and *QCR6* (JG3673/3674)) were amplified from WT yeast template (JGY43)

and cloned into the XhoI/HindIII sites of pJG1314. Yeast strains (WT (JGY43), *cbf1* (JGY1227) *psk1psk2* (JGY1244) and *psk1psk2cbf1* (JGY1261)) were transformed with LacZ fusion plasmids containing each promoter region (pJG1321, (p*LAC1*-LacZ), pJG1322 (p*LAG1*-LacZ), pJG1315 (p*ATP3*-LacZ), pJG1316 (*pCOX4*-LacZ), pJG1317 (p*HAP4*-LacZ), pJG1318 (p*NDI1*-LacZ), pJG1320 (p*QCR6*-LacZ), grown in selective SD-Leu media for 2 days, then diluted 1:50 in fresh media and grown until $OD_{600}$ ~0.5-1.0. Beta-galactosidase assays were performed as previously described by John Strebbins, Triezenberg lab. Cell extracts were normalized by the Bradford assay to ensure equal amounts of total protein were used. Samples were run at least twice in duplicate and averages were taken.

Mitochondrial isolation

WT, *cbf1* and *psk1psk2* yeast were grown overnight in YPAD, diluted 1:100 into YPAGly/EtOH, and grown until $OD_{600}$ ~1.0-2.0. Preparation of Isolated Mitochondria by Differenting Centrifugation (Diekert et al., 2001) procedure was followed with the exception of Lyticase (Sigma-Aldrich) being used in place of Zymolase. Mitochondria were quantified using the Bradford assay.

SDH and CS assays

Following mitochondrial isolation, SDH and CS activity were assayed in WT (JGY43), *cbf1* (JGY1227) and *psk1psk2* (JGY1244) yeast using kits from BioVision (Milpitas, CA). Samples were run in triplicate from biological duplicates. Student's t-test was used to compare each strain against the WT.

ACKNOWLEDGMENTS

We would like to thank Michael Standing (Brigham Young University) who imaged our yeast for the electron micrographs and Dennis Winge (University of Utah, Salt Lake City, UT) for the Sdh1 and porin antibodies. Funding for this work was supported by National Institutes of Health Grant R15 GM100376-01, a Brigham Young University Mentoring Environmental Grant to J.H.G, Brigham Young University Cancer Research Center Fellowships to D.D and J.A.P, and the Brigham Young University Department of Microbiology and Molecular Biology and College of Life Sciences.

TABLE 4.3. Strains, plasmids and primers used in this study

| Strain | Background | Genotype | Abbreviation | a/α | Reference or source |
|---|---|---|---|---|---|
| JGY1 | W303 | *ade2-1, can1-100, his3-11,15 leu2-3,112 trp1-1, ura3-1* | WT | a | David Stillman, University of Utah |
| JGY43 | BY4741 | *his3-1, leu2-0, met15-0, ura3-0* | WT | a | (Winzeler et al., 1999) |
| JGY1227 | BY4741 | *cbf1::*kan-MX4*, his3-1, leu2-0, met15-0, ura3-0* | *cbf1* | a | (Winzeler et al., 1999) |
| JGY1244 | BY4741 | *psk1::*hph-MX4*, psk2::*nat-MX4*, his3-1, leu2-0, met15-0, ura3-0* | *psk1psk2* | a | This study |
| JGY1261 | BY4741 | *psk1::*hph-MX4*, psk2::*nat-MX4*, cbf1::*kan-MX4*, his3-1, leu2-0, met15-0, ura3-0* | *psk1psk2cbf1* | a | This study |
| JGY1348 | BY4741 | *psk1::*kan-MX4*, his3-1, leu2-0, met15-0, ura3-0* | *psk1* | a | (Winzeler et al., 1999) |
| JGY1349 | BY4741 | *psk2::*kan-MX4*, his3-1, leu2-0, met15-0, ura3-0* | *psk2* | a | (Winzeler et al., 1999) |
| JHG504 | BL21DE3 | $F^-$ ompT hsdSB($rB^-mB^-$) gal dcm (DE3) | BL21 | | Novagen |

| Plasmid | Gene | Description | Backbone | Yeast origin | Selection | Reference or source |
|---|---|---|---|---|---|---|
| pJG121 | EV | Empty pRS415 plasmid | pRS415 | CEN | LEU | |
| pJG725 | EV | pAdh-myc | pRS416 | CEN | URA | (DeMille et al., 2014) |
| pJG727 | Library | Yeast genomic library | pRS426 | 2u | URA | Jared Rutter |
| pJG728 | Library | Yeast genomic library | pRS426 | 2u | URA | Jared Rutter |
| pJG1009 | EV | pET15b with James Y2H MCS | pET15b | | AMP | (DeMille et al., 2014) |
| pJG1025 | *IPP1* | *IPP1* into pET15b (pJG1009) | pET15b | | AMP | (DeMille et al., 2014) |
| pJG1031 | *CBF1* | *CBF1* into pET15b (pJG1009) | pET15b | | AMP | (DeMille et al., 2014) |
| pJG1125 | *CBF1* | Cbf1 into pJG725 | pRS416 | CEN | URA | (DeMille et al., 2014) |
| pJG1146 | *CBF1* | Cbf1-T212A | pET15b | | AMP | This study |
| pJG1181 | *PSK1* | pGAL1-10-*PSK1*-Myc | pRS426 | 2u | URA | (DeMille et al., 2014) |
| pJG1207 | *CBF1* | Cbf1-T211A | pET15b | | AMP | This study |
| pJG1232 | *USF1* | USF1 in pCMV | pCMV6-XL5 | | AMP | OriGene |
| pJG1233 | *USF1* | *USF1* into pET15b (pJG1009) | pET15b | | AMP | This study |
| pJG1246 | *USF1* | *USF1* into pJG725 | pRS415 | CEN | URA | This study |
| pJG1314 | *LACZ* | *LACZ* into pJG121 | pRS415 | CEN | LEU | This study |

| | | | | | | |
|---|---|---|---|---|---|---|
| pJG1315 | *ATP3* | *ATP3-LACZ* | pRS415 | CEN | LEU | This study |
| pJG1316 | *COX4* | *COX4-LACZ* | pRS415 | CEN | LEU | This study |
| pJG1317 | *HAP4* | *HAP4-LACZ* | pRS415 | CEN | LEU | This study |
| pJG1318 | *NDI1* | *NDI1-LACZ* | pRS415 | CEN | LEU | This study |
| pJG1319 | *QCR6* | *QCR6-LACZ* | pRS415 | CEN | LEU | This study |
| pJG1321 | *LAC1* | *LAC1-LACZ* | pRS415 | CEN | LEU | This study |
| pJG1322 | *LAG1* | *LAG1-LACZ* | pRS415 | CEN | LEU | This study |
| pJG1335 | *CBF1* | T211A-Cbf1 into pJG725 | pRS416 | CEN | URA | This study |
| pJG1336 | *CBF1* | T212A-Cbf1 into pJG725 | pRS416 | CEN | URA | This study |

| Primer | Sequence |
|---|---|
| JG3456 | GGCCTCGAGCGTTGCTGTCATTCTTGATGACG |
| JG3457 | GGCCTCGAGGTTGCTGTCATTCTTGATGACG |
| JG3458 | CGAATTCATGAAGGGGCAGCAGAAAACAGCTG |
| JG3683 | GGCAAGCTTATGACCATGATTACGGATTCACTGG |
| JG3684 | GGCGGATCCTTTTTGACACCAGACCAACTGGTAATG |
| JG3669 | GGCAAGCTTTAGAAAAGTCTTTGCGGTCATGATTC |
| JG3670 | GGCCTCGAGTTTCATCAAGGACTAAAGTTTTCTTATG |
| JG3671 | GGCAAGCTTTGATACAATTCTTGACAACATGACTAC |
| JG3672 | GGCCTCGAGGGCAAGCTTGACCTTTACTTTCCTCTCTAAAAGCC |
| JG3673 | GGCAAGCTTTTCCAACATGCCCATTTTCTATTTC |
| JG3674 | GGCCTCGAGCGAACAGCACAAGACGCGTATCAC |
| JG3675 | GGCAAGCTTTAGTGAAAGCATTGTGCTTGTTATC |
| JG3676 | GGCCTCGAGGCGGATTCCAAAGGCGTCCTTC |
| JG3679 | GGCAAGCTTCTTCGATAGCATAGTGGTTTTTAG |
| JG3680 | GGCCTCGAGGACCGGCGCTACCCGGTTAAG |

REFERENCES

Auer, S., Hahne, P., Soyal, S.M., Felder, T., Miller, K., Paulmichl, M., Krempler, F., Oberkofler, H., and Patsch, W. (2012). Potential role of upstream stimulatory factor 1 gene variant in familial combined hyperlipidemia and related disorders. Arterioscler Thromb Vasc Biol *32*, 1535-1544.

Byrne, K.P., and Wolfe, K.H. (2007). Consistent patterns of rate asymmetry and gene loss indicate widespread neofunctionalization of yeast genes after whole-genome duplication. Genetics *175*, 1341-1350.

Cai, M., and Davis, R.W. (1990). Yeast centromere binding protein CBF1, of the helix-loop-helix protein family, is required for chromosome stability and methionine prototrophy. Cell *61*, 437-446.

Conant, G.C., and Wolfe, K.H. (2007). Increased glycolytic flux as an outcome of whole-genome duplication in yeast. Mol Syst Biol *3*, 129.

Coon, H., Xin, Y., Hopkins, P.N., Cawthon, R.M., Hasstedt, S.J., and Hunt, S.C. (2005). Upstream stimulatory factor 1 associated with familial combined hyperlipidemia, LDL cholesterol, and triglycerides. Hum Genet *117*, 444-451.

da Silva Xavier, G., Rutter, J., and Rutter, G.A. (2004). Involvement of Per-Arnt-Sim (PAS) kinase in the stimulation of preproinsulin and pancreatic duodenum homeobox 1 gene expression by glucose. Proc Natl Acad Sci U S A *101*, 8319-8324.

DeMille, D., Badal, B.D., Evans, J.B., Mathis, A.D., Anderson, J.F., and Grose, J.H. (2015). PAS kinase is activated by direct SNF1-dependent phosphorylation and mediates inhibition of TORC1 through the phosphorylation and activation of Pbp1. Mol Biol Cell *26*, 569-582.

DeMille, D., Bikman, B.T., Mathis, A.D., Prince, J.T., Mackay, J.T., Sowa, S.W., Hall, T.D., and Grose, J.H. (2014). A comprehensive protein-protein interactome for yeast PAS kinase 1 reveals direct inhibition of respiration through the phosphorylation of Cbf1. Mol Biol Cell *25*, 2199-2215.

DeMille, D., and Grose, J.H. (2013). PAS kinase: a nutrient sensing regulator of glucose homeostasis. IUBMB Life *65*, 921-929.

Di Taranto, M.D., Staiano, A., D'Agostino, M.N., D'Angelo, A., Bloise, E., Morgante, A., Marotta, G., Gentile, M., Rubba, P., and Fortunato, G. (2015). Association of USF1 and APOA5 polymorphisms with familial combined hyperlipidemia in an Italian population. Mol Cell Probes *29*, 19-24.

Grassi, L., Fusco, D., Sellerio, A., Cora, D., Bassetti, B., Caselle, M., and Lagomarsino, M.C. (2010). Identity and divergence of protein domain architectures after the yeast whole-genome duplication event. Mol Biosyst *6*, 2305-2315.

Grose, J.H., Smith, T.L., Sabic, H., and Rutter, J. (2007). Yeast PAS kinase coordinates glucose partitioning in response to metabolic and cell integrity signaling. EMBO J *26*, 4824-4830.

Hao, H.X., Cardon, C.M., Swiatek, W., Cooksey, R.C., Smith, T.L., Wilde, J., Boudina, S., Abel, E.D., McClain, D.A., and Rutter, J. (2007). PAS kinase is required for normal cellular energy balance. Proc Natl Acad Sci U S A *104*, 15466-15471.

Haynes, B.C., Maier, E.J., Kramer, M.H., Wang, P.I., Brown, H., and Brent, M.R. (2013). Mapping functional transcription factor networks from gene expression data. Genome Res *23*, 1319-1328.

Holzapfel, C., Baumert, J., Grallert, H., Muller, A.M., Thorand, B., Khuseyinova, N., Herder, C., Meisinger, C., Hauner, H., Wichmann, H.E.*, et al.* (2008). Genetic variants in the USF1 gene are associated with low-density lipoprotein cholesterol levels and incident type 2 diabetes mellitus in women: results from the MONICA/KORA Augsburg case-cohort study, 1984-2002. Eur J Endocrinol *159*, 407-416.

Huertas-Vazquez, A., Aguilar-Salinas, C., Lusis, A.J., Cantor, R.M., Canizales-Quinteros, S., Lee, J.C., Mariana-Nunez, L., Riba-Ramirez, R.M., Jokiaho, A., Tusie-Luna, T.*, et al.* (2005). Familial combined hyperlipidemia in Mexicans: association with upstream transcription factor 1 and linkage on chromosome 16q24.1. Arterioscler Thromb Vasc Biol *25*, 1985-1991.

Kolaczkowski, M., Kolaczkowska, A., Gaigg, B., Schneiter, R., and Moye-Rowley, W.S. (2004). Differential regulation of ceramide synthase components LAC1 and LAG1 in Saccharomyces cerevisiae. Eukaryot Cell *3*, 880-892.

Komulainen, K., Alanne, M., Auro, K., Kilpikari, R., Pajukanta, P., Saarela, J., Ellonen, P., Salminen, K., Kulathinal, S., Kuulasmaa, K.*, et al.* (2006). Risk alleles of USF1 gene predict cardiovascular disease of women in two prospective studies. PLoS Genet *2*, e69.

Laplante, M., and Sabatini, D.M. (2012). mTOR signaling in growth control and disease. Cell *149*, 274-293.

Lee, J.C., Weissglas-Volkov, D., Kyttala, M., Sinsheimer, J.S., Jokiaho, A., de Bruin, T.W., Lusis, A.J., Brennan, M.L., van Greevenbroek, M.M., van der Kallen, C.J.*, et al.* (2007). USF1 contributes to high serum lipid levels in Dutch FCHL families and U.S. whites with coronary artery disease. Arterioscler Thromb Vasc Biol *27*, 2222-2227.

Lin, Z., Wang, T.Y., Tsai, B.S., Wu, F.T., Yu, F.J., Tseng, Y.J., Sung, H.M., and Li, W.H. (2013). Identifying cis-regulatory changes involved in the evolution of aerobic fermentation in yeasts. Genome Biol Evol *5*, 1065-1078.

MacIsaac, K.D., Wang, T., Gordon, D.B., Gifford, D.K., Stormo, G.D., and Fraenkel, E. (2006). An improved map of conserved regulatory sites for Saccharomyces cerevisiae. BMC Bioinformatics *7*, 113.

Maclean, C.J., and Greig, D. (2011). Reciprocal gene loss following experimental whole-genome duplication causes reproductive isolation in yeast. Evolution *65*, 932-945.

Makino, T., and McLysaght, A. (2012). Positionally biased gene loss after whole genome duplication: evidence from human, yeast, and plant. Genome Res *22*, 2427-2435.

Meex, S.J., van Vliet-Ostaptchouk, J.V., van der Kallen, C.J., van Greevenbroek, M.M., Schalkwijk, C.G., Feskens, E.J., Blaak, E.E., Wijmenga, C., Hofker, M.H., Stehouwer, C.D.*, et al.* (2008). Upstream transcription factor 1 (USF1) in risk of type 2 diabetes: association study in 2000 Dutch Caucasians. Mol Genet Metab *94*, 352-355.

Mymrikov, E.V., Seit-Nebi, A.S., and Gusev, N.B. (2011). Large potentials of small heat shock proteins. Physiological reviews *91*, 1123-1159.

Naukkarinen, J., Ehnholm, C., and Peltonen, L. (2006). Genetics of familial combined hyperlipidemia. Curr Opin Lipidol *17*, 285-290.

Naukkarinen, J., Gentile, M., Soro-Paavonen, A., Saarela, J., Koistinen, H.A., Pajukanta, P., Taskinen, M.R., and Peltonen, L. (2005). USF1 and dyslipidemias: converging evidence for a functional intronic variant. Hum Mol Genet *14*, 2595-2605.

Naukkarinen, J., Nilsson, E., Koistinen, H.A., Soderlund, S., Lyssenko, V., Vaag, A., Poulsen, P., Groop, L., Taskinen, M.R., and Peltonen, L. (2009). Functional variant disrupts insulin induction of USF1: mechanism for USF1-associated dyslipidemias. Circ Cardiovasc Genet *2*, 522-529.

Ng, M.C., Miyake, K., So, W.Y., Poon, E.W., Lam, V.K., Li, J.K., Cox, N.J., Bell, G.I., and Chan, J.C. (2005). The linkage and association of the gene encoding upstream stimulatory factor 1 with type 2 diabetes and metabolic syndrome in the Chinese population. Diabetologia *48*, 2018-2024.

Pajukanta, P., Lilja, H.E., Sinsheimer, J.S., Cantor, R.M., Lusis, A.J., Gentile, M., Duan, X.J., Soro-Paavonen, A., Naukkarinen, J., Saarela, J.*, et al.* (2004). Familial combined hyperlipidemia is associated with upstream transcription factor 1 (USF1). Nat Genet *36*, 371-376.

Perkins, E.M., and McCaffery, J.M. (2007). Conventional and immunoelectron microscopy of mitochondria. Methods Mol Biol *372*, 467-483.

Petti, A.A., McIsaac, R.S., Ho-Shing, O., Bussemaker, H.J., and Botstein, D. (2012). Combinatorial control of diverse metabolic and physiological functions by transcriptional regulators of the yeast sulfur assimilation pathway. Mol Biol Cell *23*, 3008-3024.

Plaisier, C.L., Horvath, S., Huertas-Vazquez, A., Cruz-Bautista, I., Herrera, M.F., Tusie-Luna, T., Aguilar-Salinas, C., and Pajukanta, P. (2009). A systems genetics approach implicates USF1, FADS3, and other causal candidate genes for familial combined hyperlipidemia. PLoS Genet *5*, e1000642.

Porta, C., Paglino, C., and Mosca, A. (2014). Targeting PI3K/Akt/mTOR Signaling in Cancer. Front Oncol *4*, 64.

Reiner, A.P., Carlson, C.S., Jenny, N.S., Durda, J.P., Siscovick, D.S., Nickerson, D.A., and Tracy, R.P. (2007). USF1 gene variants, cardiovascular risk, and mortality in European Americans: analysis of two US cohort studies. Arterioscler Thromb Vasc Biol *27*, 2736-2742.

Rutter, J., Michnoff, C.H., Harper, S.M., Gardner, K.H., and McKnight, S.L. (2001). PAS kinase: an evolutionarily conserved PAS domain-regulated serine/threonine kinase. Proc Natl Acad Sci U S A *98*, 8991-8996.

Rutter, J., Probst, B.L., and McKnight, S.L. (2002). Coordinate regulation of sugar flux and translation by PAS kinase. Cell *111*, 17-28.

Semplici, F., Vaxillaire, M., Fogarty, S., Semache, M., Bonnefond, A., Fontes, G., Philippe, J., Meur, G., Diraison, F., Sessions, R.B.*, et al.* (2011). Human Mutation within Per-Arnt-Sim (PAS) Domain-containing Protein Kinase (PASK) Causes Basal Insulin Hypersecretion. J Biol Chem *286*, 44005-44014.

Shimobayashi, M., and Hall, M.N. (2014). Making new contacts: the mTOR network in metabolism and signalling crosstalk. Nat Rev Mol Cell Biol *15*, 155-162.

Smith, T.L., and Rutter, J. (2007). Regulation of glucose partitioning by PAS kinase and Ugp1 phosphorylation. Mol Cell *26*, 491-499.

Sugino, R.P., and Innan, H. (2005). Estimating the time to the whole-genome duplication and the duration of concerted evolution via gene conversion in yeast. Genetics *171*, 63-69.

Takahara, T., and Maeda, T. (2012). Transient sequestration of TORC1 into stress granules during heat stress. Mol Cell *47*, 242-252.

van der Vleuten, G.M., Isaacs, A., Hijmans, A., van Duijn, C.M., Stalenhoef, A.F., and de Graaf, J. (2007). The involvement of upstream stimulatory factor 1 in Dutch patients with familial combined hyperlipidemia. J Lipid Res *48*, 193-200.

Winzeler, E.A., Shoemaker, D.D., Astromoff, A., Liang, H., Anderson, K., Andre, B., Bangham, R., Benito, R., Boeke, J.D., Bussey, H.*, et al.* (1999). Functional characterization of the S. cerevisiae genome by gene deletion and parallel analysis. Science *285*, 901-906.

# CHAPTER 5: Conclusions

PAS kinase, the focus of this work, is a key nutrient sensing kinase required for proper glucose allocation in yeast, mice and man. In yeast, PAS kinase allocates glucose away from glycogen storage towards structural carbohydrates through the phosphorylation of Ugp1 (Grose et al., 2007; Smith and Rutter, 2007). In mice, PAS kinase-deficiency causes decreased weight gain and lipid accumulation as well as an increased metabolism in animals that are fed a high fat diet (Hao et al., 2007). In humans, hyperactivating mutations in PAS kinase cause an increase in basal insulin levels as well as the development of Maturity-Onset Diabetes of the Young (MODY) (Semplici et al., 2011). Despite its obvious importance as a therapeutic target for the treatment of epidemic diseases like obesity, diabetes, cardiovascular disease and cancer, the molecular mechanisms behind PAS kinase function, including substrates, is largely unknown (see Chapter 1). Through this work we have identified and characterized novel substrates of PAS kinase that provide mechanisms for its known roles in glucose allocation as well as define new roles for its function.

In order to identify substrates of PAS kinase, we first conducted large-scale protein-protein interaction studies for yeast PAS kinase 1 (Psk1). We utilized both the yeast two-hybrid as well as copurification followed by mass spectrometry techniques (see Chapter 2). From these screens, 93 novel putative binding partners were identified for Psk1. Remarkably, 73% of the putative binding partners appear to have a human homolog, whereas only 20-30% of the yeast proteome is reportedly conserved with humans (Makino and McLysaght, 2012); supporting the evolutionary conservation of PAS kinase and its important role in regulating central metabolic pathways. Additionally, the majority of associated diseases for these binding partners point

towards lipid disorders, supporting the dramatic lipid phenotype in the PAS kinase-deficient mice (Hao et al., 2007).

Two of the 93 hits were retrieved in both the yeast two-hybrid and copurification screens (Pbp1 and Prb1), giving support that they are likely substrates of Psk1. Pbp1 became one focus to further characterize its interaction with Psk1. Pbp1 inhibits TORC1 by sequestering it to stress granules (Takahara and Maeda, 2012). TORC1 is also a highly conserved sensory kinase and is a key regulator of cell growth and proliferation pathways (see recent reviews (Laplante and Sabatini, 2012; Porta et al., 2014; Shimobayashi and Hall, 2014)). We hypothesized that Psk1 could be inhibiting TORC1 through the activation of Pbp1. In addition to the connection between Psk1 and TORC1, we retrieved another sensory kinase, Snf1 (AMPK), from our copurification study. We hypothesized that it could play part in this regulation and provide a model herein for the cross-talk that occurs between these three master regulators. The results of our studies support a model in which Snf1 (AMPK) senses low energy, phosphorylates and activates Psk1 which then phosphorylates and activates Pbp1 which sequesters TORC1 to stress granules, ultimately downregulating cell growth and proliferation pathways (see Chapter 3).

Another protein that became of interest for further characterization was Cbf1 (see Chapter 2), due to its human homolog being highly associated with hyperlipidemia. Transcriptome data suggested that Cbf1 regulates expression of genes involved in lipid metabolism as well as respiration (Haynes et al., 2013; Kolaczkowski et al., 2004; Lin et al., 2013; Petti et al., 2012). We first investigated respiration rates of Cbf1- and PAS kinase-deficient yeast. To our knowledge, we provided the first reports of PAS kinase and/or Cbf1 having direct effects on respiration (see Chapter 2). To determine the mechanisms behind these respiration phenotypes, we tested the hypothesis that Cbf1 was increasing respiration by

increasing mitochondrial mass and/or electron transport chain activity (see Chapter 4). PAS kinase-deficient yeast have an increased respiration rate and it appears this is due to an increase in mitochondrial mass as well as an increase in SDH activity; whereas Cbf1-deficient yeast have decreased respiration due to decreased SDH activity but not SDH protein levels. Further work to investigate how Cbf1 is affecting SDH activity led us to a high-copy suppressor screen where we identified two novel regulators of respiration, Mck1 and Cot1.

Through this work we have uncovered complex pathways by which the cell regulates its central metabolism, including respiration, lipid biogenesis, and cell growth. These pathways are key to understanding the most prevalent diseases in developed countries, including heart disease obesity, diabetes and cancer. Future work of PAS kinase is aimed at further identifying and characterizing substrates of PAS kinase from the large protein binding partner screens to help us understand more of its cellular roles and regulation in allocating glucose throughout the cell.

REFERENCES

Grose, J.H., Smith, T.L., Sabic, H., and Rutter, J. (2007). Yeast PAS kinase coordinates glucose partitioning in response to metabolic and cell integrity signaling. EMBO J *26*, 4824-4830.

Hao, H.X., Cardon, C.M., Swiatek, W., Cooksey, R.C., Smith, T.L., Wilde, J., Boudina, S., Abel, E.D., McClain, D.A., and Rutter, J. (2007). PAS kinase is required for normal cellular energy balance. Proc Natl Acad Sci U S A *104*, 15466-15471.

Haynes, B.C., Maier, E.J., Kramer, M.H., Wang, P.I., Brown, H., and Brent, M.R. (2013). Mapping functional transcription factor networks from gene expression data. Genome Res *23*, 1319-1328.

Kolaczkowski, M., Kolaczkowska, A., Gaigg, B., Schneiter, R., and Moye-Rowley, W.S. (2004). Differential regulation of ceramide synthase components LAC1 and LAG1 in Saccharomyces cerevisiae. Eukaryot Cell *3*, 880-892.

Laplante, M., and Sabatini, D.M. (2012). mTOR signaling in growth control and disease. Cell *149*, 274-293.

Lin, Z., Wang, T.Y., Tsai, B.S., Wu, F.T., Yu, F.J., Tseng, Y.J., Sung, H.M., and Li, W.H. (2013). Identifying cis-regulatory changes involved in the evolution of aerobic fermentation in yeasts. Genome Biol Evol *5*, 1065-1078.

Makino, T., and McLysaght, A. (2012). Positionally biased gene loss after whole genome duplication: evidence from human, yeast, and plant. Genome Res *22*, 2427-2435.

Petti, A.A., McIsaac, R.S., Ho-Shing, O., Bussemaker, H.J., and Botstein, D. (2012). Combinatorial control of diverse metabolic and physiological functions by transcriptional regulators of the yeast sulfur assimilation pathway. Mol Biol Cell *23*, 3008-3024.

Porta, C., Paglino, C., and Mosca, A. (2014). Targeting PI3K/Akt/mTOR Signaling in Cancer. Front Oncol *4*, 64.

Semplici, F., Vaxillaire, M., Fogarty, S., Semache, M., Bonnefond, A., Fontes, G., Philippe, J., Meur, G., Diraison, F., Sessions, R.B.*, et al.* (2011). Human Mutation within Per-Arnt-Sim (PAS) Domain-containing Protein Kinase (PASK) Causes Basal Insulin Hypersecretion. J Biol Chem *286*, 44005-44014.

Shimobayashi, M., and Hall, M.N. (2014). Making new contacts: the mTOR network in metabolism and signalling crosstalk. Nat Rev Mol Cell Biol *15*, 155-162.

Smith, T.L., and Rutter, J. (2007). Regulation of glucose partitioning by PAS kinase and Ugp1 phosphorylation. Mol Cell *26*, 491-499.

Takahara, T., and Maeda, T. (2012). Transient sequestration of TORC1 into stress granules during heat stress. Mol Cell *47*, 242-252.